STUDIES ON CARBON-CARBON BOND FORMATION REACTIONS OF ORGANIC MOLECULES OVER ZEOLITES AND OTHER MOLECULAR SIEVE CATALYSTS

A THESIS

SUBMITTED TO THE

UNIVERSITY OF PUNE

FOR THE DEGREE OF

DOCTOR OF PHILOSOPHY

(**IN CHEMISTRY**)

BY

MRS. SMITA GIRISH WAGHOLIKAR

CATALYSIS DIVISION

NATIONAL CHEMICAL LABORATORY

PUNE 411008, INDIA

APRIL 2005

CERTIFICATE

Certified that the work incorporated in the thesis **"Studies on C-C Bond Formation Reactions of Organic Molecules Over Zeolites and Other Molecular Sieve Catalysts"** submitted by **Mrs. Smita Girish Wagholikar,** for the degree of **Doctor of Philosophy,** was carried out by the candidate under our supervision in Catalysis Division, National Chemical Laboratory, Pune, India. Materials obtained from other sources have been duly acknowledged in the thesis.

Dr. S. Sivasanker — **Research Guide**

Dr. D. Srinivas — **Research Co-guide**

DEDICATED

TO

MY BELOVED PARENTS

Acknowledgements

It is a immense pleasure to acknowledge with respect the invaluable guidance, numerous discussions, constructive suggestions, encouragement and support given by my research guide, Dr. S. Sivasanker, Emeritus Scientist and former Head of Inorganic and Catalysis Division, NCL, Pune, throughout the course of this investigation. This thesis would not have taken its shape without his patience. I am indebt to him forever.

I take this opportunity to express my deepest sense of gratitude and reverence to my co-guide, Dr. D. Srinivas and Dr. Mrs. S. Mayadevi for their constant inspiration and for guiding me throughout the course of this work.

I express my profound gratitude to Dr. S.A. Pardhy, Dr. S.S. Deshpande, Ms. M.S. Agashe Dr. S.V. Awate, Dr. M.K. Dongare, Dr. S.G. Hegde, Dr. S. Umbarkar, Dr. A.A. Belhekar, Dr. K. Kamble, Dr. C.V.V. Satyanarayana, Dr. V. Ramaswamy, Dr. A..J. Chandwadkar, Dr. T. Raja, Dr. A.P .Singh, Ms. V. Samuel, Ms. N. E. Jacob, Mr. R. Jha, Dr. S.P. Mirajkar, Dr. S.B. Halligudi, Dr. P. Manikandan, Dr. V.R. Chumbhale, Dr. Rajamohan and all other scientific and technical staff for their help, inspiration and guidance. I express my gratitude towards Dr. P.N. Joshi, Dr. Chaphekar, Mr. Niphadkar, Mr. Gaydhankar, Catalysis Pilot Plant for the help extended by them for this research work.

I would like to thank my friends, Surekha, Suresh, Bennur, Vasu, Prashant, Mahesh, Pallavi, Neelam, Pai, Kala, Dhanashri, Trissa, Shanbhag, Sanker, Rohit, Sneha, Sonal and many others for their encouragement, cooperation and moral support rendered by them.

I find no words to express my deepest sense of gratitude to my parents and brother for all the love, unfailing support, tremendous patience and understanding that they have shown to me. This work would not have taken its shape had it not been backed by their cooperation and encouragement. I wish to thank my husband, Mr. Girish Wagholikar, for all the support, understanding and cooperation extended by him. I thank my son, Omkar, for making my life complete and more cheerful than it was.

I take this opportunity to thank Dr. S. Sivaram, Director, NCL, Pune, Dr. Rajiv Kumar, Head, Inorganic and Catalysis Division, NCL, Pune, Dr. A.V. Ramaswamy, former Head, Inorganic and Catalysis Division, NCL, Pune for allowing me to carry out research at NCL. Finally, I would like to thank Council of Scientific and Industrial Research (CSIR), New Delhi for providing me a research fellowship.

Smita Wagholikar

CONTENTS

Chapter 1 General Introduction

Chapter 1

Introduction

1.1 General Introduction:

Zeolites are crystalline aluminosilicates whose framework structures consist of three dimensional networks of oxygen atoms that enclose cavities or channels, which run throughout the structure. The general empirical formula of zeolites is:

$$(M^{n+})_{x/n}[(AlO_2)_x(SiO_2)_y]^{x-}.m\ H_2O$$

where, 'M' is the cation, 'm' is the number of moles of water of crystallization, x and y are the number of $[AlO_4]^{5-}$ and $[SiO_4]^{4-}$ tetrahedra in the unit cell. The Si to Al ratio (y/x) in synthetic zeolites may vary considerably, from one (for zeolite A) to near infinity (for silicalites). The network has an overall negative charge because of the presence of aluminium that is balanced by the incorporation of exchangeable cations, M^{n+}. The $[AlO_4]^{5-}$ and $[SiO_4]^{4-}$ tetrahedra can be arranged in many ways to form different porous crystal structures (zeolites). One condition here is that two aluminium atoms can never be in adjoining tetrahedra, but are separated by at least one silicon-oxygen tetrahedron [1].

Classification of zeolites can be made on the basis of their morphological characteristics [2-4], crystal structure [6,7], chemical composition [6,8], effective pore diameter [6] and natural occurance.

There are only three pore openings known to date in the aluminosilicate pore system that are of practical interest for catalytic applications: they are descriptively referred to as 8,10 and 12 ring openings. Zeolites may be referred to as small (8 membered ring), medium (10 membered ring) and large (12 membered ring) pore types. Zeolites of type A (LTA), ZK-5 (KFI) and erionite (ERI) are some examples of small (8 membered ring) pore materials, ZSM-5 (silicalite; MFI), ZSM-11 (MEL) and ferrierite (FER) are examples of

medium (10 membered ring) pore ones and faujasite (FAU), mordenite (MOR) and beta (BEA) are examples of zeolites with large pore openings.

Some common zeolites and microporous materials are listed in Table 1.1.

Table 1.1: Characteristics of some common zeolites and microporous materials

Molecular sieve type	IZA code	Si / Al ratio	Ring size[a]	Pore diameter[b](Å)	Pore dimensionality	Relative pore size
Zeolite A	LTA	1-1.5	8-8-8	4.1	3	Small
Chabazite	CHA	1-1.5	8-8-8	3.8 x 3.8	3	Small
ZSM-5	MFI	7-100	10-10-10	5.4 x 5.6	3	Medium
ZSM-11	MEL	20-90	10-10-10	5.3 x 5.4	3	Medium
ZSM-48	-	50	10	5.3 x 5.6	1	Medium
SAPO-11	AEL	-	10	3.9 x 6.3	1	Medium
Faujasite (Y)	FAU	1.5-3.0	12-12-12	7.4	3	Large
Faujasite (X)	FAU	1-1.5	12-12-12	7.4	3	Large
Linde type L	LTL	4.5-12.0	12	7.1	1	Large
Mordenite	MOR					large
Beta	BEA	10-100	12-12	6.4 x 7.6	3	Large
ETS-10	-	-	12-12-7	4.9 x 7.6	3	Large
VPI-5	VPI	-	18	12.1	1	Very large

a = number of T or O atoms comprising smallest rings in channel, b = pore diameter of largest channel

After the initial consideration of the pore size of the zeolite, it is important to examine the finer details of the channel systems. This second level of complexity includes

two features: (1) the number of dimensions the pores encompass and (2) pore mouth shape. By considering these features one distinguishes between zeolites within the small, medium

(a)

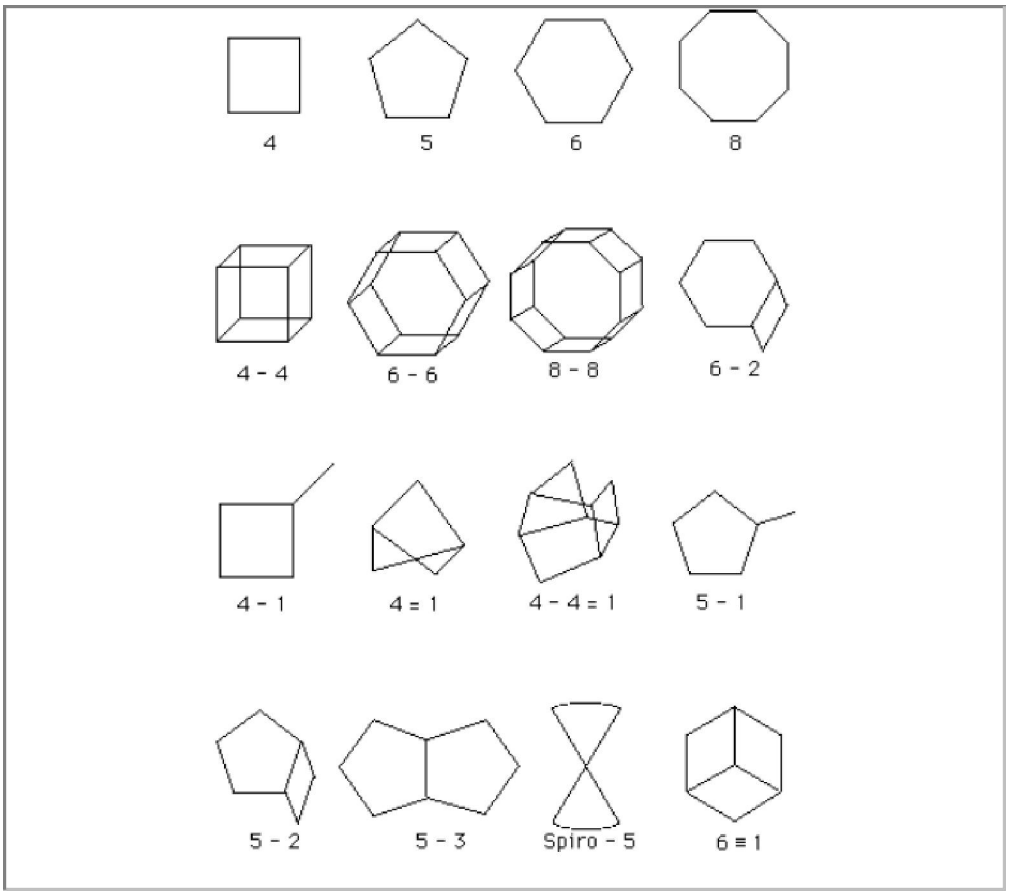

(b)

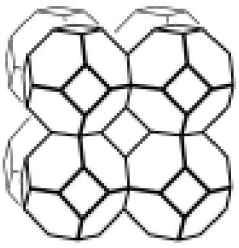

Sodalite (SOD; Pores ~ 3Å)

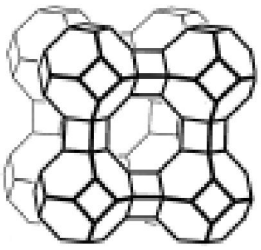

Zeolite A (LTA Pores ~ 4 Å)

Fig.1.1 (a) Examples of Secondary Building Units found in zeolite molecular sieves and (b) two typical zeolite framework structures formed from SBU's

and large pore classifications. Differences in dimensionality and shape of pore opening can also contribute to differences in catalytic and adsorption behavior in these zeolites.

For the ideal planar configuration using 2.7 Å as the diameter of the oxygen atoms, an 8 member ring opening is 4.4 Å and that of the 10 and 12 membered rings would be 6.0 and 7.7 Å, respectively. The actual values however deviate from these values as it is the structure of the zeolite that shapes the pore mouth. For example, Zeolite A, a small pore zeolite, has a pore dimension estimated from its structure to be 4.1 Å. Erionite, also a small pore zeolite has a pore diameter of 5.2 and 3.2 Å, reflecting the elongated nature of its channel system. Though the structure dictates the shape of the pore opening, this opening can be further modified; for example, the number of cations present within the pores of the structure also affects the size of the opening.

The primary building unit of a zeolite structure is the individual tetrahedral TO_4 unit, where T is either Si or Al. A secondary building unit (SBU) consists of selected groupings of those tetrahedra. There are sixteen such secondary building units that can be used to describe all of the known zeolite structures. These secondary building units consist of 4, 6 and 8 membered single rings, 4-4, 6-6 and 8-8 double membered rings and 4-1, 5-1 and 4-4-1 branched rings. The SBU's are linked three dimensionally to derive the different zeolite structures. The SBU's and framework structures of two zeolites are shown in Fig.1.1.

1.1.1. Zeolites in catalysis:

Industrial use of zeolites as catalysts began in the beginning of the 1960's as replacements for amorphous aluminosilicate cracking catalysts. Their catalytic activity is associated with the presence of acid centers (Brönsted and Lewis) in the intracrystalline surface. Acidity in zeolites arises from the substitution of a trivalent metal atom such as Al,

Ga, Fe and B for silicon in the framework position. When the charge compensating cation is a hydrogen ion (proton), the zeolite framework exhibits Brönsted acidity. Lewis acidity arises from trigonal aluminium or other cationic species. Brönsted acidity is related to the trivalent metal ion content in the framework.

The most important application of zeolites is in reactions catalyzed by Brönsted and Lewis acids. The change from a homogeneous (mineral acid) to a heterogeneous catalyst (zeolites) results in advantages of easy separation, reusability, disposal of the catalyst and avoidance of corrosion. Zeolites show the following properties that make them attractive as heterogeneous catalysts.

- Well defined crystalline structure
- High internal surface area
- Uniform pores of one or more discrete sizes
- Good thermal stability
- Ability to adsorb and concentrate hydrocarbons
- Highly acidic sites in the protonated form

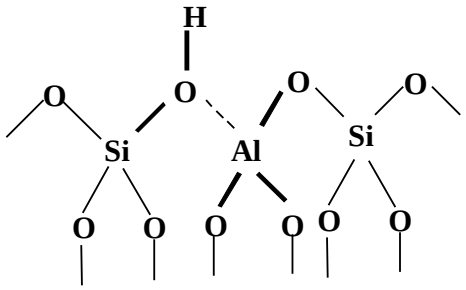

Fig. 1.2 The bridging hydoxyl group and the oxo ligands of the Al-atom act as bifunctional Brönsted acid-Lewis base sites

1.1.2 Some typical zeolites and mesoporous materials:

ZSM-5 (MFI):

ZSM-5 is a synthetic high silica zeolite first reported in 1973 by Argauer and Landolt [9]. The MFI-type topology shows a three-dimensional 10-membered channel system. The first syntheses were performed in the presence of Na^+ and organic additives. About 25 organic species have been claimed to be useful [10], among which the tetrapropyl ammonium cations are the most structure-directing. Indeed, ZSM-5 is easily synthesized with this template in a very broad range of experimental conditions. Organic-free synthesis in the presence of only Na^+ cations has also been reported [11-13].

Zeolites with FAU-type structures:

Zeolite X and zeolite Y of faujasite type (FAU) can be obtained from starting mixtures essentially differing in the Si / Al ratios (larger for Y than X) in the temperature range 293 –393 K and 293 – 448 K respectively [3]. The framework structure of zeolite Y consists of truncated octahedral sodalite units, linked by hexagonal prisms. The polyhedra formed in this way enclose a super cage (α-cage) of about 12Å diameter. The unit cell of zeolite-Y is given as $[M_xSi_{(192-x)}Al_xO_{384}]$. Zeolite Y has a three dimensional channel system consisting of 12 member rings, having an opening of 0.74 nm.

Beta (BEA):

Zeolite beta is a large pore (twelve membered ring aperture), high silica zeolite (Si/Al from about 10 to 100) and has a three dimensional pore system made up of two different types of channels with diameters of 0.73 nm and 0.55nm. It was first synthesized in 1967 [14] from alkaline aluminosilicate gels in the presence of fluoride ions as the mineralizing agent and 1,4 diazabicyclo [2,2,2] octane (DABCO) and methyl amine as the organic species. With this route the zeolite obtained is less siliceous (Si/Al = 9 - 22) than when prepared in alkaline medium with Na^+ and Et_4N^+ cations. The observation that complete exchange of cations in beta is possible [8,15] indicates the absence of small cages.

Mordenite (MOR):

Mordenite is a natural high silica zeolite whose typical unit cell formula is $Na_8Al_8Si_{40}O_{26}$. 24 H_2O. It has two types of pores that are perpendicular to each other, twelve-membered ring (12-MR) elliptical pores (0.67 - 0.71 nm) parallel to the c-axis and eight-membered ring (8-MR) pores (0.29 – 0.57 nm) parallel to the b-axis. As one of the pore systems is small (8-MR) and not useful for catalysis, mordenite can be considered as having an essentially one-dimensional channel system [16].

Engelhard's titanosilicate (ETS-10):

ETS-10 (Engelhard's titanosilicate-10) is a large pore titanosilicate molecular sieve, first synthesized at Engelhard Corporation, USA [16a]. The framework structure of ETS-10 consists of corner shared oxygen ions of $[TiO_6]^{8-}$ octahedra and $[SiO_4]^{4-}$ tetrahedra. ETS-10 possesses a three dimensional pore system made up of 12-membered ring (12-MR) channels with a pore diameter of 7.6 Å. The structure is made up of interconnecting rings of 3, 4, 5, 7 and 12 members. Each Ti is connected via oxygen to four Si atoms in two 3 membered rings and also via oxygen to other two Ti atoms. All Si atoms, except those at the apex of each 5 membered ring are connected to three Si atoms and one Ti atom via oxygen [Si (3 Si, 1 Ti)]. The apical Si in each 5 membered ring is a [Si (4Si, 0 Ti)]. Two rods of Ti perpendicular to each other join together by forming a 7 membered ring. The Ti chain rods are regularly arranged along the X and Y axes with a period of 15 Å and a large channel with 12 membered ring aperture is formed.

1.2 Modification of Zeolites:

Modification of zeolites is important as it makes available a large variety of catalytic materials and extends the scope for increasing or decreasing the pore size or acidity of the zeolite [17]. Replacing the protons in the zeolite structure by alkali or alkaline earth metal ions helps in altering the size of the zeolite pore. Dealumination of a zeolite helps in tailoring its acidic properties. Though the number of acid sites decreases on dealumination,

the acid site strength increases in some systems (FAU). Zeolites contain surface acid sites that cause non-shape selective catalytic behavior leading to undesirable products. Modification of zeolites by selectively poisoning the surface acid sites decreases the formation of these undesirable products.

1.2.1 Modification by ion exchange:

Zeolites, in a narrow definition, are crystalline aluminosilicates having a uniform pore structure and exhibiting ion-exchange behavior. A higher ion exchange capacity is observed in zeolites of low Si/Al ratio. The major applications of ion exchanged zeolites are as water softeners in laundry detergents (low cost and non-polluting substitute for phosphate), adsorbents in gas purification and in the preparation of various types of catalysts.

Usually ion exchange is performed by simply contacting the zeolite with a salt solution of a different cation at ambient or higher temperatures. The rate of ion exchange depends upon the concentration of the ions of a size capable of penetrating the pores of the zeolite. At ambient temperature, a solution of a large hydrated ion may contain very few partially hydrated ions of a size smaller than the pore opening of the zeolite, so the exchange is very slow. The rate of exchange increases with rising temperature, as water is stripped from the ions and the hydration equilibrium shifts toward less hydrated ions.

1.2.2 Modification by dealumination:

The Si/Al ratio of the zeolites can be increased significantly by chemical treatment leading to the removal of some of the Al from the framework. This is called dealumination. Dealumination by steaming or acid extraction are post synthesis methods to control the acidity of zeolites. Steaming of the acid form causes a decrease in the concentration of the tetrahedral framework aluminium while octahedral species are generated. The removal of framework aluminium by acid leaching leads to the formation of hydroxyl nests. Mild acid

leaching is also used to remove extra-framework-aluminium without extracting aluminium from the framework. The selective removal of non-framework aluminium species can also be achieved by treatment with Na_2H_2EDTA or $(NH_4)_2$ H_2EDTA. Acetyl acetone is also effective in removing the non-framework aluminium. In general, thermal stability and zeolites increases substantially as a result of dealumination.

Zeolite Y is dealuminated to form ultrastable zeolite Y by repeated sequences of ammonium exchange and calcination:

NaY ⟶ NH_4^+ Exchange ⟶ Calcination at 813 K

⟶ NH_4^+ Exchange ⟶ Final calcination at 1088 K

The extent of dealumination is limited by the degree of ammonium exchange of the starting material and depends on the temperature and partial pressure of steam during the thermochemical treatment.

1.3 Shape Selectivity of Zeolites:

In shape selective catalysis over zeolites, both the molecular dimensions of the pores and the active sites inside these pores are exploited to control the catalytic reaction. Molecular sieving is the selective adsorption of molecules, whose dimensions are critically below a certain size, into the intracrystalline void system of the molecular sieve. Obviously, it is not only the size of the pores that controls shape selectivity, but also the relative dimensions of the reacting and diffusing molecules and the transition state that play a decisive role. By applying these criteria, shape selectivity in zeolites is classified as:

(1) Reactant shape selectivity: This results from the limited diffusibility of some molecules in a mixture of molecules; the molecules smaller in dimensions than the pore openings can effectively enter and diffuse inside the zeolite pore system, while molecules of larger dimensions cannot.

(2) Product shape selectivity: This occurs when slowly diffusing product molecules cannot rapidly escape from inside the zeolite crystal and undergo secondary reactions, the observed product of the reactions being therefore mainly the molecules that can diffuse out rapidly.

(3) Restricted transition state selectivity: In a zeolite with a given pore (or cavity) dimensions, there will be just enough space for the accommodation of certain transition states and intermediates of some reactions, but no room for the formation of bulkier transition states and intermediates of other reactions. The net effect will be the suppression of the latter reactions. Restricted transition state selectivity is due to the intrinsic chemical effects that emerge from the limited space around the intracrystalline active sites.

1.4 Physicochemical Characterization of Zeolites:

A number of techniques are used to characterize zeolites. Each of the technique is unique by itself and provides important information about the sample molecular sieve. Among these, X-ray diffraction, sorption studies, nuclear magnetic resonance, transmission electron microscopy, scanning electron microscopy, temperature programmed desorption, infrared and ultra violet spectroscopy are the important and useful techniques.

1.4.1 X-ray diffraction:

Powder X-ray diffraction is the most important and commonly used tool to identify and measure the uniqueness of structure, phase purity, degree of crystallinity and unit cell parameters of crystalline materials. As the powder pattern is the fingerprint of the molecular sieve structure, phase purity and percent crystallinity of the synthesized molecular sieve can be ascertained by comparing with the standard pattern for the molecular sieve under investigation. The zeolite structure can be identified by comparison of d-spacings of the typical Bragg's reflections with those given for the known zeolites in straightforward compilations. It is also used to study cation distribution inside the zeolite matrix [16,18].

Microporous solids show characteristic peaks in the 2θ range 5-50^{o} whereas ordered mesoporous materials exhibit characteristic peaks in the low angle region between 0.8 – 10^{o}.

1.4.2 Sorption studies:

The sorption properties of molecular sieves provide information about their hydrophilic/ hydrophobic character, pore size distribution and pore volume as well as surface area before and after post synthesis modifications like encapsulation/ dealumination etc. Also, sorption studies on zeolites can provide information about their void volumes, percentage crystallinity, acidity, diffusion properties and pore blockage if any. The sorption of nitrogen measured by at low pressures and at liquid N_2 temperature (77K) and application of the Brunauer-Emmett-Teller (BET) equation is the standard method for the determination of surface areas of zeolites and molecular sieves [19, 20] even though the validity of the BET equation for these materials is questionable. However, the BET method can be satisfactorily used for comparative purposes.

1.4.3 Nuclear magnetic resonance:

High–resolution magic angle spinning nuclear magnetic resonance (NMR) spectroscopy in the solid state is a powerful complementary method to diffraction techniques for the investigation of zeolite molecular sieve structures [21]. The main fields of application are:

(i) evaluation of the environment of the silicon framework atoms,

(ii) n_{Si}/n_{Al} ratio of the zeolite framework,

(iii) silicon and aluminium ordering,

(iv) identification of framework and non-framework aluminium,

(v) dealumination and aluminium re-insertion,

(vi) incorporation of metals into zeolite framework and

(vii) determination of acidity of hydroxyl groups.

^{29}Si MAS NMR:

A particularly useful feature of the ^{29}Si NMR spectra is that the Si/Al ratio of the lattice can be calculated directly. Also, the method has the advantage that it detects the Al atoms indirectly from their effect on the Si atoms in the framework and thus detects only the framework Al atoms and the Si/Al ratio for the framework. Considerable information can be obtained from the spectra of highly silicious zeolites, where the Al content is so low that it does not affect the spectrum. In highly silicious zeolites, the resonance lines observed are due mainly to Si[4Si] groupings and are extremely narrow. Because of their excellent resolution, these spectra can be exploited in a number of ways to obtain subtle information regarding zeolite structures not easily obtainable by other techniques.

^{27}Al MAS NMR:

The ^{27}Al MAS NMR spectra of the tetrahedral lattice aluminium in zeolites reveal only a single resonance, because every Al has the environment Al[4Si]; the Al chemical shifts of individual zeolites have, however, characteristic values at a particular field strength. For $AlPO_4$ molecular sieves, the ^{27}Al spectra provide different types of information. In certain cases, some of the framework aluminium atoms can become hydrated, changing the coordination from four to six and the topology from tetrahedral to octahedral. Such changes are clearly detectable in the ^{27}Al MAS NMR spectra.

1.4.4 UV-Vis spectroscopy:

This spectroscopy is known to be a very sensitive and useful technique for the identification of the electronic state of the metal atom as well as ligand geometry in intrazeolite complexes. It gives information about the d-orbital splitting through d-d

transitions and the ligand-metal interaction through the ligand to metal charge-transfer transitions.

UV-Vis spectroscopy is useful in confirming the presence of metal ions in the framework structure of metallosilicates, such as titanosilates (TS-1) and vanadosilicates (VS-1). For example, the diffuse reflectance spectrum of TS-1 exhibited a strong transition around 212 nm (47000 cm^{-1}), whereas the silicalite –1 did not show any such signal [22]. Pure TiO_2 (anatase) absorbs at 312 nm (32000 cm^{-1}) [23]. Boccuti et al. [24] have also observed a transition around 48000 cm^{-1} in TS-1 and assigned it to an electronic transition having charge transfer character involving Ti (IV) sites. The charge transfer probably occurs from the excitation of an oxygen 2p electron in the valence band to the empty d orbitals of titanium ions [23].

1.4.5 Fourier transform infrared (FTIR) spectroscopy:

FTIR spectroscopy in the framework region (400-4000 cm^{-1}) provides additional information about the structural details of the zeolite. The bands observed in the mid infrared region have been classified into two main categories, viz. bands due to internal vibrations of the TO_4 tetrahedra (T = Si or Al) and external vibrations of the tetrahedral linkages eg., in double rings (as in A-,X-, Y-type) or pore openings (as in mordenite). Assignments of zeolite lattice vibrations are listed below [25].

Table 1.2: Assignments of zeolite lattice vibrations

Internal Tetrahedra	Vibrations, cm^{-1}	External Linkages	Vibrations, cm^{-1}
Asym. stretch	1250-950	Double ring	650-500
Sym. Stretch	720-650	Pore opening	420-300
T-O bend	500-420	Sym. Stretch	820-750
		Asym. Stretch	1150-1050 sh.

Acidic sites (such as acidic –OH groups; Brönsted acid centres) and basic Lewis sites (such as basic oxygen atoms or alkaline metal clusters) are encountered in zeolites and are of paramount importance in acid-base catalysis over zeolites. By IR spectroscopy, only the Brönsted acid sites may be investigated with and without probe molecules, whereas acidic Lewis sites, cations and basic sites can be identified and quantitatively determined only with the help of probes. Probe molecules frequently employed are typically pyridine, substituted pyridine, ammonia and amines, for acidic centres and carbon dioxide or pyrrole for basic sites.

1.4.6 Electron paramagnetic resonance (EPR) spectroscopy:

Transition metal ions can be investigated by ESR spectroscopy. Some of the ions that have been well studied are:

d^1 ions: Mo^{5+}, V^{4+}, Ti^{3+}, Cr^{5+}, W^{5+}

d^5 ions: Fe^{3+}, Mn^{2+}

d^9 ions: Cu^{2+}, Ni^{+}, Ag^{+}

These ions may either be incorporated within a host lattice at interstitial or substitutional positions or deposited at the surface of a catalyst or at cationic positions of a zeolite. The location and unusual oxidation states of these metal ions in zeolites are revealed by ESR [26].

1.4.7 Temperature programmed desorption (TPD):

This technique can be used characterize the acid sites present in the zeolite sample. Relative rapidness of the experiment and sufficient precision are an advantage to this method. Probe molecules like ammonia or pyridine are commonly used for acidity determination. Ammonia is frequently is used because of its size, stability and strong basic

strength [27]. First the zeolite is contacted with a base to neutralize the acid sites present. Then the temperature is raised at a constant rate and the amount desorbed is recorded.

In a TPD spectrum, one or more peaks may be observed, the ones at low temperature corresponding to NH_3 desorbing from the weaker acidic sites and the ones at higher temperature corresponding to the stronger acidic sites. The areas under these peaks give information about the amount of acidic sites of different acidity whereas, the peak (– maximum –) temperatures give information about the relative acid strengths [28].

1.5 Carbon – Carbon Bond Formation Reactions:

C-C bond formation reactions are the most important reactions in organic synthesis. A few of these are listed in Table 1.3.

Table 1.3: Some important C-C bond formation reactions

Reaction	Typical reactants	Products
Alkylation	Aromatic compounds and alkyl halides / alcohols or olefins	Alkyl aromatics
Acylation	Aromatic compounds and acyl halides / anhydrides or acids	Acyl aromatics / aromatic ketones
Heck	Aryl halide and acrylate	Cinnamic acid derivatives
Suzuki	Alkyl halide and phenyl boronic acid	Diaryl compound
Molecular Rearrangements		
(a) Claisen	Allyl phenyl ether	o-allyl phenol
(b) Fries	Acetophenone	o & p-acyl phenols
(c) Benzidine	Hydrazobenzene	4,4’ diamino biphenyl

(d) Wolff	Acyl halide	carboxylic acid
(e) Cope	1,5 dienes	rearranged diene

Alkylation and acylation of aromatics, coupling of aryl halides with olefins as in Heck reaction or phenyl boronic acid in Suzuki reaction are well known. Homologation of acids in Wolff rearrangement and methylene insertion to aldehydes and ketones with diazomethane are widely used. Rearrangements like Claisen, Benzidine, Cope and Diels–Alder are interesting examples of sigmatropic reactions. Dienone-phenol and Di-π methane rearrangements, and cyclization reactions like Fischer indole synthesis are also C-C bond formation reactions. Inrecent times some of these reactions have been reported to be catalyzed by zeolites. Some of the important C-C bond formation reactions are discussed in detail in this section.

1.5.1 Alkylation of aromatics:

Alkylation of an aromatic substrate is an electrophilic substitution reaction, where the electrophile is a carbocation from an alkyl halide, alcohol or an olefin often generated with the help of an acid catalyst. The essential feature of the reaction is the replacement of a

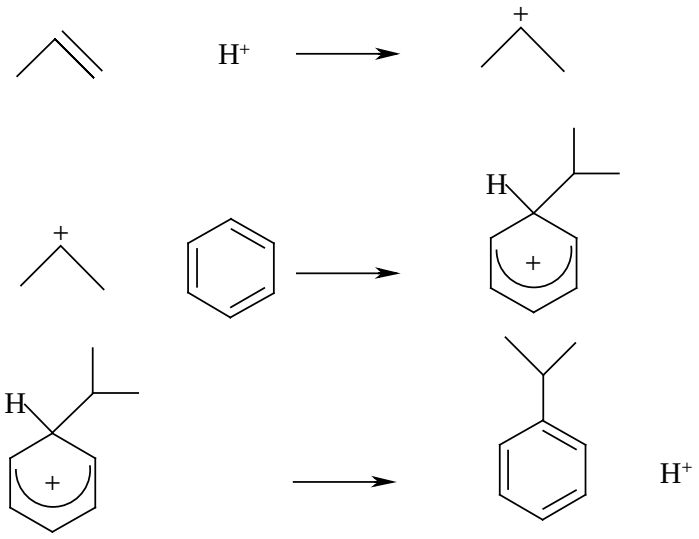

Scheme 1.1: Mechanism of a typical alkylation reaction

hydrogen atom of an aromatic compound by an alkyl group derived from an alkylating agent (Scheme 1.1). In catalysis by solid acids, the intermediate carbocation is generated with the help of acid sites on the catalyst surface.

In view of the great theoretical and practical interest in alkylation, several review articles that provide valuable information on both mechanistic and synthetic issues have been published [29-34].

1.5.2 Alkylation of phenol:

Alkylated phenols are important intermediates in the chemical industry for a great variety of products. These include pharmaceuticals, dyes and antioxidants. The major markets are nonionic detergents, phenolic resins, polymer additives, agrochemicals [35,36] and lubricating oils. Alkyl phenols containing 3-12 carbon alkyl groups are obtained by alkylating phenol with the corresponding alkene using acid catalysts. Conventional catalysts are sulphuric acid, phosphoric acid, activated montmorillonite clay, boron trifluoride and aluminium chloride.

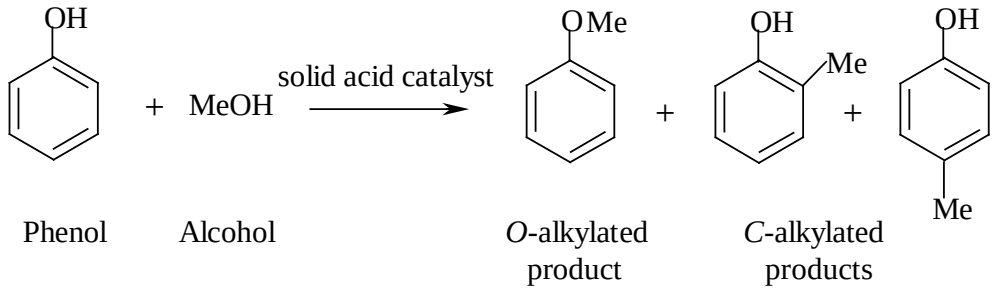

Scheme 1.2: Phenol alkylation with alcohol over zeolite catalysts

Alkylation of phenol over different zeolites using several alkylating agents, including alcohols, dimethyl carbonate [37,38], alkyl and allyl halides [39], aldehydes [40], ketones [41,42], olefins [43,44] and cyclo olefins[45-46] has been extensively studied. The most common alkylating agents are methanol [47], isopropanol [48], propylene [49], t-butanol [50] and butenes [51]. Alkylation of phenol using methanol has been reported over H-ZSM-5, H-Y, H-beta, H-mordenite, H-MCM-22 [52]. The selectivity towards o-cresol, p-cresol and anisole depends on reaction conditions. In the alkylation of phenol with methanol [47a], the *O*-alkylated product, anisole, was found to be the major and kinetically favoured product along with the *C*-alkylated products (o- and p-cresol; Scheme 1.2). The formation of the *C*-alkylated products was found to be dependent on reaction conditions like temperature and acidity of the catalyst, *C*-alkylation requiring stronger acid sites than *O*-alkylation. It was observed that in phenol methylation over medium pore zeolites, the reaction network was entirely determined by the available intracrystal space and that restricted transition state selectivity played a dominant role. The t-butylation of phenol with isobutene [53,54] or with t-butyl alcohol [55-57] over zeolites H-beta [58,62], H Y [59], H-mordenite [60] have been reported in vapour phase conditions to produce p-t-butyl phenol (p-TBP), o-t-butyl phenol (o-TBP) and 2,4-di-tert-butyl phenol (2,4-DTBP) [58,62]. Zeolite X, alkali loaded zeolite X and SAPO-11 have also been investigated as catalysts for the reaction [61,62]. The product distribution depends on the acidity of the zeolite and reaction conditions. The alkylation of phenol using isobutene in three phase conditions has been reported over H-beta [63]. Phenol alkylation with long chain olefins like hexene [64], octene [65,66], nonene [65,67], 1-decene [65,67], 1-dodecene [68,69] and other long chain olefins [70-72] and long chain alcohols [72] has also been reported. The alkylation of phenol with 1-hexene over modified natural aluminosilicates led to the formation of o- and p-(2-hexyl phenol), the ortho isomer being the predominant product. In the study of o-

alkylation of phenol with 1-dodecene in presence of aluminium oxide, the maximum yield was 66.7 % at a mol ratio of phenol: dodecene = 2:1. it is suggested that the alkylation reaction was found to take place on the Lewis acid sites of the catalyst [68]. The use of BF_3-etherate as a homogeneous catalyst has been reported for the alkylation of phenol with 1- and 2-octene in the absence of a solvent by Sonavane et al. [73]. The use of zeolites [74-76] and mesoporous materials [77,78] in the alkylation of phenol has been studied by several research groups.

1.5.3 Alkylation of naphthalene:

Isopropylation of naphthalene to produce 2,6-dialkylated naphthalene (2,6-DIPN) is a commercially important reaction. The product is an intermediate in the making of advanced polymeric materials and liquid crystalline polymers (Scheme 1.3). Alkylation of naphthalene has been widely studied by several groups over different zeolites [79-85] and mesoporous catalysts [86,87]. Pu et al. [87] studied the reaction over Al-MCM-48 and Al-MCM-41. Al-MCM-48 possessed a higher activity due to its larger pore size and three dimensional pore system, which are more advantageous for molecular diffusion than the relatively narrow and one dimensional pore system of Al-MCM-41.

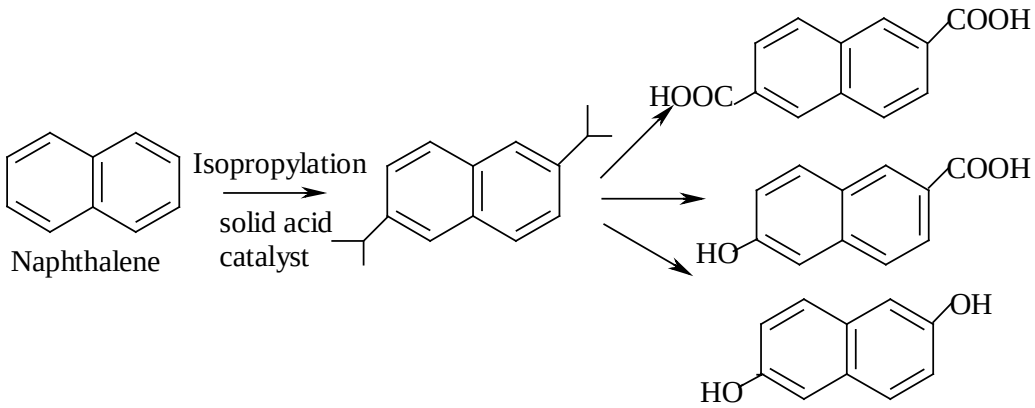

Scheme1.3: Conversion of naphthalene to 2,6-diisopropyl naphthalene (2,6-DIPN) and derivatives

Isopropylation of naphthalene has been studied in both liquid [88-90] and gas phases [91,92] over zeolite catalysts with the aim of achieving high yields of 2,6-DIPN. Different alkylating agents like isopropanol [90], propene and isopropyl bromide have been used for alkylation. Song and Kirby [90] reported that the 2,6- / 2,7-DIPN ratio is dependent on the alkylating agent used. Several research groups [89,90] have reported that 2,6 DIPN can be obtained with high selectivities over H-mordenite by the alkylation of naphthalene with propene and iso-propanol. Also, dealumination of mordenite [86,93,94] caused an improvement in selectivity towards the desired product. This may be attributed to reduced contribution of external acid sites and the reduction of the unit cell dimensions [95]. Schmitz et al. [93] have optimized the reaction conditions for 2,6-DIPN formation (over mordenites) using propene as alkylating agent. The naphthalene/ catalyst ratio was found to be important for product selectivity, a ratio of 10 being most suitable for 2,6-DIPN formation at 473 K. Also, longer reaction times favoured an increase in conversion and 2,6-DIPN yield. Poisoning of the external acid sites by silylation [88], by adsorption of water [96] and deposition of cerium oxide [89,97,98] was found to enhance the selectivity of H-mordenite for the formation of 2,6-DIPN. The impregnation of cerium followed by calcination led to the deactivation of the external acid sites without a decrease in the pore radius. The deactivation reduced non-regioselective alkylation and isomerization thereby increasing the selectivity for the desired 2,6-DIPN.

1.5.4 Acylation of aromatics:

Acylation reactions are also electrophilic aromatic substitution reactions in which an electrophile is generated from an acyl halide [99], anhydride [100], carboxylic acid [101] or an α, β unsaturated organic acid [102]. Friedel-Crafts acylation is a convenient route for the preparation of aromatic ketones [102,103] (Scheme 1.4).

The most commonly used aromatics in acylation reactions are benzene, toluene, xylene, phenol [104], naphthalene [105], 1-naphthol [106], 2-methoxynaphthalene [107], anisole and veratrol [108]. There are reports of the use of zeolites [101,109], heteropoly acids [102,110], cation-exchanged montmorillonite [111], phosphotungstic acid [112], cesium substituted dodecatungstophosphoric acid [113], superacids [114], scandium triflate [115], hafnium triflate [116], sulfated zirconia [117], ytterbium (III) methide [118] microwave modified $ZnCl_2$/ H-Y [119], zeolites treated with silane [120], pentasil type zeolites [121], and rare earth exchanged zeolites [109] as catalysts for acylation reactions.

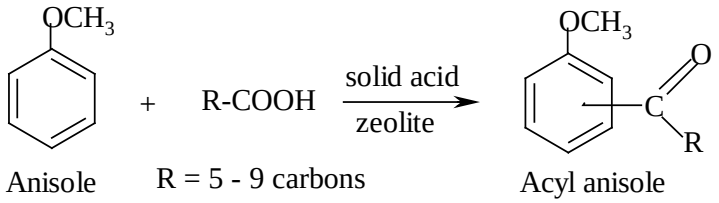

Scheme 1.4: Acylation of anisole over zeolites

The use of zeolites eliminates the problems associated with the classical Friedel-Crafts catalysts namely, poor selectivity for the products, use of more than stiociometric amount of catalysts and destruction of the catalyst during work-up. The use of acyl halides and anhydrides is widely reported in the study of acylation of aromatics over zeolite catalysts. However, there are only a few reports on the use of alkanoic acids as acylating reagents.

1.5.5 Rearrangement of allyl aryl ethers over zeolites (Claisen Rearrangement):

Claisen rearrangement involves the conversion of allyl phenyl ethers to o-allyl phenols at elevated temperatures of about 473K. The reaction has, however, been reported to be catalysed by Lewis and Brönsted acids [122,123]. In the presence of acid catalysts, the o-allyl phenols further undergo cyclization to form dihydrobenzofuran derivatives (Scheme

1.5). The reaction, therefore, presents an attractive route to the synthesis of benzofuran derivatives from substituted allyl aryl ethers [124]. Similarly S and N containing heterocycles are obtained with thio-Claisen [125] and amino-Claisen [126] rearrangements, respectively.

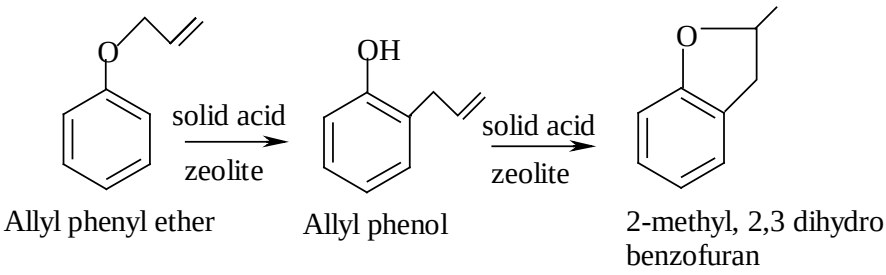

Scheme 1.5: Claisen rearrangement of allyl phenyl ether over zeolites

Reports on the use of solid acids in Claisen rearrangement are rather scarce. Pitchumani et al. have observed shape selectivity in ZSM-5 and ZSM-11 during their study of photo assisted Claisen rearrangement [127]. Sheldon et al. have investigated the use of H-FAU and H-MOR in the rearrangement of allyl phenyl ether in benzene medium [128,129]. The reaction was accompanied by the formation of dimers and oligomers, which could be suppressed by triphenylphosphine treatment of the catalysts. This treatment led to enhanced selectivities for the Claisen products in the case of H-BEA. Other solid acid catalysts that have been investigated are mesoporous silica [130] and bentonite [131]. The response to solvents and substituents was investigated by Joseph Gajewski [132]. The use of homogeneous catalysts like $Mo(CO)_6$ [133] gave good yields of both Claisen and cyclized products. Cyclopalladated amine [134] was found to be a better catalyst for non-activated allyl imidate. $SnCl_4$ catalyzed Cope and Claisen rearrangements of N-allylanilines and N-allylenamines [135] readily give 2-allyl aniline as the Claisen product. $Cu(OTf)_2$ and $Yb(OTF)_3$ catalysts have been reported for the rearrangement of 2-alkoxycarbonyl

substituted allyl vinyl ethers [136]. Pd catalysts were reported [137] to be good for Cope, Claisen and other 3,3 sigmatropic rearrangements. $ZnCl_2$ [138], organo-Al [130], $TiCl_4$ [139], lithium perchlorate [140], and Pd and Ni have been reported to be good catalysts for thio-Claisen rearrangement [141,147]. Also, the use of a three component system, $Ru_3(CO)_{12}$ / imidazolinium salt / Cs_2CO_3 [142] and a low molecular weight polyethylene [143] have been reported for the Claisen rearrangement of allyl homoallyl and diallyl ethers. Secondary deuterium isotope effects and transition state structure in aromatic claisen rearrangement (non-catalytic) indicate that the reaction has a concerted transition state in which bond making and breaking, have proceeded to major extents [144]. Other probe methods are discussed by Kunkeler et al. [145,146].

1.5.6 Coupling of alkyl halides with olefins (Heck Reaction):

Heck reaction was discovered by R. F. Heck in 1973. The reaction involves the coupling of an alkyl halide with an olefin (acrylates/ styrene) using palladium complexes as catalysts to form cinnamic acid derivatives (Scheme 1.6). These derivatives are industrially important as UV absorbers, antioxidants in plastics and intermediates in pharmaceuticals, agrochemicals and fragrances. Heck reaction is an excellent tool for the synthesis of numerous styrene derivatives due to its tolerence for a wide variety of functional groups on both reactants [148]. Suzuki coupling is also a Pd catalyzed C-C bond formation reaction involving aryl boronic acid and aryl halide / diazonium salt or triflate to produce a biaryl.

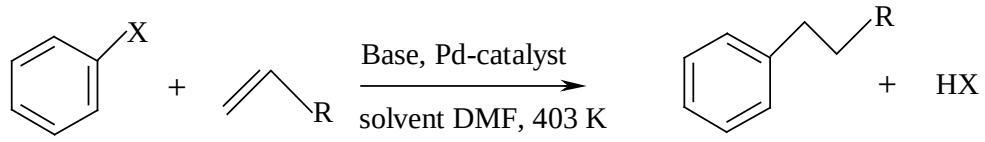

X = I, Br, Cl R = Ph, -COOEt (Et or any alkyl group)

Coupling product

Scheme 1.6: Typical example of a Heck reaction

The use of homogeneous Pd catalysts for Heck coupling is well established [148,149]. In order to overcome the problems arising from separation, recovery and reuse of Pd complexes [150], a variety of heterogeneous catalysts [150-152] have been investigated for the Heck reaction. These include Pd supported on carbon, different metal oxides [153,154], clays mesoporous silica, zeolites [155, 156] and Pd nanoparticles [157]. The use of Cu, Ni, Co and Mn heterogeneous catalysts is also known [158]. However, only a few references are available on the use of metal supported basic catalysts for the Heck reaction [156,159].

1.6 Objectives and Scope of the Thesis:

It is evident from the literature survey on zeolites and microporous materials that these materials have opened new opportunities in organic synthesis and production of fine chemicals. The objective of the present work is to study some important C-C bond formation reactions, typically used in synthesis of fine chemicals, over the large pore acidic zeolites H-FAU, H-BEA and H-MOR. The influence of dealumination of zeolites on their acidity and catalytic activity will be investigated. Additionally, a large pore microporous zeolite-like material, ETS-10, with basic properties will be used as support for Pd in the Heck reaction.

The use of solid acids has become a prominent feature in the alkylation of aromatics. The alkylation of phenol has been reported over different catalysts with alcohols, allyl and alkyl halides and olefins. Phenol alkylation with olefins is commonly carried out in the vapour phase. Reports on the alkylation of phenol in the liquid phase with long chain olefins are less common. Octyl, nonyl and decyl phenols are widely used in detergents as surfactants. Hence, an investigation of phenol alkylation in the liquid phase using long chain olefins will be carried out. Investigations on the effect of temperature, mole ratio, different

zeolites, catalyst amount and poisoning of the catalyst is to be done. A study of the thermodynamics and kinetics of the reaction has also been done.

Shape selective isopropylation of naphthalene has been extensively investigated by earlier workers in the presence of organic solvents. The present work has been undertaken to study the isopropylation of naphthalene on different zeolites in the absence of organic solvents. The isopropylation of naphthalene in the absence of an organic solvent is of interest as it reduces load on down stream separation [83,84]. The influence of reaction parameters will be studied and the activity of different zeolites compared.

Friedel-Crafts acylation is an important C-C bond formation reaction and a convenient route for the preparation of aromatic ketones [102,103] that are useful as reactive intermediates in the production of pharmaceuticals, perfumes, dyes, insecticides and other fine chemicals. The use of acyl halides and anhydrides has been widely reported in the acylation of aromatics over zeolite catalysts. However, there are only a few reports of the use of alkanoic acids as acylating reagents. The use of long chain carboxylic acids as acylating reagents in the acylation of anisole over zeolite catalysts will be investigated in this work. The influence of reaction parameters such as mole ratio, temperature effect, catalyst amount and different zeolite catalysts will also be studied.

Claisen rearrangement is well known as a thermal reaction. However, Sheldon et al. have reported the use of zeolites as catalysts [128,129] with benzene as the medium for the rearrangement. A detailed study of the rearrangement will be carried out in the presence of different solvents at different temperatures and catalyst amounts over different zeolites and dealuminated zeolites. Rearrangement of other ethers such as, allyl cresyl ethers and the diallyl ether of hydroquinone will also be investigated. A kinetic analysis of the rearrangement presents will be carried out to understand the reaction better.

The coupling of an alkyl halide with an olefin to form cinnamic acid or its derivative is well known as the Heck reaction. The use of homogeneous catalysts, typically Pd complexes has been well established for this reaction. To overcome the problems of separation and recovery, palladium loaded on a variety of solid supports has been reported. However, very few references are available on the use of metal supported basic catalysts for the Heck reaction [156,159]. Therefore, the use of Pd supported on the novel basic ETS-10 molecular sieve as a catalyst for the Heck reaction will be investigated. The study will focus on the carbon – carbon coupling of different aryl halides with ethyl acrylate over Pd-ETS-10. The influence of Pd content, nature of the base and reactivity of different substrates and reactants are to be examined.

1.7 Outline of the Thesis:

The thesis is divided into seven chapters:

Chapter I: Introduction

Chapter 1 presents a general introduction to the importance and wide application of the environmentally friendly solid acid catalysts, zeolites, in C-C bond formation reactions. A general introduction to zeolites and their structure is presented. The most important characteristic of zeolites is that their properties can be tailored according to the requirement. The modification of zeolites is therefore discussed. The properties of some commercially important zeolites, their characterization and the role of zeolites in catalysis are summarized. A number of C-C bond forming reactions, such as alkylation, acylation, Claisen rearrangement and Heck reaction are discussed. The application of solid acids, especially micro and mesoprous materials in the above reactions is presented.

Chapter II: Materials, Methods and Physicochemical Characterization

This chapter contains a description of the materials and experimental setup used and methodology adopted in this work. The first part of the chapter presents information about

the zeolites used in this study, their modification by ion exchange and dealumination and their chemical analysis. Information about other chemicals, especially the synthesis of the substrates is also presented. The experimental techniques used in the catalytic reaction studies and product analysis are described. The second part presents the different characterization techniques used to evaluate the structural, textural and acidic properties of the catalysts. The methodology used in the kinetic analysis of the reactions is also presented at the end.

The dealumination of zeolites H-BEA and H-MOR was carried out to prepare samples with different Si/Al ratios. H-FAU samples with different Si/Al ratios were obtained from commercial sources. The zeolite samples were used in different C-C bond formation reactions.

The parent zeolite samples and the dealuminated forms were characterized by X-ray diffraction (XRD), N_2 sorption studies for the determination of surface area and temperature programmed desorption of NH_3 to determine the acidity of the different zeolites. ^{27}Al MAS NMR was used to study the nature of Al in the samples and X-ray fluorescence analysis was used to determine the aluminium and silicon content in the samples. The results of the characterization studies are reported and discussed.

The catalytic reactions were carried out in a round bottomed flask fitted with a water cooled reflux condenser under N_2 atmosphere or in a Parr autoclave in the presence of N_2.

The chapter also discusses the application of reaction kinetics to analyze the experimental results of the alkylation of phenol with 1-octene, Claisen rearrangement of allyl phenyl ethers and the acylation of anisole. The rate equations that have been set up for the reactions to derive the rate constants for the various steps are described. The reactions have been analyzed as first (or second) order parallel and series reactions.

Chapter III: Alkylation of Phenol and Naphthalene

This chapter is divided into two sections. The liquid phase alkylation of phenol with 1-octene over wide pore zeolites reported in section A of this chapter. The shape-selective isopropylation of naphthalene with i-propanol is presented in section B.

Chapter 3-A: The reaction between phenol and 1-octene affords oxygen alkylated (*O*-alkylated) and carbon alkylated (*C*-alkylated) products. These are formed simultaneously and contain isomeric (2-, 3- and 4-) octyl phenyl ethers (*O*-alkylates) and octyl phenols (*C*-alkylates). The relative activity of the zeolites for the reaction, in terms of phenol conversion is given as H-BEA > USHY (FAU) > H-MOR. H-BEA and H-MOR favor *C*-alkylate formation. On USHY, *O*-alkylates are formed preferentially compared to *C*-alkylates.

The influence of process variables such as temperature, mole ratio of reactants, catalyst concentration, poisoning of the catalyst and duration of run have been investigated. The kinetics of the reaction was examined assuming second order series and parallel reactions.

Chapter 3-B: The reaction has been carried out at different pressures in the presence of nitrogen and in the absence of organic solvents. The influence of reaction parameters has been studied and the activity of different zeolites has been compared. A comparison of the activity of HY (FAU), REY, H-BEA and H-MOR in the isopropylation of naphthalene with isopropanol shows that H-BEA is the most active and H-MOR is the most shape selective. A comparison of the reaction in cyclohexane, N_2 and without any medium shows that the reaction proceeds better in N_2 with higher activity and selectivity.

Chapter IV: Acylation of Aromatics

The present study reports the use of the long chain carboxylic acids (hexanoic, octanoic and decanoic) as acylating reagents in the acylation of anisole over zeolite

catalysts. Reaction parameters such as mole ratio, temperature and catalyst amount have been investigated. The reaction kinetics has been analyzed as a pseudo-first order reaction.

Chapter V: Rearrangement of Allyl Aryl Ethers

This chapter presents the studies on the rearrangement of allyl aryl ether over zeolite catalysts. The Claisen rearrangement of allyl phenyl ether (APE) to o-allyl phenol was investigated over zeolite beta with different Si/Al ratios. Over the zeolite catalyst, the product of the rearrangement of the allyl phenol cyclized to produce 2,3-dihydro-2-methyl benzofuran. The influence of the reaction temperature and catalyst Si/Al ratio on the reaction was examined by a kinetic analysis. Also, a study of the effect of solvents was carried out. The intermediate allyl phenol reacted with aromatic solvents to produce byproducts. Assuming a first order consecutive reaction, detailed kinetic analysis of the formation of the products is presented. The rearrangement of the isomeric allyl cresyl ethers and the diallyl ether of hydroquinone was also investigated over zeolite beta. The rearrangement was also carried out over the other large pore zeolites, mordenite and faujasite, with different Si/Al ratios.

Chapter VI: Heck Reaction of Aryl Halides with Olefinic Compounds

This chapter describes the use of palladium loaded ETS-10 catalyst for the Heck reaction. The carbon – carbon coupling of different aryl halides with ethyl acrylate over Pd-ETS-10 in the presence of a basic compound was carried out. The influence of Pd content, nature of the base and reactivity of different substrates and reactants was examined.

Pd-ETS-10 (reduced in H_2) exhibits a high activity towards the Heck coupling of aryl iodides and bromides with acrylates, under typical reaction conditions. A TON value of ~ 10,000 is achieved for a 0.2 wt % Pd-ETS-10 catalyst. Organic bases lead to higher catalytic activity than inorganic bases and electron withdrawing substituents enhance the reactivity of the aryl halides.

Chapter VII: Summary and Conclusions.

This chapter presents the overall summary of the work done and describes the major findings of the studies.

1.8 References:

1. R. Szostak, "Molecular Sieves: Principles of Synthesis and Identification" Van Nostrand Reinhold, New York (1989).
2. A. F. Cronstedt, Svenska Vetenskaps Akademiens Handlinger, Stockholm, 17 (1956) 120.
3. D.W. Breck, "Zeolite Molecular Chemistry: Structure, Chemistry and Use" Wiley , London (1974).
4. W.H. Meier and D.H. Olson, "Atlas of Zeolite Structure Types", Butterworths-Heinemann, Boston, MA, 3rd eds. (1992).
5. W.L. Bragg, "The Atomic Structure of Minerals", Cornell University press, Ithaca, New York (1937).
6. R.M. Barrer, "Hydrothermal Chemistry of Zeolites", Academic press, New York, (1982).
7. W.H. Meier, "Molecular Sieves", Society of Chem. Ind., London 10, (1968).
8. E.M. Flanigen, "Proceedings of the 5th Int. Conf. On Zeolites," L.V.C Rees (eds.) Naples, Italy, June 2-6, (1980) 760.
9. R.J. Argauer, G.R. Landolt, US Patent 3702886 (1972).
10. B.M. Lok, T.R. Cannan, C.A. Messina, Zeolites 3 (1983) 282.
11. C.J. Plank, E.J. Rosinski, M. K. Rubin, US Patent 4175114 (1979).

12. R.W. Grose, E.M. Flanigen, US Patent 4257885 (1981).

13. W.J. Bale, D.G. Stewart, Eur. Pat. Appl. 30811 (1981).

14. R.L. Wadlinger, G.T. Kerr, E.J. Rosinski, US Pat 3308069 (1967).

15. (a) H. Tsuji, F. Yagi, H. Hattori, and K.Kita, "Proceedings of 10th Int Cong. on Catalaysis", L. Guczi, F. Solymosi and P. Tetenyi (eds). Akademiai Kiado, Budapest, (1993) 1171.

16. A. Kozlov, K. Asakura, Y. Iwasawa, Micropor. and Mesopor. Mater. 21, (1998) 571. (a) S.M. Kuznicki, U.S. Patent 5011591 (1991)

17. J.L. Guth and H. Kessler, "Catalysis and Zeolites: Fundamentals and Applications" J. Weitkamp. L. Puppe (eds.) Springer-Vergag, Heidelberg, New York.

18. K.J. Balkus Jr., A.K. Khanmamsedova, K.M. Dixonand, F. Bediou, Appl. Catal. A. 143 (1996) 159.

19. P.A. Jacobs, "Characterization of Heterogeneous Catalysts" F. Delannay (eds), Marcel Dekker, Inc. (1984) pg 367.

20. S. Brunauer, P.H. Emmett and E. Teller, J. Am. Chem. Soc., 60 (1938) 309.

21. A. Bell and A. Pines, "NMR Techniques in Catalysis" Heinemann eds., Marcel Dekker, Inc. (1994).

22. A. Thangaraj, R. Kumar, S.P. Mirajkar and P. Ratnasamy, J. Catal., 130 (1991) 1.

23. (a) A.L. Companion, R.E. Wyatt, J. Phys. Chem. Solid, 24 (1993) 1025.

(b) R.J.H. Clark, "Chemistry of Titanium and Vanadium", Elesevier, Amsterdam, (1968) 272,

24. M.R. Boccuti, K.M. Rao, A. Zecchina, G. Leofanti and G. Petrini, "Structure and Reactivity of Surfaces", Stud. Surf. Sci. Catal., 48 (1989) 133.

25. G.K. Hellmut, H. Michael, K.B. Hermann, "Catalysis and Zeolites: Fundamentals

and Applications" J. Weitkamp. L. Puppe (eds) Springer-Verlag, Heidelberg, New York (1999).

26. (a) J.C. Vedrine, "Characterization of Heterogeneous Catalysts" (F. Delannay) Marcel Dekker, Inc. (1984) p.161; C. Defosse, "Characterization of Heterogeneous Catalysts" F. Delannay) Marcel Dekker, Inc. (1984) p.225; F. Delannay and B. Delmon, "Characterization of Heterogeneous Catalysts" (F. Delannay) Marcel Dekker, Inc. (1984) p. 22. (b) B.D. Cullity, "Elements of X-Ray Diffraction", Addison-Wesley, Reading, Mass., (1956).

27. A. Satsuma, Y. Kamiya, Y. Westi, T. Hattori, Appl. Catal. A., 194 (2000) 253.

28. (a) H. Sato, Catal. Rev- Sci. Engg., 39 (1997) 395. (b) A. Alberti, Zeolites 19, (1997), 411. (b) G. Bagnasco, J. Catal., 159 (1996) 249. (c) L. Froni, F.P. Vatti, E. Ortoleva, Micropor. Mater. 3 (1995) 367.

29. G.A.Olah (eds.), "Friedel-Crafts and Related Reactions", Interscience Publishers, New York, (1963).

30. G.A.Olah (eds), "Friedel- Crafts Chemistry", Wiley, New York, (1973).

31. H. Pines, "The Chemistry of Catalytic Hydrocarbon Conversions", Academic Press, New York, (1981).

32. W. Keim, M. Röper, *Ullmann's Encylc. Ind. Chem.* 5th ed., VCH, Weinheim, Vol. A1 (1985) 185.

33. *Kirk-Othmer, Encyclopedia of Chemical Technology*, 4th eds., Wiley, New York (1991).

34. P.B. Venuto, Micropor. Mater., 2, (1994), 297.

35. J.F. Loreuc, G. Lambeth, W. Scheffer in *Kirk-Othmer, Encyclopedia of Chemical Technology*, 4th eds., Vol. 2 (1992) 113.

36. W.Keim, *Ullmann's Encylc. Ind. Chem.* 5th eds., VCH, Weinheim Vol. A1 (1985)

197; (b) H.Fiege, *Ullmann's Encylc. Ind. Chem.* 5th eds., VCH, Weinheim Vol. A8 (1987) 25; (c) H. Fiege, H.W. vogels, T. Haucamote, T, Imai, H. Miki, Y. Fujita, H.J. Buysch, D. Garbe, W. Paulus in *Ullmann's Encylc. Ind. Chem.* 5th eds., VCH, Weinheim, Vol. A19 (1991) 313.

37. F.M. Bautista, J.M. Campelo, A. Garcia, D. Luna, J.M. Marinas, A.A. Romero, React. Kinet. Catal. Lett., 63 (1998) 261.

38. M. Yamamoto, T. Mizuno, M. Okihama, Jpn. Kokai. Tokkyo Koho JP 09010597 A2 (1997). C. A. 126:173355.

39. K.Smith, G.M. Pollaud, I. Matthews, Green chem., 1 (1999), 75.

40. J. Tateiwa, E. Hayama, T. Nishimura, S. Uuemura, J. Chem. Soc., Perkin Trans., 1 (1997) 1923.

41. Y. Haseba, K. Miyazawa, H. Takeuchi, J. Tateiwa, S. Uemura, JP 97-105293 (1997). C.A. 129: 316032.

42. T.Nishimura, S. Ohtaka, A. Kimura, E. Hayama, Y. Haseba, H. Takeuchi, S. Uemura, Appl. Catal. A., 194 (2000) 415.

43. I.T. Golubchenko, Dopov. Akad. Nauk Ukr. RSR, Ser.B: Geol., Khim. Biol. Nauki, 10 (1980) 42. CA 94:139374.

44. A.V. Zorina, Yu. I. Michurov, F.B. Gershanov, G.I. Rutman, A.V. Kuchin, V.P. Yur'ev, Zh. Obshch. Khim., 50 (1980) 581; C.A. 93: 167785.

45. V.V. Fomenko, D.V. Korchagina, N.F. Salakhutdinov, I. Bagryanskaya, Yu.V Gatilov, K.G. Ione, V.A. Barkhash, Russ. J. Org. Chem., 36 (2000) 539.

46. A.E. Drabkin, A.S. Fedotov, N.F. Fedotova, Zh.Prikl.Khim. 53 (1980) 888. C.A. 93:167782. (a) R. Anand, K.U. Gore, B.S. Rao, Catal. Lett., 81 (2002) 33.

47. S. Namba, T. Yashima, Y. Itaba, N. Hara, Stud. Surf. Sci. Catal., 5 (1980) 105. (a) R. F. Parton, J. M. Jacobs, D. R. Huybrechts and P. A. Jacobs, Stud. Surf. Sci.

Catal., 46 (1988) 163.

48. S. Sato, R. Takahashi, T. Sodesawa, K. Matsumoto, Y. Kamimura, J. Catal. 184 (1999) 180.

49. Bo Wang, Wee Chul, Tian-Xi Park, Sang-Eon, Stud. Surf. Sci. Catal., 135 (2001) 4121.

50. S. Subramanian, A. Mitra, C.V.V. Satyanarayana, D. K. Chakrabarty, Appl. Catal. A., 159 (1997) 229.

51. M.Yamamoto, T. Mizuno, M. Okihama, Jpn. Kokai Tokkyo Koho JP 09010597 A2 (1997). C. A. 126: 173355.

52. G. Moon, K.P. Moellr, W. Boehringer, C. T. O' Connor, Stud. Surf. Sci. Catal., 135 (2001) 4598.

53. L. Pan, A. Zhang, Shiyou Huagong, 25 (1996) 761. C.A. 126: 30972.

54. H. Alfs, G. Boehm, H. Steiner, Ger. Offen. DE 2745589 (1979) 12. C.A. 91: 56613.

55. S. Han, K. Zhang, Huaxue Gongye Yu Gongcheng, 16 (1999) 367. C. A. 133: 254175.

56. K. Zhang, H. Zhang, G. Xu, S. Xiang, S. Lui, D. Xu, H. Li, Appl. Catal. A., 207 (2001) 183.

57. A.V. Krishnan, K.Ojha, N.C. Pradhan, Org. Proc. Res. and Develop. 6 (2002) 132.

58. R. Zhu, X. Tang, A. Zhang, L. Pan, Ranliao Huaxue Xuebao, 27 (1999) 225. C. A. 132: 24095.

59. (a) K. Zhang, F. He, X. Genhui, Chemical Industries (Dekker), 82, "Catalysis of Organic Reactions", (2001) 193.

60. K. Zhang, S. Xiang, H. Zhang, G. Xu, S. Lui, D. Xu, H. Li, React. Kinet. Catal.

Lett., 77 (2002) 13.

61. S. Lee, Si Woo Lee, Ki Seok Kim, T. J. Lee, H. Dong, J.C. Kim, Catal.Today, 44 (1998) 253. (a) S. Subramanian, A. Mitra, C.V.V. Satyanarayana, D. K. Chakrabarty, Appl. Catal. A., 159 (1997) 229.

62. K. Zhang, C. Huang, H. Zhang, S. Xiang, S. Lui, D. Xu, H. Li, Appl. Catal. A., 166 (1998) 89.

63. L. Pan, A. Zhang, Shiyou Huagong, 25 (1996) 761; C.A. 126: 30972.

64. Kh.I. Areshidze, G.O. Chivadze, M.V. Kurashev, V.V. Khakhnelide, Neftekhimiya, 19 (1979) 188. C.A. 91: 56524.

65. V. Raverdino, P. Sassetti, J. Chromatgr., 153 (1978) 181. C.A. 89: 108442.

66. I.I. Namazov, N.G. Abdullaev, R.G. Rzaev, A.T. Panina, Azerb.Neft. Khoz., 7 (1976) 59. C. A. 86: 139540.

67. K.D. Korenev, P. S. Belov, A.S. Zavadoskaya, P.P. Kapustin, G. I. Kozyreva, E.A. Uvarova, V. A. Zavorotnyi, Khim. Tekhnol.Topl. Masel, 8 (1987) 17.

68. I.T. Golubchenko, V.G. Motornyi, O.I. Gaponenko, I. A. Manza, P. N. Galich, Neftepererab. Neftekhim. 19 (1980) 19; C.A. 95:61637.

69. P.M. Galich, Visn. Akad. Nauk. Ukr. RSR., 4 (1989) 15. C.A. 111: 133707.

70. Sh.S Shchegol, E.G. Davtyan, V.N. Danishevskii, A.I. Nagiev, Nefepererab. Neftekhim. 10 (1978) 41. C.A. 90: 192979.

71. N.L. Voloshin, E.V. Lebedev, E.K. Bryanskaya, V.T. Sklyar, N.I. Vykrestyuk, Mater. Resp. Nauchno-Tekh. KOnf. Molodykh Uch. Pererab. Nefti Neftekhim., Vol 2 (1976) 14; C.A. 89: 179638.

72. V.N. Zhdamarova, S.V. Rudenko, O.K. Smirnov, S.G. Potapenko, S.M. Levi, A.D. Kopeina, Tezisy Dokl.-Simp. Sint. Primen. Poverkhn.- Akt. Veshchestv Prom-sti. Kinofotomater., 20 (1977). C.A. 89: 131483.

73. (a) H.R. Sonavane, V.G. Naik, B.C. SubbaRao, Indian J. Chem., 3 (1965) 260. (b) H.R. Sonawane, M.S. Wadia, B. C. Subba Rao, Indian J. Chem., 6 (1968) 72. (c) H.R. Sonawane, M.S. Wadia, B. C. Subba Rao, Indian J. Chem., 6 (1968) 297.

74. S. K. Badamali, A. Sathievel, P. Selvam, Catal. Lett., 65 (2000) 153.

75. X. Li, M. Han, X. Lui, Z. Pei, L. She, Stud. Surf. Sci.Catal., 105 B (Progress in Zeolite and Microporous Materials, Pt. B), (1997) 1157.

76. A. Sathievel, S. K. Badamali, P. Selvam, Micropor. Mesopor. Mater. 39 (2000) 457.

77. A. Sathievel, P. Selvam, Catal.Lett. 72 (2001) 225.

78. R. Bal, B. Tope, S. Sivasanker, J. Mol. Catal. A. Chem., 181 (2002) 161.

79. C. He, Z. Lui, F. Fajula, P. Moreau, Chem. Commun., 18 (1998) 1999.

80. G. Colon, I. Ferino, E. Rombi, P. Magnoux, M. Guisnet, Appl. Catal. A., 168 (1998) 81.

81. J. Wang, J. Park, L. Yong-Ki, W. Chul, J. Catal. 220 (2003) 265.

82. S.J. Chu and Y.W. Chen, Appl. Catal. A., 123 (1995) 51.

83. I. Matthew, S. Mayadevi, S. Sabne, S.A. Pardhy, S. Sivasanker, React. Kinet. Catal. Lett., 74 (2001) 119.

84. I. Matthew, S. Sabne, S. Mayadevi, S.A. Pardhy, S. Sivasanker, Indian J. Chem. Tech. 8 (2001) 469.

85. M. Toba, F. Mizukami, S. Niwa, A. Katayama, G. Takeuchi, S. Mitamura, Prep.-Am. Chem. soc., Div. Pet. Chem., 43 (1998) 278.

86. K.M. Reddy, C. Song, Catal. Today, 31 (1996) 137.

87. S.B. Pu, J.B. Kim, M. Seno, T. Inui, Microporous Mater., 10(1-3), (1997), 25.

88. P. Moreau, A. Finiels, P. Geneste, J. Catal., 136 (1992) 487.

89. Y.Sugi, J.H. Kim, T. Matsuzaki, T. Hanaoka, Y. Kubota, T. Tu, M. Matsumoto, Stud. Surf. Sci. Catal., 84 (1994) 1837.

90. C. Song and S. Kirby, Microporous. Mater., 2 (1994) 467.

91. S.J. Chu and Y.W. Chen, Ind. Eng. Chem. Res. 33 (1994) 3112.

92. S.J. Chu and Y.W. Chen, Appl. Catal. A., 123 (1995) 51.

93. A.D. Schmitz, C. Song, Prep. Pap.- Am. Chem. Soc., Div. Fuel. Chem., 39 (1994) 986.

94. A.D. Schmidtz, C. Song, Catal. Today, 31 (1996) 19.

95 C. Song, A.D. Schmidtz, M. Reddy, Proc. 12th Int. Zeolite Conf., Vol.2, edited by Treacy M M J, Materials Research Soc., Warrendale, Pa, (1999) 1133.

96. A.D. Schmidtz, C. Song, Catal. Lett., 40 (1996) 59.

97. J.H. Kim, Y.Sugi, T. Matsuzaki,T. Hanaoka, Y. Kubota, T. Tu, M. Matsumoto, S. Nakata, A. Kato, Appl. Catal. A., 131 (1995) 15.

98. D. Mravec, J. Chylik, M. Michvocik, M. Hronec, A. Smieskova, P. Hudec, Chem. Papers., 52 (1998) 218.

99. A. Corma, M.J. Climent, H. Garcia, J. Primo, Appl. Catal. A., 49 (1989) 109.

100. U. Freese, F. Heinrich, F. Roessner, Catal. Today. 49 (1999) 237.

101. Y. Ma, Q.L. Wang, W. Jiang, B. Zuo, Appl. Catal. A., 165 (1997) 199.

102. C. De Castro, J. Primo, A. Corma, J. Mol. Catal. A., 134 (1998) 215.

103. G.A. Olah, “Friedel-Craft and Related Reactions”, Vol I-IV, Wiley- Interscience, New York, (1963).

104. E.V. Sobrinho, E. Falabella, S. Aguiar, D. Cardoso, F. Jayat, M. Guisnet, Proc. Int. Zeolite Conf., 12th meeting, 2, (1998), 1463.

105. A. Chatterjee, D. Bhattacharya, T. Iwasaki, T. Ebina, J. Catal., 185 (1999) 23.

106. O. Kobayashi, N. Hashizume, Jpn. Kokai Tokkyo Koho JP 10087549 A2 (1998)

7. C.A. 128: 257234.

107. H.K. Heinichen, W. F. Holderich, J. Catal., 185 (1999) 408.

108. M. Spagnol, L. Gilbert, D. Alby, Ind. Chem. Libr., 8 (1996) 29. C.A. 126: 18590.

109. B. Chiche, A. Finiels, C. Gauthier, P. Geneste, J. Org. Chem., 51 (1986) 2128.

110. J. Kaur, K. Griffin, B. Harrison, I. V. Kozhevnikov, J. Catal., 208 (2002) 448.

111. B. Chiche, A. Finiels, C. Gauthier, P. Geneste, J. Mol. Catal.A., 42 (1987) 229.

112. C. Castro, A. Corma, J. Primo, J. Mol. Catal. A., 177 (2002) 273.

113. G. D. Yadav, N. S. Asthana, V.S. Kamble, J. Catal., 217 (2003) 88

114. K. Arata, H. Nakamura, M. Shouji, Appl. Catal. A., 197 (2000) 213.

115. J.R. Desmurs, S. David, J. C. Bigouraux, FR 2756279 A1 (1998). C.A. 129: 81578.

116. O. Kobayashi, Jpn. Kokai Tokkyo Koho JP 09227442 A2 (1997). C. A. 127: 278063.

117. J. Deutsch, A. Trunschke, D. Mueller, V. Quaschning, E. Kemnitz, H. Lieske, Catal. Lett., 88 (2003) 9.

118. A. G. M. Barrett, N. Bouloc, C. D. Braddock, D. Chadwick, D.A. Henderson, Synlett, 10 (2002) 1653.

119. D. Yin, D. Dulin, Z. Fu, Fenzi Cuihua, 12 (1998) 401. C. A. 130: 182224.

120 M. Morimoto, M.Inohara, Y. Mori, Jpn. Kokai Tokkyo Koho JP 10120612 A2 (1998), 10. C. A. 129: 15965.

121 M.Masahiro, M. Morimoto, Y. Mori, Jpn. Kokai Tokkyo Koho JP 10120613 A2 (1998), 7. C. A. 129: 15964.

122 J. March, “Advanced Organic Chemistry”, 4th eds., Wiley, New York, (1992).

123 R.P. Lutz, Chem. Rev., 84 (1984) 205.

124 K. Pitchumani, M. Warrier, V. Ramamurthy., Res. Chem. Intermediates, 25

(1999) 623.

125 R. Sreekumar, R. Padmakumar, Tetrahedron Lett., 38 (1997) 2413.

126 P.J. Kunkeler, J.A. Elings, R.S. Downing, H. Van Bekkum, Spec.Publ.- R. Soc. Chem., 216 (1998) 7.

127 K. Pitchumani, M. Warrier, V. Ramamurthy., J. Amer. Chem. Soc., 118 (1996) 9428.

128 J.A. Elings, R.S. Downing, R.A. Sheldon, Stud. Surf. Sci. Catal., 94 (1995) 487.

129 R.A. Sheldon, J.A. Elings, S.K. Lee, H.E.B. Lempers, R.S. Downing, J. Mol. Catal. A: 134 (1998) 129.

130 (a) K. Takai, I. Mori, K. Oshima, H. Nozaki, Tertahedron Lett., 22 (1981) 3985. (b) I. Sucholeiki, M.R. Pavia, C.T. Kresge, S.B. McCullen, A. Malek, S. Schram, Mol. Diversity, 3 (1998) 161. C.A. 129: 202736 (1999).

131 R. Cruz-Almanza, F. Perez-Flores, L. Brena, E. Tapia, R. Ojeda, A. Fuentes, J. Heterocycl.Chem., 32 (1995) 219.

132 J. Gajewski, Acc. Chem. Res., 30 (1997) 219.

133 A.M. Bernard, M.T. Cocco, V. Onnis, P.P. Piras, Synthesis, 1 (1997) 41. C.A. 126: 144068.

134 P. Leung, Khim-Hui Ng, Y. Li, Andrew J.P. White, D.J. Williams, Chem. Commun., 23 (1999) 2435.

135 A.G. Mustafin, A.R. Gimadieva, K.A. Tambovtsev, G.A. Tolstikov, I.B. Abdrakhmanov, Russ. J. Org. Chem., 34 (1998) 90. C.A. 130:3647.

136 T.P.Yoon, Vy M. Dong, David W.C. MacMillan, J. Am. Chem. Soc., 121 (1999) 9726.

137 (a) H. Nakamura, Y. Yamamoto, “Handbook of Organopalladium Chemistry for Organic Synthesis”, 2 (2002) 2919. (b) T. Hayashi, A. Yamamoto, Y. Ito, Synth.

Commun., 19 (1989) 2109.

138 T. Hayashi, M.Goto, Nippon Kagaku Kaishi, 7 (1978) 1007. C.A. 89: 128852.

139 M. R. Saidi, Heterocycles, 19 (1982) 1473.

140 P.A. Grieco, J.D. Clark, C.T. Jagoe, J. Am. Chem. Soc., 113 (1991) 5488.

141 D.J. Watson, P.N. Devine, A.I. Meyers, Tetrahedron Lett., 41 (2000) 1363.

142 J. Le Notre, L. Brissieux, D. Semeril, C. Bruneau, P.H. Dixneuf, Chem. Commun., 16 (2002) 1772.

143 K.A. Swiss, R.A. Firestone, J.Org. Chem., 64 (1999) 2158.

144 K.D. McMichael, G.L. Korver, J. Am. Chem. Soc., 103 (1981) 1757.

145 P.J. Kunkeler, J.A. Elings, R.A. Sheldon, H. Van Bekkum, Proc. Int. Zeolite Conf., 3 (1998) 1975.

146 P.J. Kunkeler, D. Moeskops, H. Van Bekkum, Microporous Mater., 11 (1997) 313.

147 L. Wang, B. Li, T. Chen, Q. Jin, J. Wang, S. Tang, D. Ding, Wuji Huaxue Xuebao, 16 (2000) 591. C.A. 133: 334925.

148 R.F. Heck, “Palladium Reagents in Organic Synthesis”, Academic Press, New York, (1985). (a) A. Wali, S.M. Pillai and S. Satish, React. Kinet. Catal. Lett. 60 (1997) 189.

149 (a) B.M. Trost, I. Flemming (eds.), Comprehensive Organic Synthesis, Vol. 4, p. 585 and 833 and references cited therein. (b) A. de Meijiere, F.E. Meyer, Angew. Chem. 106 (1994) 2473, and references cited therein. (c) A.F. Littke, and G. C. Fu, J. Am. Chem. Soc., 123 (2001) 6989. (d) D. Nair, J. T. Scarpello, I. F. J. Vankelecom, L.M. F. D. Santos, L.S. White, R.J. Kloetzing, T. Welton and A.G. Livingston, Green Chem. 4 (2002) 319.

150 I.P. Beletskaya, A. V. Cheprakov, Chem. Rev., 100 (2000) 3009.

151 (a) F.R. Hartley, “Supported Metal Complexes: A New Generation of Catalysts”, Riedel, Dordrecht, (1985). (b) Y.I. Ermakov and L.N. Aezamaskova, Stud. Surf. Sci. Catal. 27 (1986) 459. (c) A. Eisenstadt, “Catalysis of Organic Reactions”, eds. F. E. Hecks, Marcel Dekker, Basel (1988) 415.

152 R.S. Varma, K.P. Naicker and P.J. Liesen, Tetrahedron Lett. 40 (1999) 439.

153 H. Hagiwara, Y. Shimizu, T. Hoshi, T. Suzuki, M. Ando, K. Ohkubo and C. Yokoyama, Tetrahedron Lett. 42 (2001) 4349.

154 F. Zhao, B.M. Bhanage, M. Shirai and M. Arai, Eur. J. Chem., 6 (2000) 843.

155 (a) J. Zhao, R. Zhao, L.Mo, S. Zhao, X. Zheng, J. Mol. Catal A: Chem. 178 (2002) 289. (b) M. Dams, L. Drijkoningen, D. De Vos and P. Jacobs, Chem. Commun., (2002) 1062.

156 (a) K. Kohler, M. Wagner and L. Djakovitch, Catal. Today 66 (2001) 105. (b) A. Corma, H.Garcia, A. Levya, A. Primo, Appl. Catal. A., (2003), in press.

157 M.T. Reetz, E. Westermann, Angew. Chem. Int. Eds. 39 (2000)165.

158 (a) M.V. Rajasekharan and R.V. Chaudhari, Catal. Lett. 41 (1996) 171. (b) S. Iyer, V.V. Thakur, J. Mol. Catal A., 157 (2000) 275.

Chapter 2

Materials, Methods and Physicochemical Characterization

PART 1 : Materials and Methods

2.1 Zeolites and their Modification:

BEA, MOR and FAU:

The H-forms of zeolites beta (BEA), Y (FAU with different Si/Al ratios) and mordenite (MOR) were obtained from PQ Corp., USA. The zeolites were calcined at 723 K for 4h and stored in tightly sealed bottles. XRD patterns of the zeolites matched well with their standard patterns. Compositional analyses of the zeolites were carried out by XRF (Table 2.1).

Table 2.1: Si/Al ratios of the commercial zeolite samples

Zeolite[a]	Si/Al Ratio
BEA(15)	15.0
MOR(11)	11.0
FAU(2.6)	2.6
FAU(6)	6.0
FAU(15)	15.0
FAU(40)	40.0

[a] The number in the parenthesis is the Si/Al ratio of the sample

ETS-10:

The hydrothermal synthesis of ETS-10 using $TiCl_4$ was carried out with a gel of molar composition: 3.70 Na_2O: 0.95 K_2O: TiO_2: 5.70 SiO_2: 171 H_2O following published procedures [1]. After crystallization, the product was filtered, washed, dried at 383 K for 10 h and calcined at 723 K in dry air for 6 h. The ETS-10 molecular sieve used in this study

had the chemical composition, $[Na_{16.6}K_{14.4}(Ti_{16.21}Si_{79.74}O_{208})]$ (by atomic absorption spectroscopy) and a N_2 adsorption (BET) surface area of 460 m^2/g [2].

Pd-loaded ETS-10 was prepared for studying the Heck reaction. Pd (0.2 to 6 wt %) was loaded on the molecular sieve by wet impregnation using a solution of $[Pd(NH_3)_4]Cl_2$ at 353 K. The Pd-loaded samples were dried at 383 K (6h), calcined at 673 K (6h) in air, reduced at 623 K in H_2 for 6h and stored under nitrogen.

REY:

Rare earth exchanged Y zeolite (REY) was prepared from commercial Na-Y (Si/Al = 2.6) (Zeolyst) by ammonium and RE-exchanges. Ammonium exchange was done by stirring the Na-Y powder with a 2 M solution (10 ml / g zeolite) of NH_4NO_3 for 4h at 353 K. The mixture was cooled, the supernatant liquid was decanted and the procedure repeated twice. After the third exchange, the NH_4-zeolite was washed well with deionized water and dried at 383 K. The RE exchange procedure was similar, but a 5 % solution of $RECl_3$ (didymium chloride, supplied by Indian Rare Earths Ltd., Cochin, India; composition: Ce, <2%, Nd, ~ 35%, La / Y ~ 45%, Pr ~ 10% other lanthanides, rest; pH of solution was adjusted to ~ 5.2) was used and two exchanges were carried out on the NH_4-Y. The sample was finally dried (383 K, 6h) and calcined (723 K, 4h). The RE_2O_3 content of the sample was 15 % on dry basis. Surface area (BET) measured by N_2 adsorption was 720 m^2/g. The REY was blended and extruded with alumina (30 %) and calcined at 773 K (6h). The extrudates were sized to 1mm length and activated at 773 K for 4h in air before use.

Dealumination of beta and mordenite:

(a) H-beta (BEA(15) was dealuminated by treating the dried catalyst with HNO_3 (55 %) using 60 g of acid per g of beta. The mixture was heated to 358 K and was kept under magnetic stirring for different periods of time to obtain samples with different Si/ Al ratios.

The dealuminated samples were extensively washed with deionised water and dried at 373 K [3,4]. The Si/Al ratios of the samples are presented in Table 2.3.

(b) Mordenite samples with different Si/Al ratios were also prepared by acid leaching. Aluminium was removed from MOR(11) by refluxing it with 6M hydrochloric acid (4ml per g of MOR) for different time periods. The solution was filtered, washed repeatedly with distilled water followed by dilute ammonia solution (1 %) to remove residual acid. The material was dried at 373 K for two hours and heated at 723 K for four hours to obtain the dealuminated sample. The Si/Al ratios of the samples are presented in Table 2.3.

Poisoning of BEA with alkali metals:

Poisoning of beta with the alkali metals, sodium and potassium was carried out by treating the zeolite (NH_4-BEA) with different quantities of 0.03M solutions of the alkali metal carbonates at 353 K for one hour. The zeolite was then filtered, dried (373 K, 12h) and calcined (773 K, 6h). The alkali metal content was estimated by atomic absorption spectroscopy. The samples contained 0.1 to 0.4 mmol of alkali metal per g (Table 2.5).

2.2 Chemicals and Reagents:

The chemicals and reagents used in the present work are listed in Table 2.2 along with the chemical formula and the source. Their purity as determined by GC is also presented in the table.

Preparation and purification of substrates:

Preparation of isomeric octyl phenols:

The isomeric octyl phenols were obtained by a two step process. First the conversion of octyl alcohol to octyl bromide was carried out followed by reaction with phenol to yield the desired compounds.

Preparation of 2-bromooctane: 2-Bromooctane was prepared by refluxing 2-octyl alcohol in toluene with HBr. In a two-necked RB flask (100 ml) equipped with a magnetic stirrer and Dean Stark apparatus, octyl alcohol (4.0 g) was taken with toluene (30 ml) and then HBr (47%, 10 ml) was added to it. The reaction mixture was refluxed for 6h and the reaction was monitored by TLC. The reaction mixture was then cooled and washed well with sodium hydroxide (6N, 50 ml) and then with HCl (10%, 100ml) followed by distilled water (100 ml). The reaction mixture was then dried over anhydrous sodium sulphate. Toluene was removed by distillation to give 2-bromooctane (yield 4.0 g). A similar procedure was used to prepare 3-bromooctane from 3-octyl alcohol.

Alkylation of phenol with 2-/ 3- bromooctane: Phenol (0.94 g) and 2- (or 3-) octylbromide and acetone (20 ml) were taken in a two-necked RB flask (50 ml) equipped with a magnetic stirrer and refluxed in for 8h. The reaction was monitored by TLC. The TLC showed the presence of products along with unreacted phenol and 2-bromooctane. The reaction mixture was worked up after evaporating acetone and then adding ethyl acetate. The organic layer containing the reaction mixture dissolved in ethyl acetate was washed with sodium hydroxide and water, dried over sodium sulphate and then the ethyl acetate was removed in a rotary evaporator. The product contained both *O*- and *C*- alkylated compounds. These were separated by column chromatography to give pure isomeric *O*- and *C*-alkylated products.

Preparation of allyl phenyl ether:

Allyl phenyl ether was prepared in a round-bottomed flask (250ml) equipped with a magnetic stirrer and a reflux (cold water) condenser. The flask was charged with phenol (5 g) and allyl bromide (6 g) (1:1.5 mole ratio). Acetone was used as the solvent (30 ml). Freshly dried K_2CO_3 (9.5 g) was added and the mixture was stirred for 6 h at reflux temperature. The progress of the reaction was monitored by TLC. The acetone in the

Table 2.2: List of Chemicals and Reagents used in the study

Chemical	Source	Chemical formula	Purity (%)
Phenol	Merck, India	C_6H_5OH	>99
Allyl bromide	Aldrich, U.S.A	CH_2:$CHCH_2Br$	99
o-Cresol	Aldrich, U.S.A	*o*-CH_3 C_6H_4OH	98
m-Cresol	Aldrich, U.S.A	*m*-CH_3 C_6H_4OH	98
p-Cresol	Merck, India	*p*-CH_3 C_6H_4OH	98
1-Octene	Aldrich, U.S.A	$CH_3(CH_2)_5CH$:CH_2	98
Naphthalene	s.d. Fine Chem., India.	$C_{10}H_8$	
Anisole	Merck, India	$C_6H_5OCH_3$	99
Hexanoic acid	s.d. Fine Chem., India.	$CH_3(CH_2)_3CH_2COOH$	98
Octanoic acid	Merck, India	$CH_3(CH_2)_5CH_2COOH$	>99
Decanoic acid	Aldrich, U.S.A	$CH_3(CH_2)_7CH_2COOH$	98
Iodobenzene	Aldrich, U.S.A	C_6H_5I	98
Ethyl acrylate	Aldrich, U.S.A	CH_2:$CHCOOC_2H_5$	99
Tributyl amine	Aldrich, U.S.A	$[CH_3(CH_2)_3]_3N$	98.5
Cyclohexane	Qualigens Fine Chem.	C_6H_{12}	99.5
Propan-2-ol	Merck, India	$(CH_3)_2CHOH$	99
1,2 Dichloroethane	Merck, India	CH_2ClCH_2Cl	99
1,1,2,2Tetrachloroethane	s.d. Fine Chem., India.	$CHCl_2CHCl_2$	98
Benzene	s.d. Fine Chem., India.	C_6H_6	99.7
Toluene	s.d. Fine Chem., India.	$C_6H_5CH_3$	98

reaction mixture was distilled off using a rotary evaporator and the contents of the flaskwere dissolved in ethyl acetate. The potassium carbonate was removed by pouring the reaction mixture in a separating funnel and washing with water. The unreacted phenol was removed by washing the organic layer with 10% sodium hydroxide (100 ml). The reaction mixture was further washed with water and brine solution, and the organic layer was dried over anhydrous sodium sulphate. Further, it was concentrated by evaporating the solvent using a rotary evaporator and purified by column chromatography. The purity and chemical structure were ascertained by GC, GC-MS and GC-IR.

The allyl cresyl ethers were prepared by following a similar procedure.

2.3 Reaction and Product Analysis:

The experimental setup and reaction conditions for all the reactions are presented in this section.

2.3.1 Alkylation of phenol with 1-octene:

The reactions were carried out in a two-necked RB flask (25 ml) using equimolar amounts of phenol and 1- octene (10 mmol each) and 0.2 g of freshly calcined catalysts, in a N_2 atmosphere. Aliquots of the reaction were collected at different time intervals and analyzed by gas chromatography (Varian Star 3400 C_X; capillary column: CP Sil 5CB, 30 m and i.d. 0.05 mm). The reaction products were identified by GC-MS and GC-IR.

2.3.2 Isopropylation of naphthalene:

Isopropylation experiments were carried out in a batch mode in a 300 ml stainless steel Parr autoclave. The catalyst (1g; 1 mm particles) enclosed in a stainless steel wire mesh was attached to the stirrer blades to ensure good contact with the reacting fluids. The reactor was loaded with the required amount of naphthalene and isopropyl alcohol (IPA), and filled with nitrogen to the required pressure. After carrying out the reaction for the desired time, the reactor and its contents were cooled, the product mixture dissolved in

diethyl ether, and analyzed by GC (Perkin-Elmer Auto System XL; column: Ultra 2 (cross linked 5 % PHME siloxane, film thickness: 0.52 µm, length: 25 m, i.d.: 0.32 mm; FID detector). The conversions were calculated based on naphthalene.

2.3.3 Acylation of anisole:

The reactions were carried out in a two-necked RB flask using anisole (0.02 moles) and carboxylic acid (0.005 mmol) with 0.15 g of freshly calcined H-forms of the zeolites as catalysts, in N_2 atmosphere. Aliquots of the reaction were collected at different time intervals and analyzed by gas chromatography (Varian Star 3400 C_X; capillary column: CP Sil 5CB, 30 m and i.d. 0.05 mm). The reaction products were identified by GC-MS and GC-IR. The conversions were calculated based on the acid.

2.3.4 Rearrangement of allyl aryl ether (Claisen rearrangement):

The reactions were carried out under N_2 in a two-necked round-bottomed flask (25ml) equipped with a magnetic stirrer and a reflux (cold water) condenser. The flask was charged with the substrate allyl ether (1.25 mmol) and the solvent (3 g). Freshly calcined catalyst was added and the mixture was stirred for 6 h at the required temperature. The progress of the reaction was monitored by withdrawing samples at different time intervals and analyzing them by gas chromatography (Varian Star 3400 C_X; column: CP Sil 5CB, 30m and i.d. 0.05 mm). The reaction products were identified by GC-MS and GC-IR.

2.3.5 Coupling of aryl halide with olefin (Heck Reaction):

The reactions were carried out in the liquid phase in a 50-ml round-bottomed flask fitted with a reflux condenser. The flask was charged with the substrate (1 mmol), olefin (5.0 mmol), base (typically, tributylamine, (TBA); 2 mmol), solvent (dimethyl formamide, (DMF); 5g) and the catalyst (0.025 g), and placed in an oil bath kept at 403 K. The progress of the reaction was monitored by a gas chromatograph (Varian Star 3400 C_X; column: CP

Sil 5CB, 30m and i.d. 0.05mm). The reaction products were identified by GC-MS and GC-IR. Conversions were calculated based of the substrate (aryl halide).

PART 2 : Catalyst Characterization

2.4 Experimental:

The catalysts were characterized by several characterization techniques. The Si/Al ratios of all the samples were determined by X-ray fluorescence. Also, X-ray diffraction, surface area studies and temperature programmed desorption of adsorbed NH_3 were carried out for all the catalysts. ^{27}Al MAS Nuclear Magnetic Resonance spectra were also recorded for the catalysts.

2.4.1 Elemental analysis:

The quantification of the aluminium and silicon content in the zeolite for the determination of the Si/Al ratio was done by X-ray fluorescence technique using a Rigaku 3070 X-ray wavelength dispersive spectrometer. The sample was prepared by making a solid solution of the zeolite in $LiBO_2$ melt followed by rapid cooling to a glassy material. For calibration, standard zeolite samples with known compositions were used.

Atomic Absorption Spectrophotometer was used to determine the amount of palladium leached into the solution from the Pd-ETS-10 catalysts during the Heck reaction. The analysis was carried out on a Hitachi Z8000, Polarized Zeeman Spectrophotometer.

The alkali metal content in the poisoned BEA samples were obtained by flame photometric analysis of the acid extracts (by digestion) of the samples.

2.4.2. X-ray diffraction:

The phase purity and crystallinity of the zeolites were examined by XRD (Rigaku, Miniflex) in the 2θ range of 5-50^o. The parent zeolite samples, BEA(15), MOR(11) and FAU(2.6) and the dealuminated samples were characterized.

2.4.3. Sorption studies:

The total surface areas of the samples were obtained from N_2 adsorption at liquid N_2 temperature by the BET method using a commercial instrument (Quantachrome, Nova 1200). As the applicability of the BET equation to microporous materials is questionable, surface areas were also calculated from the monolayer volumes (V_m) obtained from the isotherms by the point B method assuming the area of the N_2 molecule to be 16.2 $Å^2$ [5]. The external areas of the samples were obtained by the t-plot method.

2.4.4. Temperature programmed desorption:

Acidity of the zeolite samples was characterized by the TPD of adsorbed NH_3 (Micromeritics, Autochem Z910). The standard procedure for TPD measurements involved the activation of the zeolite in flowing He at 873 K (3h), cooling to 298 K and adsorbing NH_3 from a stream of He-NH_3 (10%), removing the physically adsorbed NH_3 by desorbing in He at 373 K for 1h and finally carrying out the TPD experiment by raising the temperature of the catalyst in a programmed manner (10 $K.min^{-1}$). The TPD curves were deconvoluted into two peaks and the areas under the peaks were converted into meq NH_3 per g catalyst based on injection of known volumes of the He-NH_3 mixture at similar conditions.

2.4.5. ^{27}Al MAS Nuclear magnetic resonance:

The ^{27}Al MAS nuclear magnetic resonance spectra of BEA(15), MOR(11) and FAU(2.6) and the dealuminated samples were recorded on a Bruker (model: DRX-500) instrument. The spinning factor was 130.3MHz, spinning speed was 10 KHz and pulse length was 10sec. The number of scans for every sample was approximately 1000.

2.5 Results and Discussion:

The Si/Al ratios determined for the dealuminated samples of zeolites BEA(15), MOR(11) and FAU(2.6) are presented in the Table 2.3 along with the sorption data. The

XRD patterns of all the dealuminated samples were similar to the parent sample (Fig.2.1). The crystallinty of the samples was not significantly affected by dealumination, the relative intensities of the prominent lines being within 10% of those of the parent sample. The total surface areas (by the BET and point-B methods) and the external surface areas (by the t-plot method) calculated from N_2 adsorption at liquid N_2 temperature are reported in Table 2.3. It is noticed that the surface areas obtained by the point B method are slightly larger than those obtained from the BET equation, the deviation being in the range of 2-7 % for the samples. However, both the methods of calculating the surface areas do reveal the same trends between the samples. The external surface area of zeolites arises from the external surfaces of the crystallites, mesopores in the crystallites and amorphous material. The external areas are ~ 6 – 12% of the total area for the MOR and FAU samples, ~17- 25% for the BEA samples (Table 2.3).

The TPD profiles essentially consisted of two unresolved peaks for all the samples. These were deconvoluted into two distinct peaks with peak maxima in the range of 423 – 480 K for first peak and 623 – 723 K for the second peak for BEA and FAU and 723-823 K for MOR (Fig.2.2 a-d). It was assumed that the two peaks represent NH_3 adsorbed from weak and strong acid sites. Based on this assumption and the amount of NH_3 desorbed, as obtained from the area under the corresponding peaks, strong and weak acidity (in meq/g) have been calculated and reported in Table 2.4. However, it should be noted that the second peak is broad for many samples suggesting a range of acidity. Besides, the areas of the two peaks often overlap (for BEA and FAU) and hence the distinction as strong and weak is not accurate (though useful). The TPD profile of MOR is, however, better resolved into weak and strong acid sites. From the TPD results, MOR(11) is more acidic than BEA(15) and FAU(2.6). It possesses more strong acid sites than the other two zeolites and the position of the peak maximum of the second peak is also at a higher temperature suggesting that its

acid sites are stronger than those of BEA and FAU. However, it is to be noted that quantification of strength of acid sites based on TPD results is not realistic. The amount of acidity, especially that of the strong acid sites, is found to be related to the Al content in the different zeolites (Table 2.4).

TPD profiles of alkali metal loaded BEA samples are presented in Fig 2.3 a and b. The profiles were deconvoluted (Fig 2.3b) into two peaks and the quantitative data are presented in Table 2.5. Exchange of BEA with K-ions decreases total acidity. The decrease is mainly due to a decrease in the strong acid sites. Interestingly, exchange with sodium ions does not cause significant decrease in total acidity. In fact, it appears that the weak acid sites decrease and the strong acid sites increase. This is probably due to an experimental artifact arising from deconvolution. However, as noticed in the case of K, the peak maximum of the high temperature peak decreases suggesting the transformation of the strong acid sites into weaker ones. The studies suggest that K is a better poison for the acid sites compared to Na. This is in tune with the belief that strong acid sites determined from the TPD studies are ion-exchangeable Brönsted acid sites (bridged hydroxyl groups) and Lewis acid centers (formed by dehydration of Brönsted sites). The low temperature peak (characterizing weak acidity) is mainly due to physisorbed NH_3 and that desorbed from silanol groups.

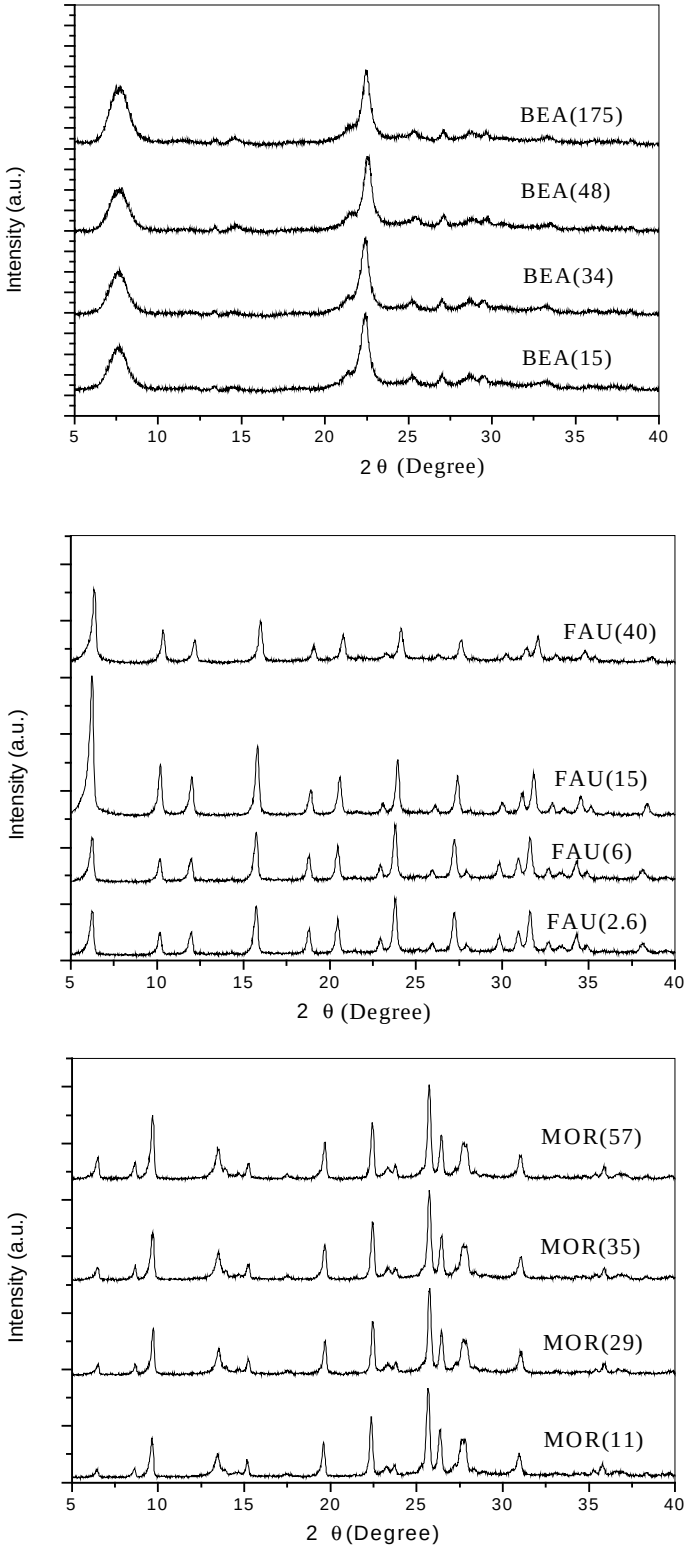

Fig. 2.1 X-ray diffraction patterns of BEA(15), MOR(11) and FAU(2.6) and the dealuminated samples (The number in the brackets is the Si/Al ratio of the sample)

Table 2.3: Physicochemical characterization of zeolites BEA(15), MOR(11) and FAU(2.6) and dealuminated samples

Sample Name[a]	Si / Al Ratio	Surface area (m^2/g)			Total Pore Volume (cc /g)
		S_{BET}	S_B[b]	External[c]	
BEA(15)	15	656	681	166	0.32
BEA(34)	34	754	800	150	0.36
BEA(48)	48	760	795	128	0.35
BEA(175)	175	580	617	131	0.28

Sample Name[a]	Si / Al Ratio	Surface area (m^2/g)			Total Pore Volume (cc /g)
		S_{BET}	S_B[b]	External[c]	
MOR(11)	11	562	593	52	0.24
MOR(29)	29.4	550	566	53	0.23
MOR(35)	35.9	519	551	35	0.22
MOR(57)	57.2	564	580	57	0.24

Sample Name[a]	Si / Al Ratio	Surface area (m^2/g)			Total Pore Volume (cc /g)
		S_{BET}	S_B[b]	External[c]	
FAU(2.6)	2.6	795	848	48	0.33
FAU(6)	6	749	787	53	0.32
FAU(15)	15	697	728	93	0.31
FAU(40)	40	747	782	77	0.34

[a]:The number in the brackets is Si/Al ratio of the sample,[b]: Surface areas calculated from V_m values obtained by the point B method, [c]: Calculated by the t-plot method.

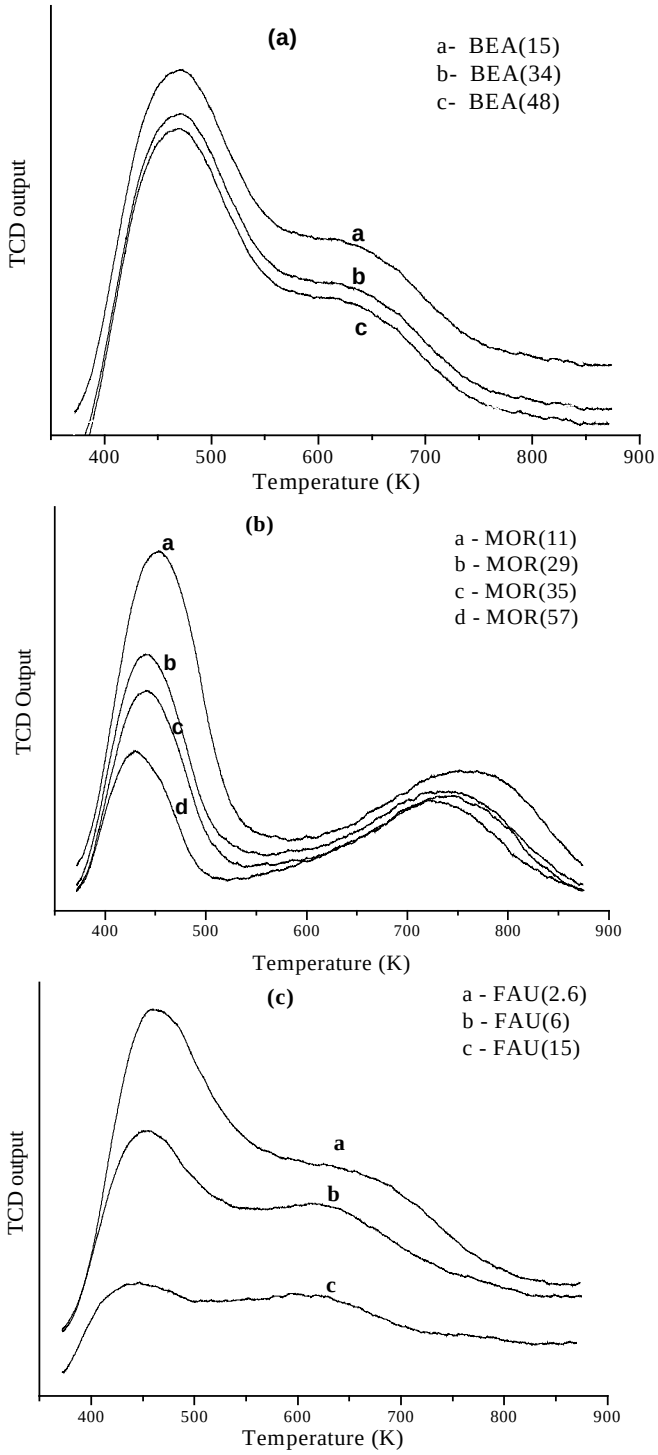

Fig. 2.2a. TPD of ammonia profiles of BEA(15), MOR(11) and FAU(2.6) and the dealuminated samples

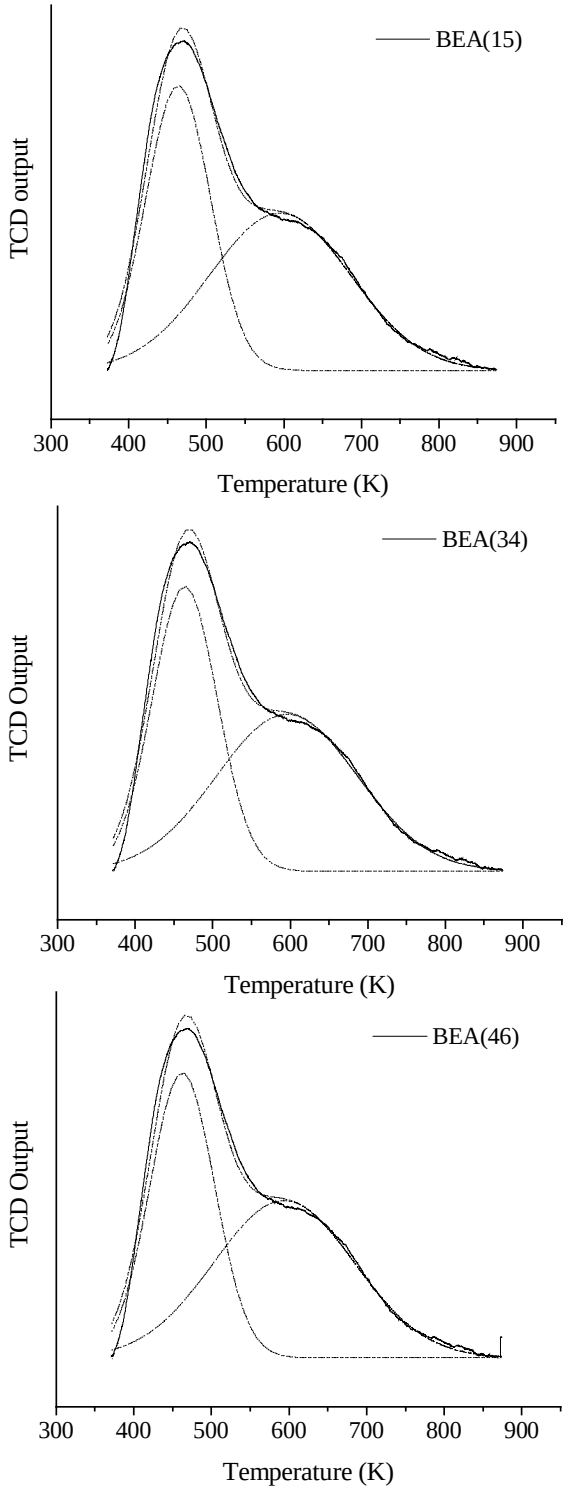

Fig. 2.2b. Deconvoluted TPD profiles for the BEA samples

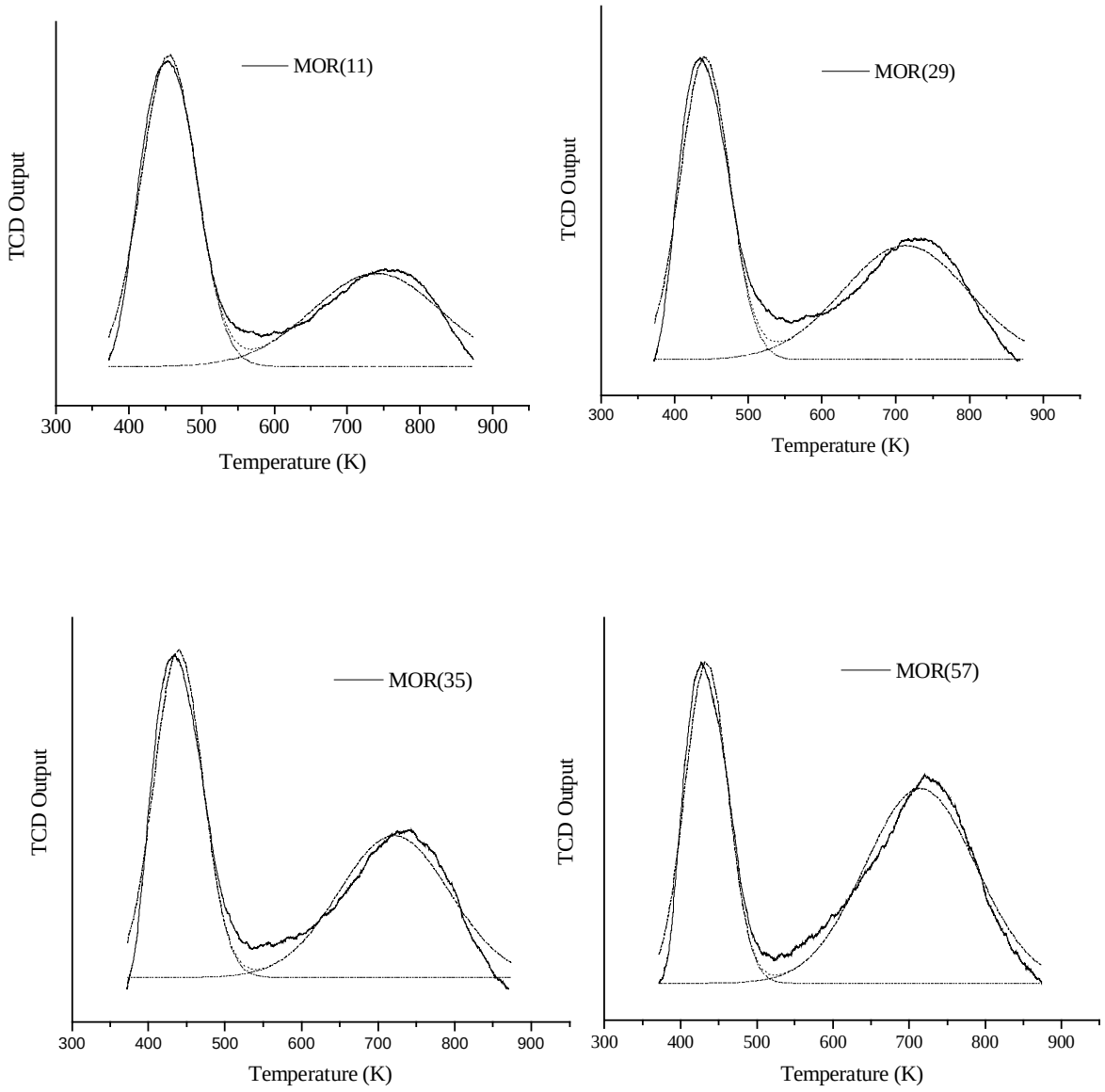

Fig. 2.2c. Deconvoluted TPD profiles for the MOR samples

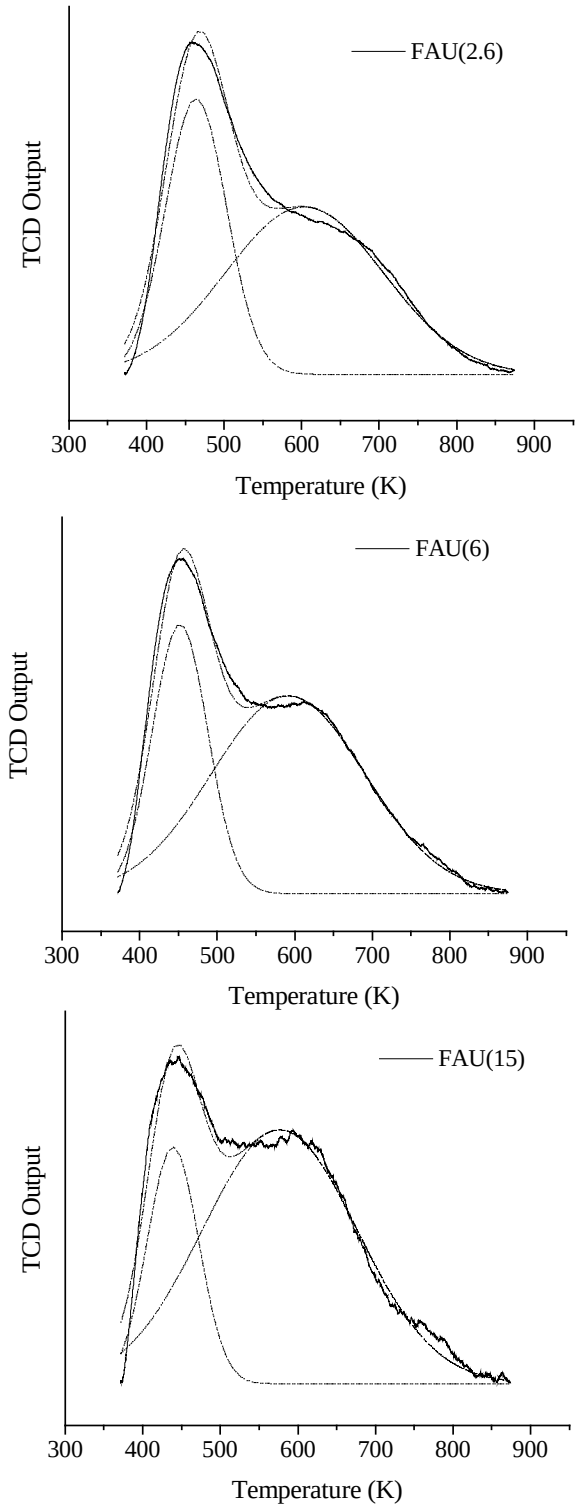

Fig. 2.2d. Deconvoluted TPD profiles for the FAU samples

Table 2.4: Al content and acidity characteristics of the zeolites

Sample	Al content (meq/g)	Acidity (meq/g)		
		Total	Weak	Strong
BEA(15)	1.04	1.22	0.55	0.67
BEA(34)	0.47	0.51	0.21	0.30
BEA(48)	0.34	0.39	0.09	0.30
BEA(175)	0.09	-	-	-

Sample	Al content (meq/g)	Acidity (meq/g)		
		Total	Weak	Strong
MOR(11)	1.39	1.87	1.05	0.82
MOR(29)	0.55	1.45	0.75	0.70
MOR(35)	0.45	1.30	0.67	0.63
MOR(57)	0.28	0.98	0.41	0.57

Sample	Al content (meq/g)	Acidity (meq/g)		
		Total	Weak	Strong
FAU(2.6)	4.65	2.23	0.89	1.34
FAU(6)	2.39	1.31	0.44	0.87
FAU(15)	1.04	0.58	0.14	0.44
FAU(40)	0.41	0.26	0.06	0.20

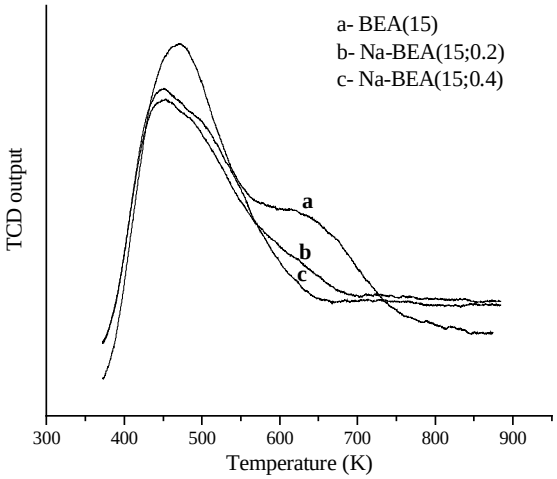

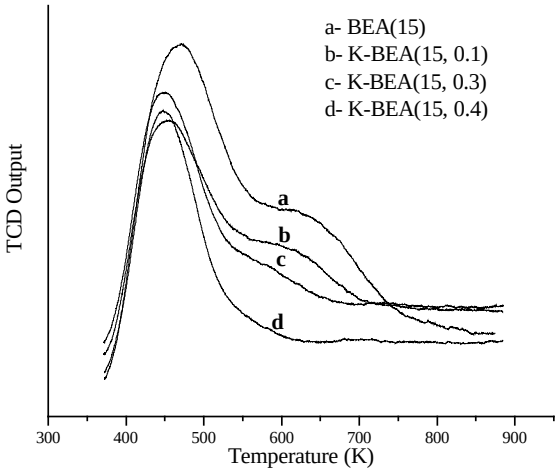

Fig. 2.3a. TPD profiles of ammonia of BEA(15) and sodium and potassium poisoned BEA(15) samples

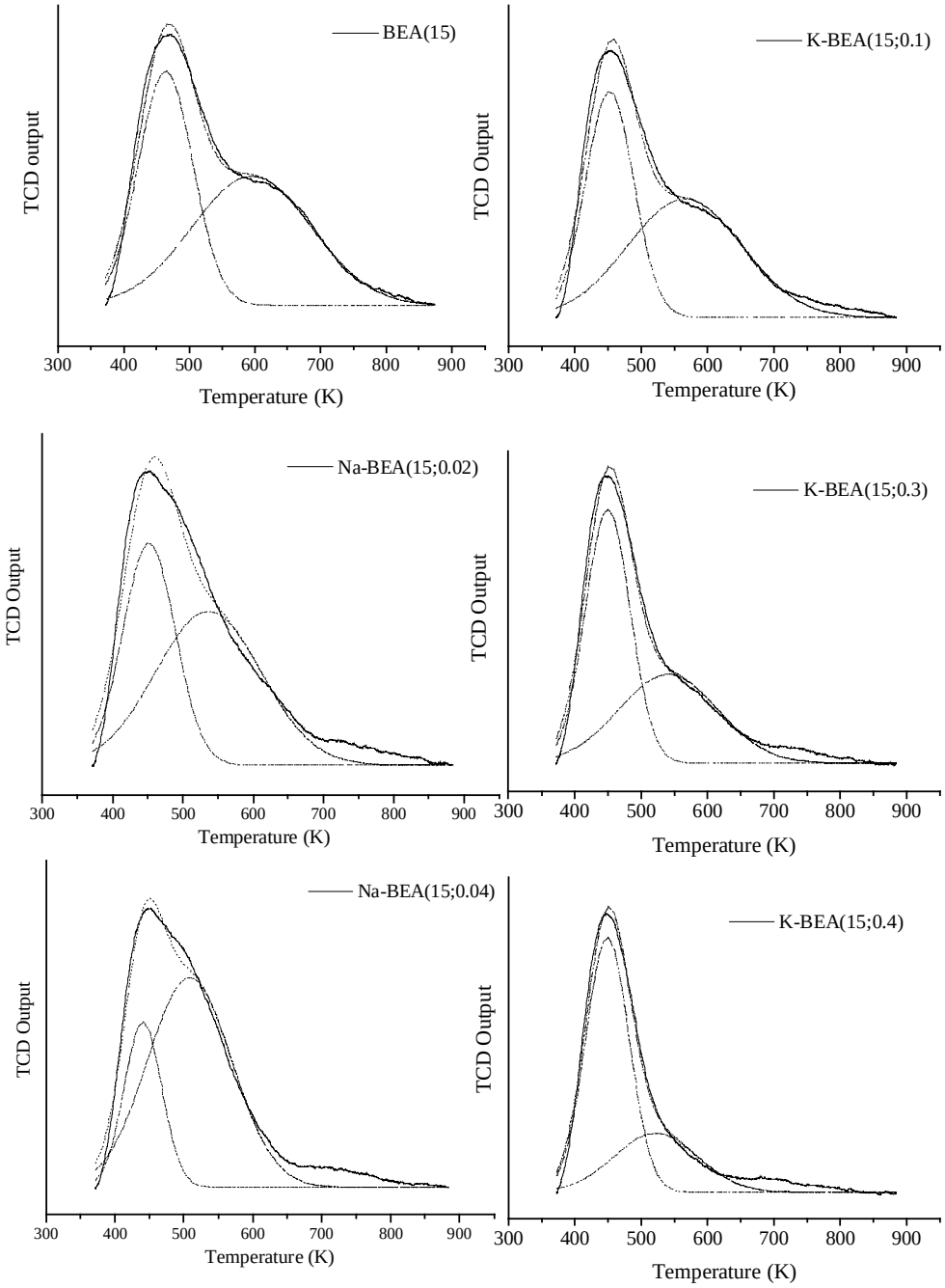

Fig. 2.3b. Deconvoluted profiles of BEA(15) and Na and K poisoned samples (The numbers in the brackets after BEA are Si/Al ratio and mmol/g of alkali metal)

Table 2.5: Acidity of parent and alkali poisoned BEA samples from TPD of NH_3

Alkali metal (mmol/g)	Acidity (meq/g)		
	Total	Weak	strong
Nil	1.21	0.55	0.655
Potassium			
0.1	1.024	0.46	0.57
0.3	0.885	0.49	0.39
0.4	0.45	0.50	0.22
Sodium			
0.2	1.08	0.46	0.63
0.4	1.02	0.26	0.76

The ^{27}Al MAS nuclear magnetic resonance spectra of the zeolites and their dealuminated samples (Fig. 2.4 a-c) show the presence of both tetrahedral Al (strong signal ~ 53-56 ppm) and octahedral Al (signal near 0 ppm). The T_d and O_h signals arise from the framework Al and extra-framework Al species respectively. It is noticed that even the parent commercial samples possess some octahedral Al. However, the intensity of the O_h signal is very much smaller than that of the T_d signal in BEA and MOR samples. The O_h signal in FAU(2.6) and (6) are quite strong suggesting the presence of substantial amounts of extra framework Al. The dealuminated samples possess smaller amount of octahedral Al due to leaching of the non-framework aluminium during acid treatment.

The Si/Al ratios reported in this study are based on bulk analysis by XRF and include both framework and non-framework Al. In view of the low intensity of the O_h signals, the reported ratios are expected to reflect mainly the framework Al in all the samples [except FAU(2.6) and (6)].

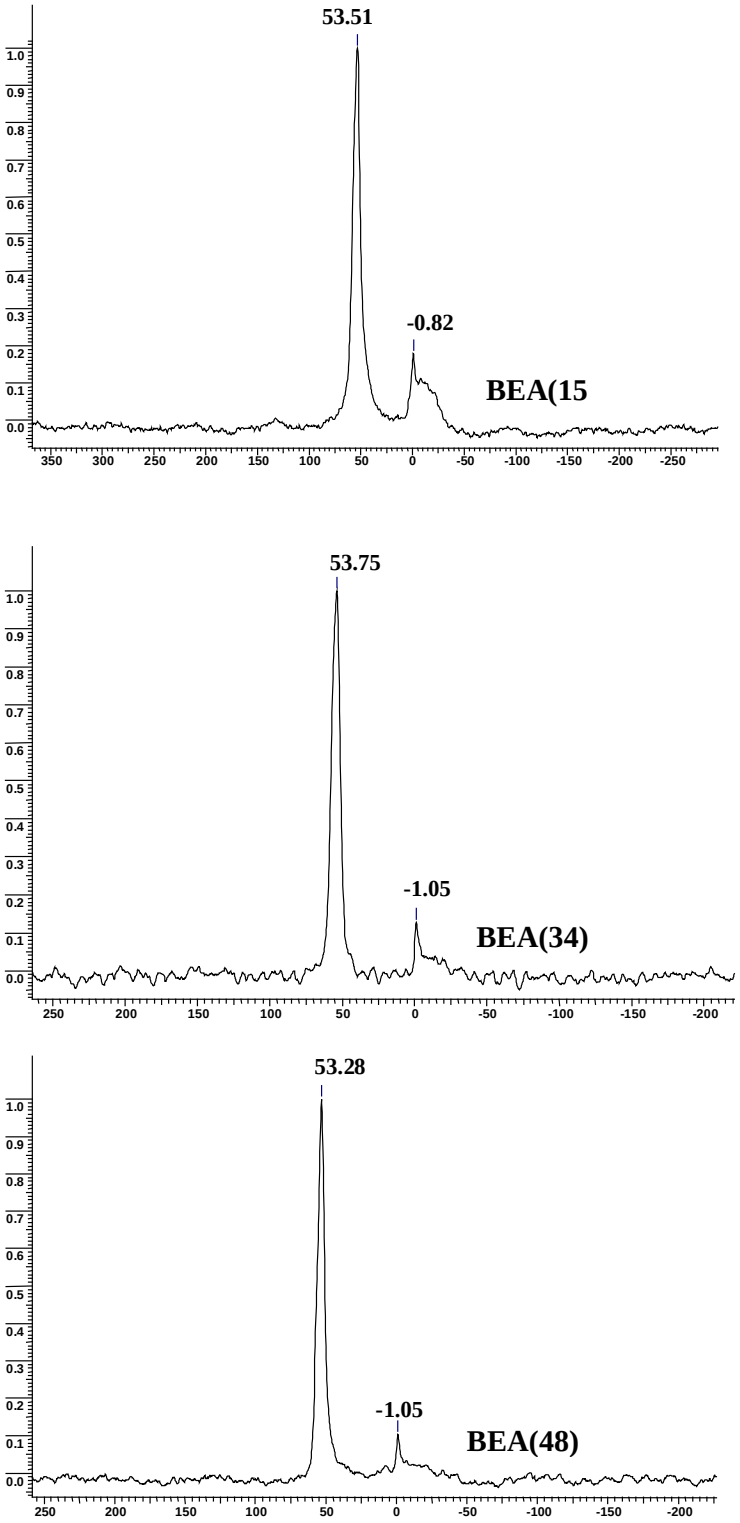

Fig. 2.4a. ^{27}Al MAS NMR spectra of BEA(15) and the dealuminated samples

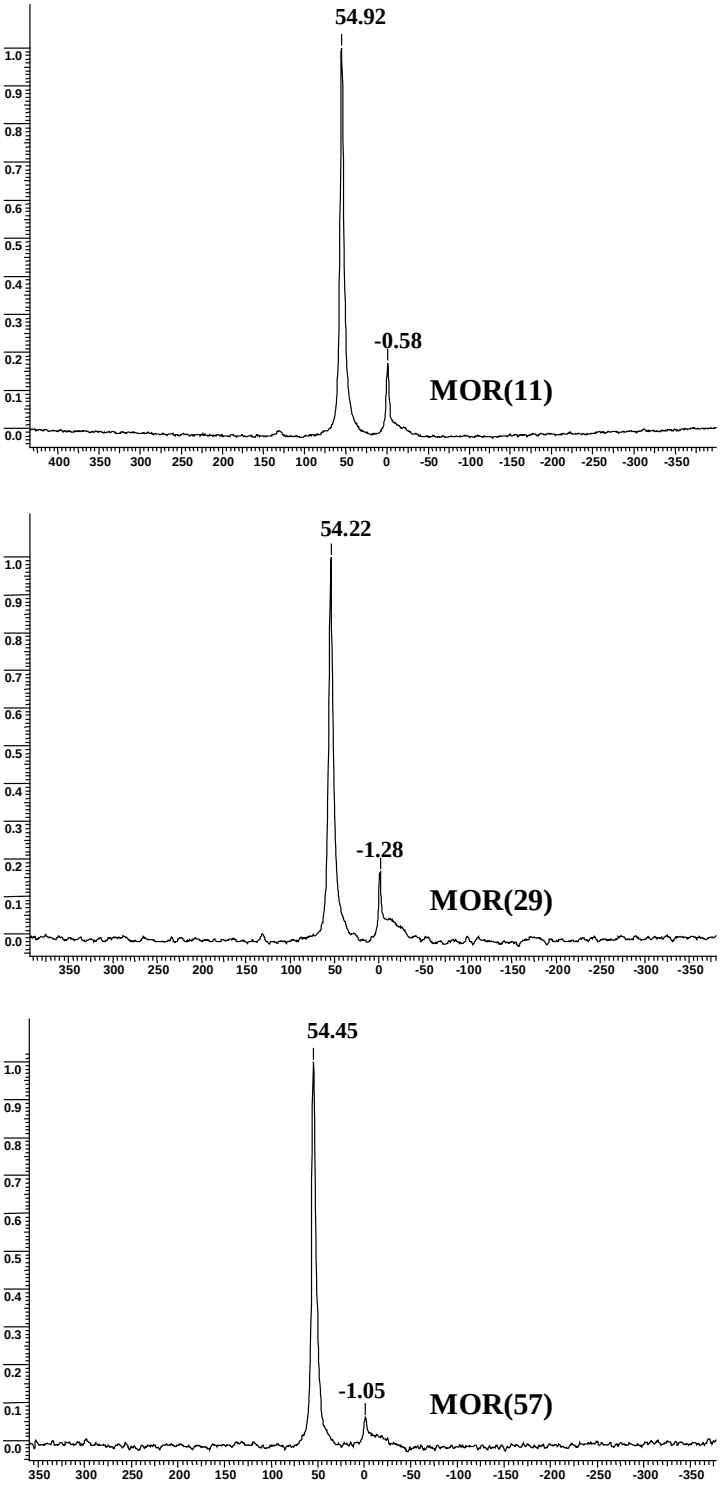

Fig. 2.4b. ^{27}Al MAS NMR spectra of MOR(11) and the dealuminated samples

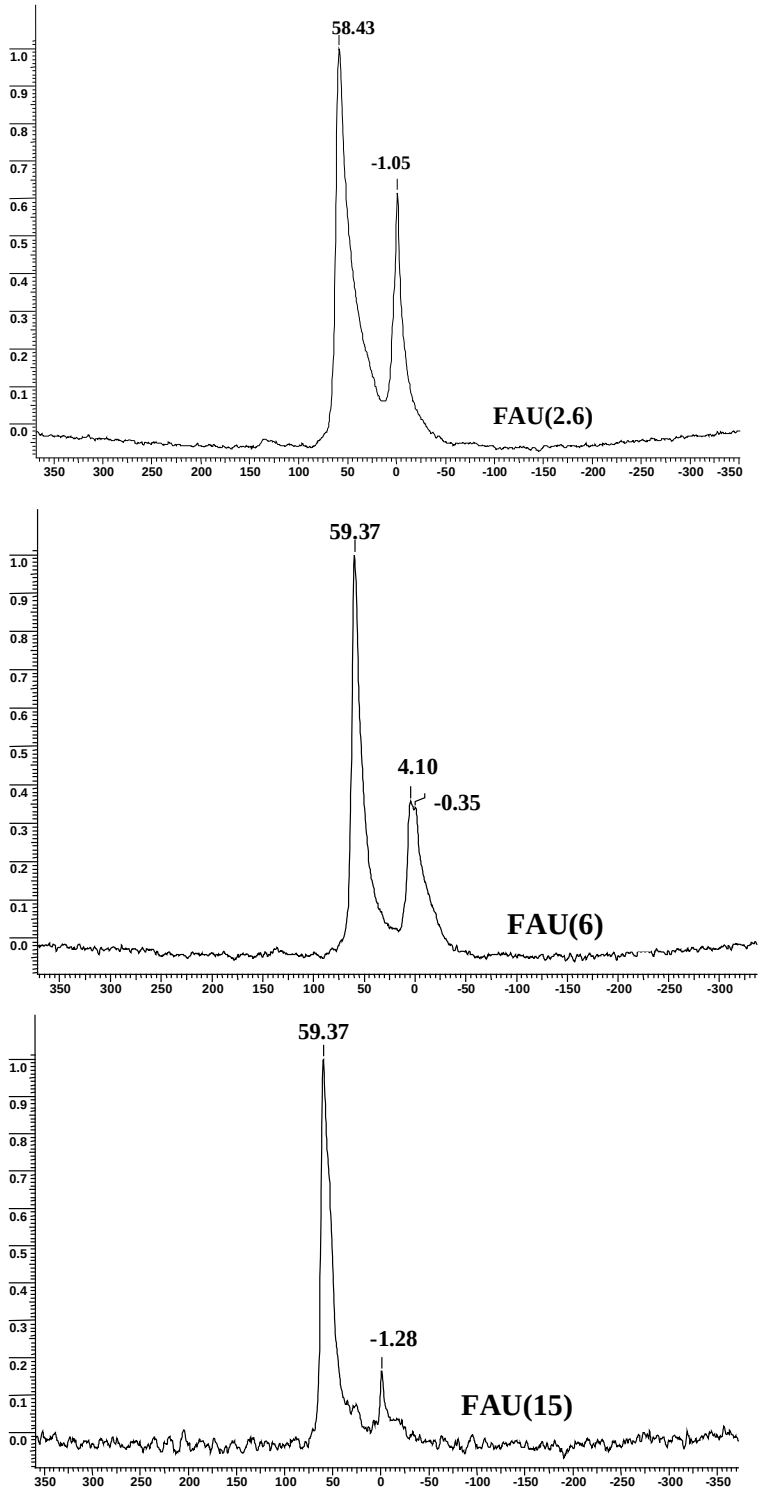

Fig. 2.4c. ^{27}Al MAS NMR spectra of FAU samples

2.6 Thermodynamics of Alkylation of Phenol with 1-Octene:

Thermochemical data on the alkykation of phenol with 1-octene were calculated using the Benson's method [6,7]. The thermodynamic parameters like enthalpy, entropy, Gibbs energy of formation and equilibrium constants for the formation of *O*- and *C*-alkylates were determined. The use of the Benson's method also facilitated the determination of the thermodynamic properties of the o- and p- substituted products. For the estimation of ΔH^o_f (298 K), S^o (298 K) and C^o_p (T) a group contribution method was used. Contributions by atoms with valencies greater than unity were considered.

The expressions for the estimation of enthalpy, heat capacity and entropy are given below. They are obtained by summing the contributions of each *i*-group (ΔHi, S^oi and C^o_p (T)) which have been tabulated by Benson et al. [8,9], taking into account the frequency of appearance n_i of each group in the molecule.

$$\Delta H^o_f (298\ K) = \Sigma\ n_i\ \Delta Hi$$

$$C^o_p (T) = \Sigma\ n_i\ C^o_p$$

$$S^o (298\ K) = \Sigma\ n_i\ S^oi - R \ln (\sigma) + R \ln (\eta)$$

The Benson's method demands corrections of the sum of entropies using the symmetry number (σ) and the number of possible optical isomers (η). The symmetry number (σ) of the molecule can be obtained by the product of the internal symmetry number (σi_{nt}) and the external symmetry number (σ_{ext}):

$$\sigma = (\sigma i_{nt}) . (\sigma_{ext})$$

The σi_{nt} parameter represents the number of symmetry elements of each group and σ_{ext} represents the number of symmetry elements of the whole molecule. For example, propane has two terminal - CH_3 groups and each group has a threefold axis of symmetry. Rotation of these *internal* groups yields σi_{nt} = (3)**.**(3) as the number of permutations. Also, the entire molecule has a single twofold axis of symmetry, so

σ_{ext} = 2. Then, $\sigma = (2).(3)^2 = 18$.

In addition to the symmetry corrections, if a molecule has optical isomers, i. e. it contains one or more asymmetric carbon atoms (as in 3-methylhexane), the number of spatial orientation is increased and a correction of + Rln (η) must be added to the number of isomers η being the number of optical isomers. The number of possible optical isomers is 2^m where *m* is the number of asymmetric carbon atoms.

The Benson method also demands fixed corrections for the following properties of ortho-isomers of aromatic compounds:

$\Delta H^o_f (298) = \Delta H^o_f - 0.57$

$S^o (298) = S^o - 1.61$

$C_{p300} = Cp^o + 1.12$

$C_{p400} = Cp^o + 1.35$

$C_{p500} = Cp^o + 1.30$

$C_{p600} = Cp^o + 1.17$

$C_{p800} = Cp^o + 0.88$

Finally, the thermodynamic properties and chemical equilibrium constant (K) of the reactions at different temperatures were estimated as follows:

$C^o_{p\,m} = C^o_p (T) - C^o_{p\,298} / 2$

$\Delta H^o_f (T) = \Delta H^o_{f\,298} + C^o_{p\,m} (T-298)$

$S_f^o (T) = S_f^o{}_{298} + C^o_{p\,m} (T / 298)$

$\Delta G^o_f (T) = \Delta H^o_f (T) - T\, S_f^o (T)$

$K (T) = \exp [-\Delta G^o_f (T) / RT]$

From the equilibrium constant and reaction equations, the molar concentrations of reactants and products at equilibrium were calculated. The calculated thermodynamic properties of the reactants and the different products are presented in Tables 2.6 and 2.7

respectively. A plot of the calculated K_p values at different temperatures for the formation of octyl phenyl ether and octyl phenols is presented in Fig 2.5 a. In the temperature range of calculations, there is a continuous decrease in K_p with temperature. The K_p value for the *C*-alkylate is larger than for the *O*-alkylate in the entire temperature range (200 to 1000 K), the difference becoming smaller at higher temperatures. The ratios of the K_p values for *O*- and *C*-alkylates increases with temperature. The corresponding molar equilibrium concentrations for *O*- and *C*- alkylates and total conversion calculated at different temperatures are presented in Fig 2.5 b. The concentration of *C*-alkylate decreases while that of the *O*-alkylate increases due to smaller decrease in K values with temperature for the *O*-alkylate compared to the *C*-alkylate (Fig.2.5a).

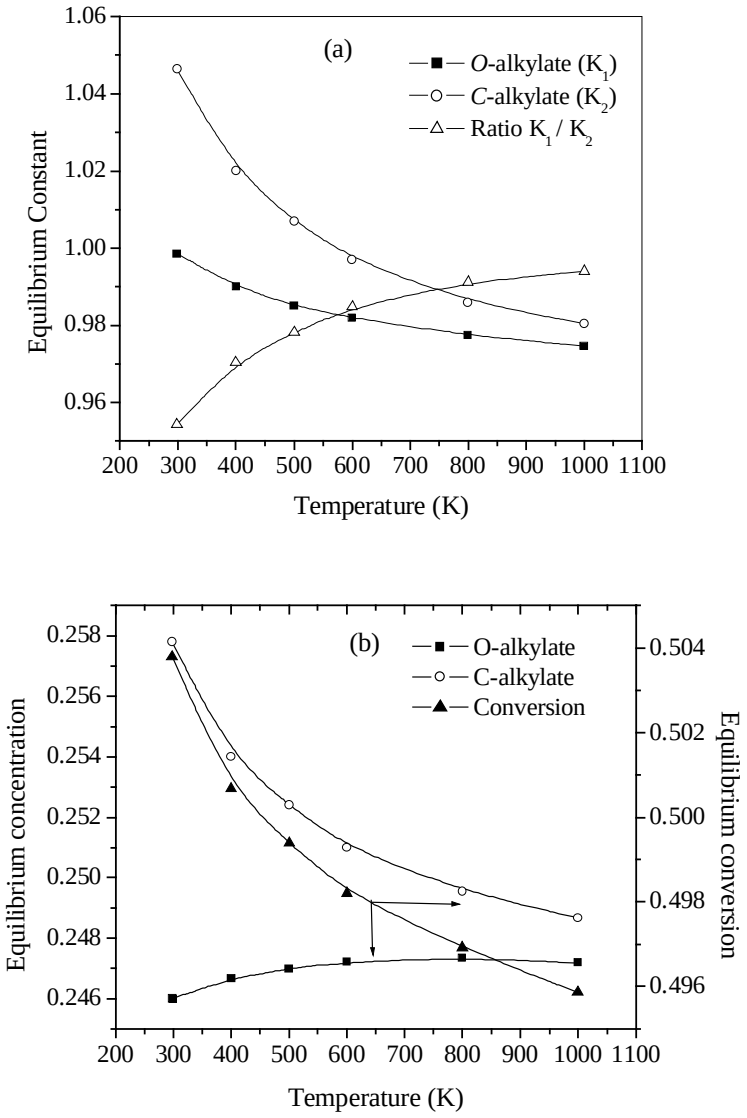

Fig. 2.5. Variations of equilibrium constants and their ratios (a), and total conversion and concentration of *O*- and *C*-alkylates (b) with temperature in the alkylation of phenol with 1-octene

Table 2.6: Thermodynamic properties of phenol and 1-octene

Temp(K)	Phenol				1-octene			
	Cp^o	ΔH_i	ΔS_i^o	ΔG_f^o	Cp^o	ΔH_i	ΔS_i^o	ΔG_f^o
298	20.14	-22.36	-18.37	-16.88	42.95	-19.81	-85.35	5.62
400	32.04	-19.70	-26.05	-9.28	53.97	-14.87	-99.62	24.98
500	38.36	-16.45	-33.51	0.303	64.14	-8.99	-113.06	47.53
600	43.37	-12.77	-40.60	11.59	72.80	-2.34	-125.85	73.17
800	50.68	-4.58	-53.34	38.09	86.38	12.65	-149.21	132.0
1000	55.62	4.23	-64.20	68.65	96.48	15.18	-169.75	198.88

The properties are expressed as: Cp^o, cal/mol.K; ΔH_i, Kcal/mol; ΔS_i^o, cal/molK; ΔG_f^o, Kcal/mol.

Table 2.7: Thermodyanmic properties of *O*-alkylate, ortho- and para-alkylates

Temp K	*O*-alkylate				o-alkylate				p-alkylate			
	Cp^o	ΔH_i	ΔS_i^o	ΔG_f^o	Cp^o	ΔH_i	ΔS_i^o	ΔG_f^o	Cp^o	ΔH_i	ΔS_i^o	ΔG_f^o
298	68.24	-59.22	-163.6	0.81	65.45	-66.67	-148.69	-11.10	64.33	-66.10	-150.30	-10.05
400	88.40	-51.23	-186.6	7.74	89.25	-58.78	-171.43	-5.90	87.90	-58.33	-172.71	-4.90
500	105.5	-41.67	-208.6	14.80	105.94	-49.36	-193.06	-0.66	104.64	-49.19	-194.0	-0.02
600	119.1	-30.94	-229.2	21.80	119.59	-38.73	-213.44	4.58	118.43	-38.50	-214.25	5.29
800	140.4	-6.85	-266.6	36.40	140.24	-15.04	-250.25	15.07	139.36	-14.97	-250.87	15.64
1000	155.4	19.28	-299.0	51.14	154.30	10.46	-281.64	24.57	154.30	10.64	-282.57	25.67

The properties are expressed as: Cp^o, cal/mol.K; ΔH_i, Kcal/mol; ΔS_i^o,cal/molK; ΔG_f^o, Kcal/mol.

2.7 Kinetic Analysis:

In a chemical reaction, the rearrangement or redistribution of the constituent atoms of the reacting species takes place leading to the formation of new molecules, which are termed as the products. The mode and mechanism of the reaction, the physical and energy changes involved and the rate of formation of the products are of importance in the study of chemical reactions. Kinetic analysis is concerned with the rate of formation of products and the factors that influence the rate. The kinetic analysis of the different carbon – carbon bond formation reactions viz. the Claisen rearrangement of allyl ethers (allyl ethers of phenol, and o-, m- and p-cresols), phenol alkylation and acylation of anisole with alkyl carboxylic acids (hexanoic, octanoic and decanoic acids) were carried out during the course of the study to have a better understanding of the reactions.

Claisen rearrangement:

The reactant conversion and the product selectivity of the reaction depend on the reaction parameters, the medium of the reaction (solvent) and the catalyst used. The products of the reaction of the Claisen rearrangement of allyl phenyl ether over H-BEA in the presence of a reactive solvent (benzene or toluene) are presented in the Fig. 2.8.

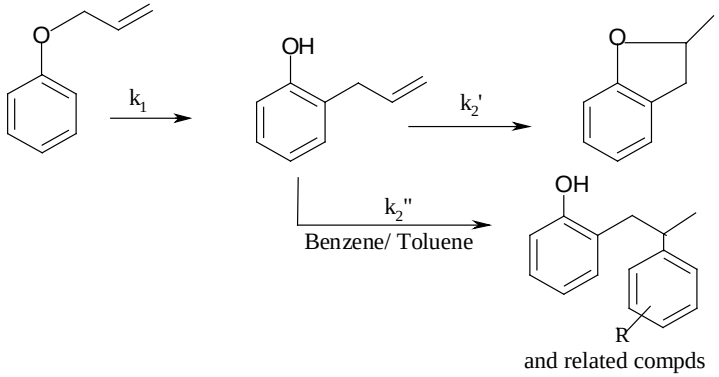

Fig. 2.8. Products of Claisen rearrangement of allyl phenyl ether over H-BEA in the presence of reactive solvents (benzene/ toluene)

This may be schematically represented as first order series and parallel reactions as shown in the Fig. 2.9.

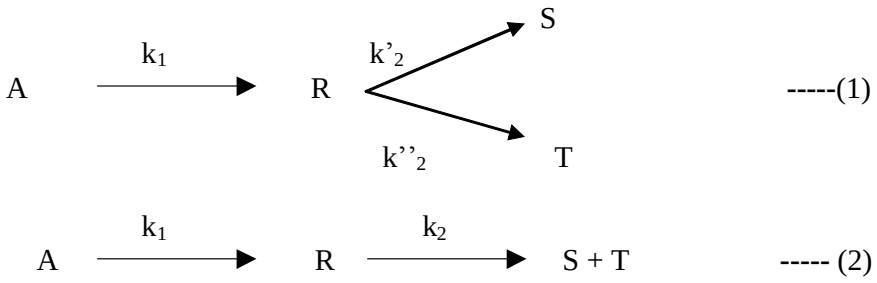

Fig. 2.9. Schematic representation of series and parallel reactions

Here, A represents the allyl aryl ether; R the intermediate phenyl allyl ether; S, the ring compound (methyl dihydrobenzofuran) and T the side products; k_1 is the first order reaction rate constant for the first step; k_2', the rate constant for the formation of S and k_2", the rate constant for the formation of T. This reaction equation may be reduced to that of a standard first order series reaction presented in equation (2); k_2 is the rate of disappearance of the intermediate. As R forming S and R forming T are a set of parallel reactions,

$$k_2 = k_2' + k_2'' \qquad \text{----- (3)}$$

and

$$k_2'/k_2'' = \text{moles of S formed / moles of T formed} \qquad \text{----- (4)}$$

The relation between the concentration, rate constant and time for first order unimolecular consecutive reactions is given by

$$C_A = C_{A0}e^{(-k1t)} \qquad \text{----- (5)}$$

and

$$C_R = C_{A0}\, k_1 \{e^{(-k1t)} - e^{(-k2t)}\} / (k_2-k_1) \qquad \text{----- (6)}$$

Here, C_{A0} is the initial concentration of the allyl aryl ether, and C_A and C_R are the concentrations of allyl aryl ether and allyl phenol, respectively at time t. Equations (5) and

(6) have been used for the estimation of the rate constants k_1 and k_2 from the experimentally obtained concentration-time profiles. The reaction times used for the calculations varied depending on the reactivity of the substrate and hence the time span of the concentration profiles were different for different substrates. The rate constants for the parallel reactions, k_2' and k_2" have been calculated from k_2 and the concentrations of the products, using equations (3) and (4). The confidence levels for the rate constants are 95 ± 5 %.

Phenol Alkylation:

The alkylation of phenol with 1-octene is rather complex involving a number of possible reactions. The major reaction products are represented in the Fig. 2.10.

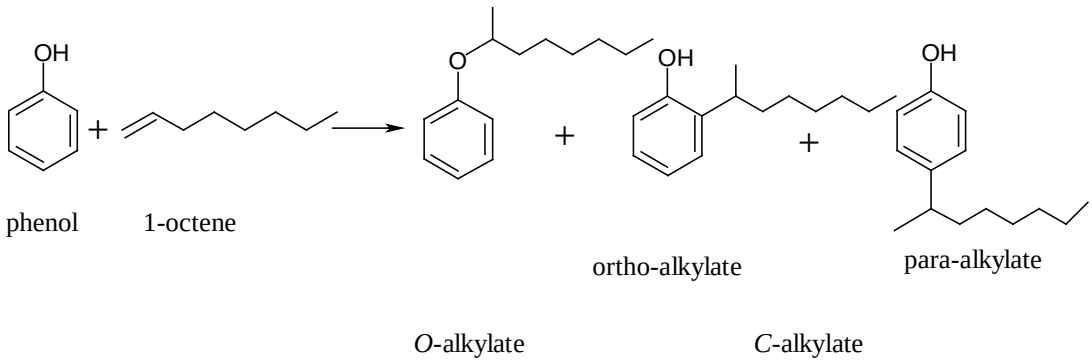

Fig. 2.10. Products of alkylation of phenol with 1-octene (chain isomers not shown)

The product analysis for this reaction, when phenol and octene are taken in the molar ratio 1:1, predominantly showed the formation of *O*-alkylation (ether) and *C*-alkylation products (*o*-alkyl phenol and *p*-alkyl phenol). For analytical simplicity, the isomerization of octene was ignored and the overall reaction was considered as a set of parallel reactions resulting in the formation of ether and alkyl phenols. This is justified as the products from octene isomers constituted only a small amount of the products of the overall reaction. This may be schematically represented as:

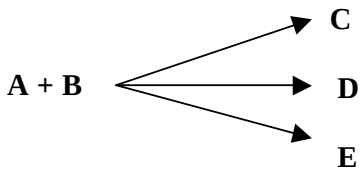

This is a set of second order reactions in parallel. The general equation for a second order irreversible reaction with equi-molar reactants is given by:

$$X_A/(1-X_A) = C_{A0}\, k\, t$$

Here X_A is the conversion of reactant A, which is the same as that of reactant B, C_{A0} is the initial number of moles of reactant A or reactant B, t is the reaction time and k is the second order reaction rate constant. The rate constants of the reactions at different reaction temperatures were calculated using the above expression and the temperature dependence of the rate constant was evaluated using the Arrhenius expression:

$$k = k_0 e^{(-E/RT)}$$

In the above expression, k_0 is the frequency factor, E is the activation energy, R is the universal gas constant and T is the reaction temperature.

Acylation of Anisole

Acylation reactions were carried out using different straight chain carboxylic acids viz. hexanoic, octanoic and decanoic acid. In all the reactions, anisole was used in excess (mole ratio of anisole to acid = 4 : 1), and the products formed were the ketone and the ester of the acid used in the reaction. Since anisole was in excess, these reactions were considered as psuedo first order with respect to the acid. So the standard first order reaction rate expression

$$-\ln (1-X_A) = kt$$

was used for the kinetic analysis of the reaction and the activation energy of the reaction was estimated using the Arrhenius expression given earlier.

2.8 References:

1. T.K. Das, A.J. Chandwadkar and S. Sivasanker, Chem. Commun., (1996), 1105.
2. S.B. Waghmode, S.G. Wagholikar and S. Sivasanker, Bull. Chem. Soc. Jpn., 76 (2003) 1989.
3. S. Krijnen, P. Sanchez, B.T.F. Jacobs and J. H. C. van Hooff, Micropor. Mesopor. Mater., 31(1999) 163.
4. E. B. Lami, F. Francis, D. Angewt and T. Des Courieres, Micropor. Mater., 1(1993) 237.
5. "Adsorption, Surface Area and Porosity", S.J. Gregg and K.S.W. Sing, Academic Press, (1967) Chapter 2, p 54.
6. "Properties of Gases and Liquids", R.C. Reid, J.M. Praunitz and T.K. Sherwood, Third edn. Mc Graw Hill Book Co. (1988) Chapter.6, p 150.
7. E.V. Sobrinho, D. Cardoso, E.F. Souza-Aguair, J. Braz. Chem. Soc., 9 (3) (1998) 225.
8. S.W. Benson, "Thermodynamical Kinetics", Wiley, New York, (1968) Chapter 2.
9. S.W. Benson, F.R. Cruickshank, D.M. Golden, G.R. Haugen, H.E.O′ Neal, A.S. Rodgers, R.Shaw, R. Walsh, Chem. Rev., 69 (1969) 279.

Chapter 3

Alkylation of Phenol

and

Naphthalene

Chapter 3-A

Alkylation of Phenol with 1-Octene

3-A.1 Introduction:

Alkylation of phenol with olefins and alcohols has been studied by different groups in both the liquid and vapour phases over solid catalysts like zeolites [1-3], SAPO-11 [4] and mesoporous materials [5,6]. The *tert*-butylation of phenol over H-beta (BEA) in the vapour phase by Zhang et al. [3] has revealed that high yields of p-TBP (p-tertiary butyl phenol) are possible at a reaction temperature of 418K and at low reactant molar ratios. It was reported that medium acid sites on the zeolite are advantageous in producing p-TBP, strong acid sites are helpful for the formation of 2,4-DTBP (2,4-ditertiary butyl phenol) and weak acid sites are responsible for the formation of o-TBP. The para selective butylation of phenol over a silicoaluminophosphate (SAPO-11; AEL) catalyst in the vapour phase revealed that o-TBP easily isomerises to p-TBP whereas, the reverse reaction is not significant [4]. Also, both the alkyl phenols were found to undergo easy dealkylation. Poisoning of the acid sites by ammonia and quinoline reduced the activity revealing the role played by weak and structural acid sites in the reaction. Silylation of SAPO-11 by dichlorodiphenylsilane to remove the external surface acid sites did not change the conversion or selectivity, which indicated that the reaction occured inside the pores. Sakthivel et al. have reported that phenol conversion increases with a decrease in the phenol: *t*-BuOH ratio over H-AlMCM-41 [5]. Also, at higher temperatures the o-TBP and p-TBP isomerize to m-TBP. When *tert*-butylation was carried out over mesoporous H-FeMCM-41, p-TBP was obtained as the major product with high selectivity [6].

The formation of octylphenol over different catalysts was studied in detail by Young [7]. The alkylation of phenol with long chain olefins or alcohols yielded a broad spectrum of products. The isomerization of 1-octene under reaction conditions to 2-, 3-, 4- octenes resulted in the formation of mixtures of isomeric products. It was found that the product distribution obtained over ZSM-12 (MTW) and mordenite (MOR) was similar. However, the product distribution over conventional REY (Rare Earth – Y; FAU) and Amberlyst-15 consisted of a complex mixture of products [7]. The REY and Amberlyst-15 catalysts showed similar product distribution but no particular or outstanding preference to any aromatic ring substitution position nor to any particular point of attachment of the phenol on the alkyl chain. In sharp contrast, the octyl phenols produced over MTW and MOR were unexpectedly rich in both para-octylphenols and in octyl phenols in which the aromatic ring was attached at the 2-position on the alkyl chain. Another unique benefit of the zeolite catalyst was the specificity in the formation of mono-alkylphenols compared to the disubstituted product. When 1-octanol reacted over 12-MR zeolites, only p- and o-alkylation occured. As the m-isomers were completely absent even at high conversions, the shape selective nature of the catalysts was reflected. Preferential para-substitution occured for each octyl phenol over all the 12-MR zeolites used [8]. For the less bulky 2-octyl phenol, the preference was about the same for the para isomer over REY, MOR and MTW. However, no regioselectivity was observed for REY as equal amounts of 2-, 3- and 4- octyl phenols were formed.

Sonawane et al. [9-11] have reported the liquid phase alkylation of phenol using 1- and 2- octenes in the absence of solvent at room temperature over a homogeneous catalyst, BF_3-etherate. The reaction produced both the ether (from alkylation at the oxygen atom) and alkyl phenols (the o- and p-isomers) from alkylation at the ring. The *O*- alkylate was found to contain isomeric octyl phenyl ethers, 2-, 3- and 4-. The 2- isomer was found to be

the predominant one at the initial stages. The percentage of the 2-isomer was observed to decrease with time. 1-Octyl phenyl ether was found to be totally absent. This suggests that the carbonium ion is preferentially generated at the second carbon atom in 1-octene and this carbonium could then react or rearrange. A comparison of activities of 1- and 2-octenes showed an increased reactivity for 1-octene. This indicates that olefins with internal double bonds are less reactive than those with a terminal double bond. In the *C*-alkylate (ortho- and para-isomers), the proportion of the 2-isomer was large in the beginning and decreased with time. However, a corresponding increase in 3- and 4- isomers was not observed. This was most probably due to further alkylation. The *O*-/*C*-alkylate ratio remained constant throughout confirming that both the alkylates were formed simultaneously. Also, it indicated that there was no conversion from *O*- to *C*-alkylate under the reaction conditions.

The present study is the use of the zeolites H-beta (BEA(15)), H-mordenite (MOR(11)) and H-USY (FAU(15)) as catalysts in the liquid phase alkylation of phenol with 1-octene. The influence of process variables such as temperature, reactant mole ratio, catalyst amount and alkali metal poisoning on the reaction has been investigated. The kinetics of the reaction was examined assuming parallel second order reactions.

3-A.2 Experimental:

The source of the catalysts used in this chapter, their characterization and experimental methods adopted are reported in Chapter.2, section 2.1, 2.4 and 2.3 respectively. Phenol and 1-octene were procured from Merck, India and Aldrich, U.S.A. respectively. The preparation of isomeric octyl phenols is described in chapter 2, section 2.2 Details of thermodynamic and kinetic studies are presented in sections 2.6 and 2.7 of the same chapter.

3-A.3 Results and Discussion:

3-A.3.1 Physicochemical properties:

All the samples exhibited the characteristic XRD patterns for the different zeolites. The total surface area, external surface area (by the t-plot method) and the pore volume of zeolites with different Si/Al ratios are presented in Chapter.2, Table 2.3. The temperature programmed desorption (TPD) profiles of the zeolites (BEA(15), MOR(11) and FAU(15)) and the Na- and K-poisoned BEA samples are presented in Chapter.2, Fig.2.2 and Fig. 2.3.. The strong and weak acidity (in meq/g) have been calculated after deconvolution of the profiles into two peaks for all the samples and reported in Chapter.2, Tables 2.4 and 2.5.

3-A.3.2 Alkylation of phenol:

Alkylation of phenol with 1-octene resulted in the selective formation of the monoalkylated products. The formation of dialkylated products was negligibly small. In the absence of a catalyst, the reaction did not proceed to any appreciable extent at the end of 6 h even at 383K. The reaction between phenol and 1-octene over the solid acid (zeolite) catalysts produced mainly oxygen alkylated (*O*-alkylated) and carbon alkylated (*C*-alkylated) products. These appear to be formed in parallel and contain isomeric (2-, 3- and 4-) octyl phenyl ethers (*O*-alkylates) and octyl phenols (*C*-alkylates) (Fig. 3-A.1). In keeping with the scheme (Fig. 3-A.1), other isomeric octenes (2-, 3- with 1-octene.and 4-octenes) were found in the reaction mixture.

A kinetic analysis of the results was carried out assuming second order parallel reactions (chapter 2, section 2.7). The overall reaction rate constant was calculated based on phenol conversion. The reaction of phenol with 1-octene to give the ether (*O*-alkylate) and the *C*-alkylate (ortho- and para-isomers) was considered as a set of reactions in parallel. Though there were skeletal isomers of the *O*-alkylated and *C*-alkylated products, according to Fig. 3-A.1, the 2-isomers were the predominant species in each set (i.e. *O*-alkylate, o-alkylate and p-alkylate). Hence all the isomers in each set were grouped together for the analysis.

The alkylation of phenol with 1-octene over BEA was investigated at different temperatures, run duration and reactant mole ratios. The influence of doping the catalyst with small amounts of Na and K on conversion and product yields was also investigated. A comparison of the performance of three wide pore zeolites, BEA, MOR and FAU, was also done. The different studies are discussed below.

3-A.3.3 Influence of run duration:

Representative plots of the change in conversion and product yields and the ratios of the different products with duration of run are presented in Fig. 3-A.2. The major products are found to be octyl phenyl ether and the ortho- and para- (o- and p-) octyl phenols (collectively called the *C*-alkylate). The m-isomer was not detected in the products of the runs. This could be due to the negligible formation (at the low temperatures used) of the kinetically less favoured m-isomer, and its not being detected at very small concentrations. At higher temperatures (say above 420 K) the o- and p-alkylates can isomerize into the thermodynamically more stable m-isomer. Earlier workers have also not reported its formation when the reaction was carried out at low temperatures [9-11]. Others have reported its presence when the reaction was carried out higher temperatures (above 420 K) over solid acid catalysts and have concluded that it is formed by the isomerization of the primary o- and p-products [5].

The overall conversion of phenol increases with duration of the run (studied upto 6h). At 373 K (Fig. 3-A.2 a), the yield of the *C*-alkylate is more than that of the *O*-alkylate (ether) though the yield of the ether is more than that of either the o- or p-alkylate. The selectivity ratio of the ether to the alkyl phenols (*O*-/*C*-alkylate ratio) decreases with duration of run. On the other hand, the o-/p-isomer ratio increases with duration of run. Earlier workers have suggested (based on studies at higher temperatures) that the ether (*O*-alkylate) is formed even over weak acid centers, while *C*-alkylation requires stronger acid

sites [6,8,12]. Also, they found that more ether was produced (increase in *O*-/*C*-alkylate ratio) with catalyst deactivation and increasing time on stream in both liquid and vapour-

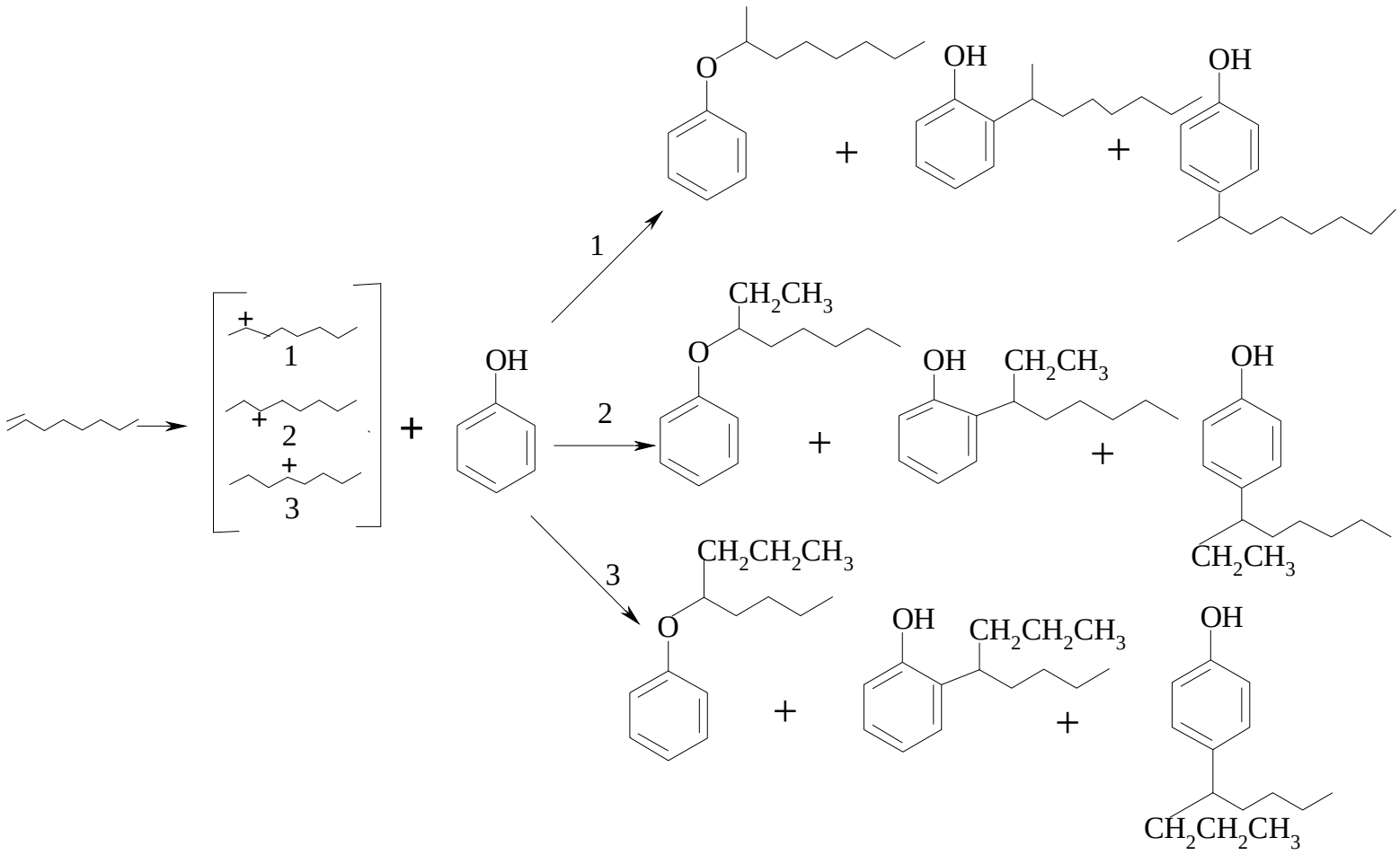

Fig. 3-A.1. Schematic representation of the reactions in the alkylation of phenol with 1-octene

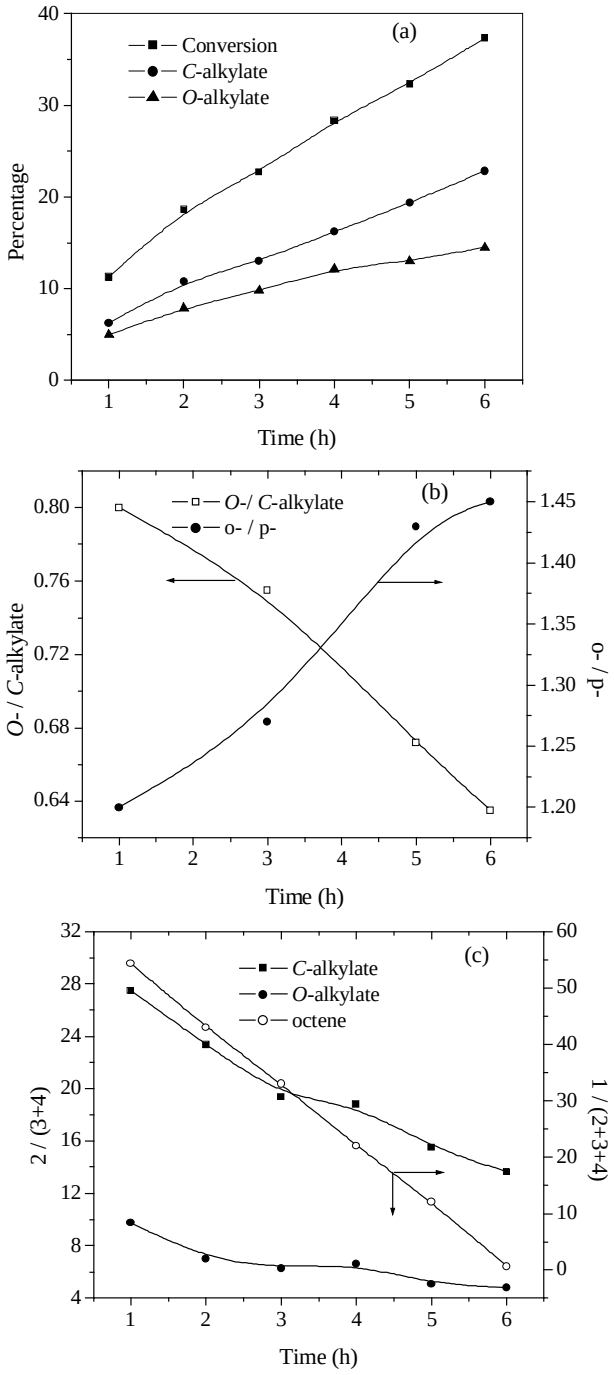

Fig. 3-A.2. Influence of duration of run on a) conversion and yields of *O*- and *C*-alkylate, b) *O*-/*C*- alkylate and o-/p-ratios and c) ratios of skeletal isomers in *O*- and *C*- alkylate and ratios of olefins (catalyst BEA, 0.2g; temperature: 373 K; phenol:1-octene (mole) = 1)

phase experiments on the alkylation of phenol with methanol carried out in the temperature range of 473 to 673 K [8,12]. The present observation on *O*-/*C*- ratio is different (Fig. 3-A.2 b).

This could be due to the different feeds used, 1-octene in this work and methanol by earlier workers [8,12]. Besides, reactions over zeolites are complicated in that a range of acid strengths are present in the samples, and the reaction can take place at the external surface, inside the pores and over amorphous material, if any. The relative contribution of the active centers in the different locations is expected to play a major role in determining the selectivity of the catalyst. In the case of the BEA sample used, it had a fairly large amount of external surface area (~ 25% of total) and it is likely that much reaction took place on the external acid sites. It also had a wide range of acid centers (Fig. 3-A.1). The decrease in *O*-/*C*- ratio and the increase in o-/p- ratio with duration of run can partly be explained by the isomerization of the ether into the alkyl phenol with increasing duration of run. Indeed, earlier workers have suggested the isomerization of anisole to *o*-cresol based on studies carried out at higher temperatures (473 – 673 K) on the alkylation of phenol with methanol over ZSM-5. However, negligible isomerization to octyl phenols was observed in this work when 2-octyl phenyl ether was heated with BEA at 373 K for 6 h. Therefore, the isomerization of the ether into alkyl phenols is not a likely reason for the present observations. The observed decrease in the *O*-/*C*- ratio is probably due to greater reactivity of the terminal olefin (1-octene), present in larger amounts in the beginning of the reaction (see below), for *O*-alkylation.

Internal olefins (isomeric octenes; 2, 3- and 4-octene) are also found in the product mixture (Fig. 3-A.2 c) confirming the occurrence of octene-isomerization. However, the observed isomer composition does not suggest the attainment of thermodynamic equilibrium even at the end of 6h at 373 K. The 1-/(2- + 3- + 4-) octene ratio at the end of 6

h is 0.66. Three isomeric *O*- and *C*-alkylates corresponding to the position of the phenoxy or phenyl group in the octane chain at 2-, 3- and 4-positions are formed (Fig. 3-A.1). The 1-isomer is not formed due to the poor stability of the 1-carbenium ion. At equilibrium, one would expect approximately equal amounts of the three isomers (2-, 3- and 4-), a 2-/(3- + 4-) ratio of about 0.5. However, it is noticed (Fig. 3-A.2 c) that the experimentally observed ratio is much higher. The deviation from equilibrium is much larger for the *C*-alkylate than for the *O*-alkylate. Within the *C*-alkylate, the *o*-isomer contains more 2- product than the p-isomer. With duration of run, the 2-/(3- + 4-) ratio decreases for both the *C*- and *O*-alkylates. Two different equilibrium steps can exist in the overall reaction: one for the equilibration of the olefin (octene) and another for the equilibration of the alkyl phenols/ethers [8]. At the low temperature used in this study (373 K), the latter equilibration reaction is expected to be much slower than olefin equilibration. The large amounts of the 2-isomer observed in the products is due the greater reactivity of the terminal olefin compared to the internal olefins [9-11] and the non attainment of olefin equilibrium. The differences in the ratios, 2- /(3- + 4-), between the *O*- and *C*- alkylates is probably due to many causes that include geometric constraints for the different transition states inside the pores, differences in the reactivity of the olefins, acidity distribution and the relative contribution from the external and internal areas to the two reactions.

3-A.3.4 Influence of catalyst amount:

The influence of catalyst amount on the alkylation of phenol with 1-octene was studied using different amounts of BEA (15). The conversion increases from 27 % to 40% as the catalyst amount is increased from 0.1 to 0.3 g (Fig. 3-A.3). The *C*- and *O*- alkylates also show an increasing trend with increase in the catalyst amount. The *O*-/*C*- and o-/p-ratios also increase with catalyst amount. The octene ratio (1/ (2+3+4)) shows a decrease as expected. It is seen from Fig. 3-A.3 that the 2- isomer is dominant and increases with

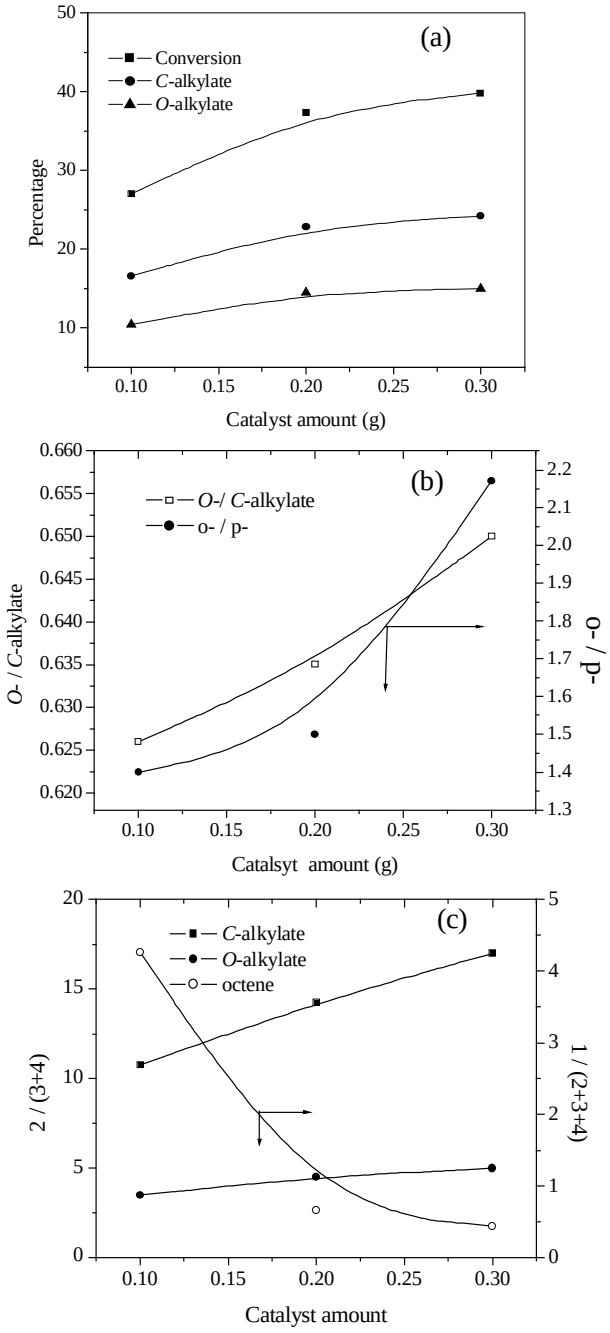

Fig. 3-A.3. Influence of catalyst amount on (a) conversion and yield of *C*-and *O*-alkylates, (b) *O*- / *C*-alkylate and o- / p- ratios and (c) ratios of skeletal isomers in *O*- and *C*- alkylate and ratios of olefins (catalyst = BEA, 0.2g; temperature: 373 K; phenol:1-octene (mole) = 1; duration of run = 6h)

increase in catalyst amount in both the *O*-and *C*- alkylates. In view of the marginal increase in conversion beyond 0.2 g catalyst loading, all other experiments were conducted using 0.2 g catalyst.

3-A.3.5 Influence of temperature:

Phenol conversion increases steadily from 12.5 % to 53.7 % as the reaction temperature is increased from 343 to 393 K (Fig. 3-A.4 a). The yields of both the *O*- and *C*-alkylates increase with temperature. The product ratios are found to be dependent on the reaction temperature, as can be seen from Fig. 3-A.4 b. The *O*-/*C*-alkylate ratio increases from 0.48 at 343 K to 0.69 at 393 K. The o-/ p- ratio also increases with temperature from 1.25 at 343 to 1.65 at 393 K. It is observed that 2-isomers are predominantly formed in both *O*- and *C*-alkylated products, though the 2- /(3- + 4-) ratio decreases with temperature (Fig. 3-A.4 c). This is in agreement with the results of the analysis of the octene isomers (Fig.3-A.4 c). The yield of the internal olefins increases with temperature, though equilibrium composition is not obtained even at 373 K. The second order rate constants of the reaction obtained at different temperatures are presented in Fig. 3-A.5. The rate constants for the overall reaction as well as the individual reactions increase with increasing temperature. The rate constant for the *C*-alkylated products ($k_{ortho\text{-alkylate}} + k_{para\text{-alkylate}}$) is higher than that for the *O*-alkylated product in the entire temperature range under study. The activation energy values (calculated from the rate constants) for the overall reaction and the two major reactions are presented in Table 3-A.1. The equations for rate constants are also given in the table. The activation energies for the two major reactions are similar, the value for *O*-alkylation being marginally larger.

In order to understand the two reactions better to and know if thermodynamic equilibria are reached in the experiments, the thermodynamic equilibrium constants (K_p) and equilibrium conversions were calculated using standard methods [13,14].

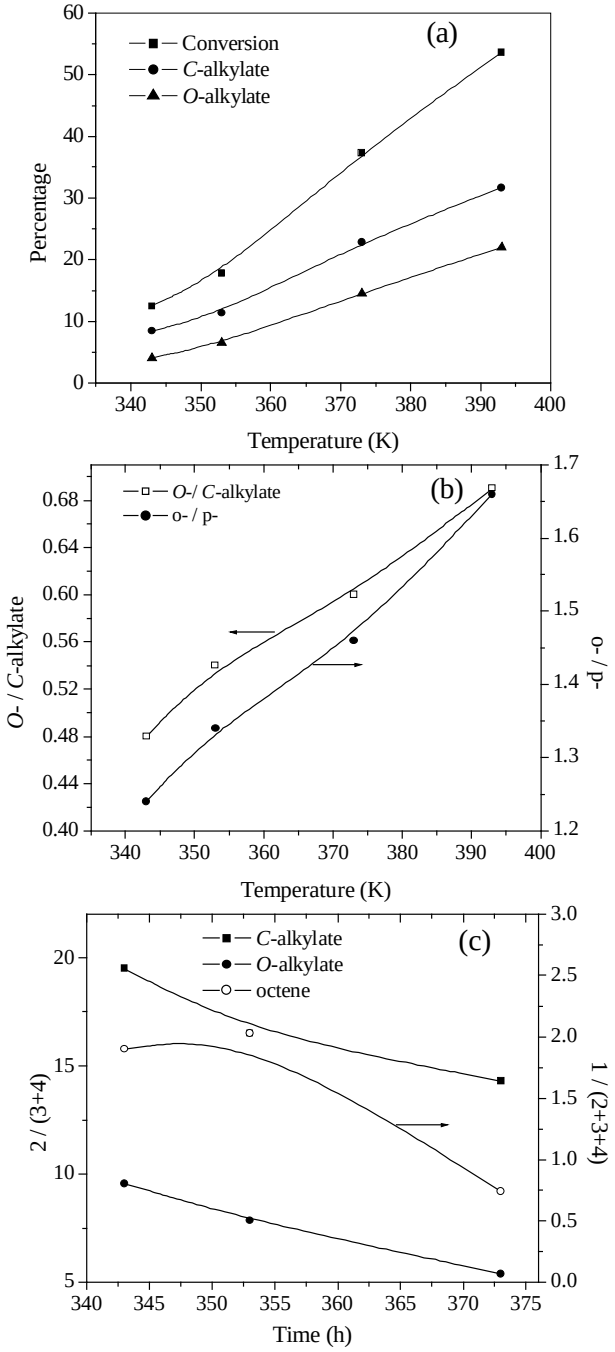

Fig.3-A.4. Influence of temperature of reaction on a) conversion and yields of *O*- and *C*-alkylate, b) *O*-/*C*- alkylate and o-/p-ratios and c) ratios of skeletal isomers in O- and C-alkylate and ratios of olefins (catalyst = BEA, 0.2g; phenol: 1-octene (mole) =1; duration of run = 6h)

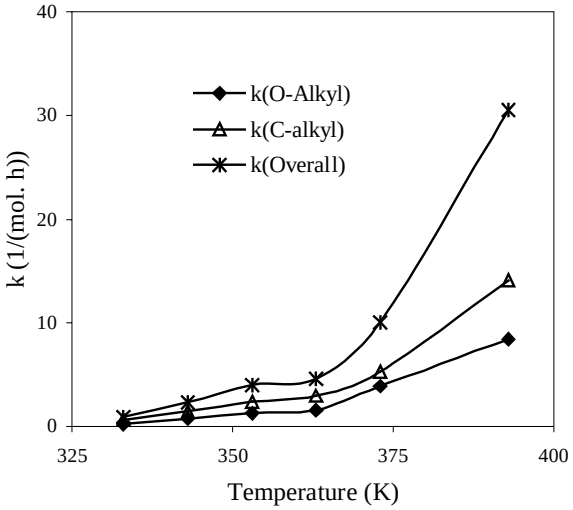

Fig.3-A.5. Influence of temperature on the rate constants for product formation in the alkylation of phenol with 1-octene (catalyst, BEA; phenol : 1-octene (mole) = 1)

Table 3-A.1: Activation energy and the equations for rate constants for phenol alkylation with 1-octene

Reaction	Activation energy (kCal/mole)	Equation for rate constant
Formation of O-alkylate	14.60	$k_{O\text{-}Alkyl} = 1.0\ E{+}09\ e^{(-14.60/RT)}$
Formation of C-alkylate	12.64	$k_{C\text{-}Alkyl} = 2.0\ E{+}08\ e^{(-12.64/RT)}$
Overall reaction	14.53	$k_{Overall} = 3.0\ E{+}09\ e^{(-14.34/RT)}$

The details of the calculations are presented in Chapter 2, section 2.6. A plot of the calculated K_p values at different temperatures for the formation of octyl phenyl ether and octyl phenols is presented in Fig. 3-A.6 a. The K_p value for the *C*- alkylate is larger than for the *O*-alkylate in the entire temperature range (200 to 1000 K), the difference becoming smaller at higher temperatures. In the temperature range of the calculations, there is a continuous decrease in K_p with temperature. The corresponding molar equilibrium

conversions and the actual conversions obtained (experimental) at different temperatures are presented in Fig. 3-A.6 b – d. In the narrow temperature range of the experiments (343 K to 393 K), the theoretical conversions remain nearly constant while the conversions experimentally obtained at the end of 6 h increase rapidly with temperature. It is noticed that experimental conversions are far below the equilibrium conversions at low temperatures and equilibrium conversions are reached only at temperatures above 380 K. It should, however, be noted that the calculated values are based on gas-phase thermodynamic data and the reactions have been carried out in the liquid phase. The excess conversions observed at high temperatures could be a result of this difference and the errors associated with the calculation of the thermodynamic data [13].

3-A.4.6 Influence of mole ratio:

The alkylation reaction was studied at three different mole ratios of phenol: 1-octene. The results of the studies are presented in Table 3-A.2. As expected, phenol conversion increases with increasing 1-octene. The *O*-/*C*-alkylate ratio decreases on increasing the amount of octene. The o-/p-isomer ratio is about the same for phenol : octene ratio of 0.5 and 1, but is larger when the ratio is two (Table 3-A.2). Earlier workers have found a decreasing trend for the *O*-/*C*-alkylate ratio for H-K-Y and an increasing trend for ZSM-5 in the reaction of phenol with methanol at temperatures (523 K for FAU and 643 K for MFI) higher than that used in this study [8,12]. Jacobs et al. have explained the observations based on the consecutive formation of the *C*-alkylates over FAU and the shape-selectivity effects of MFI [8]. As isomerization of the ether was not experimentally noticed at the low temperatures of this work over the large pore zeolite (BEA), the reasons have to be different (and are not yet clear). The ratios of the skeletal isomers (2- /(3- + 4-)) decreases on increasing the octene amount for both the *O*- and *C*-alkylates.

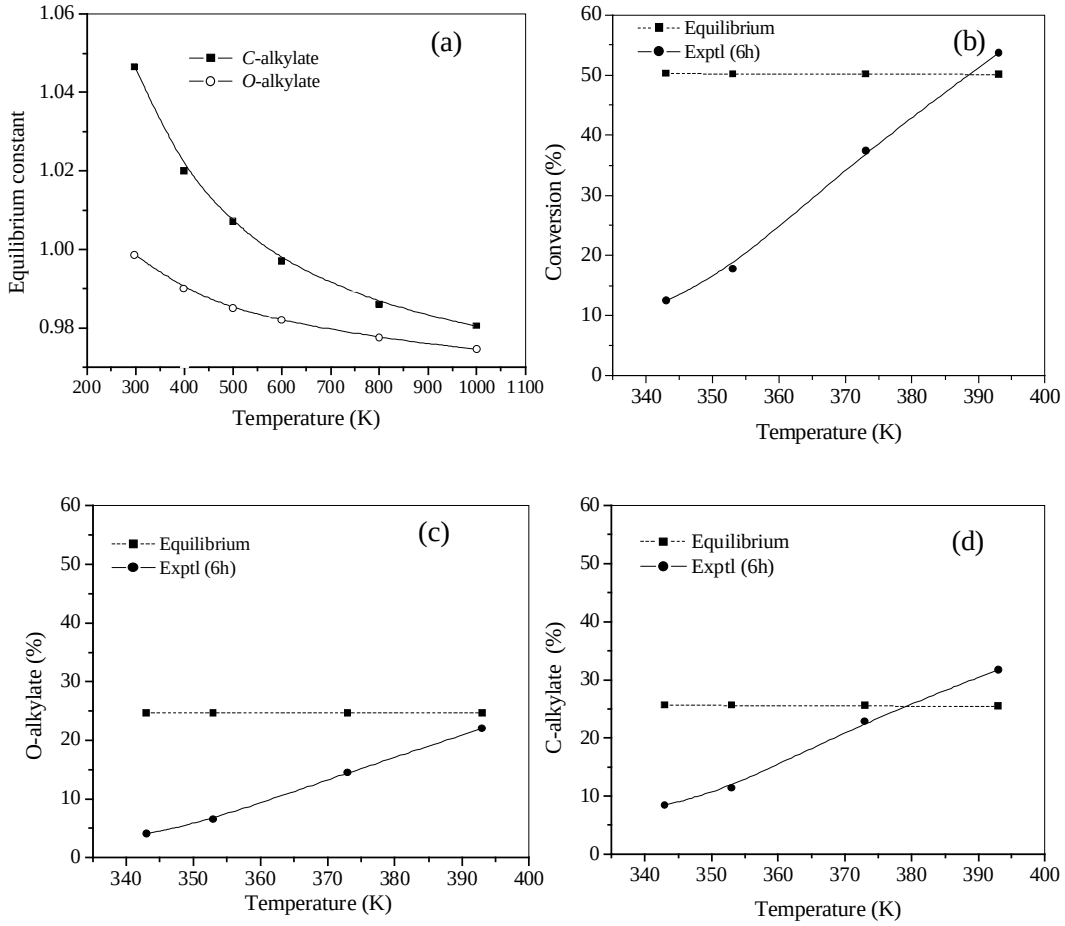

Fig. 3-A.6. (a) Influence of temperature on calculated equilibrium constant values for *O*- and *C*-alkylate and (b), (c) and (d) comparison of experimental conversions, *O*- and *C*-alkylate yields (respectively) with calculated equilibrium values at different temperatures (catalyst = BEA, 0,2g; phenol: 1-octene (mole) =1; duration of run = 6h)

Table 3-A.2: Effect of mole ratio of phenol: 1-octene on conversion and product yield (temperature: 373 K; catalyst: BEA(15), 0.2 g; reaction time: 6h; atmosphere: N_2)

Phenol :1-octene (mole)	Conversion of phenol (%)	Product yield (%)			*O*-/ *C*-alkylate	o-/ p-alkylate	2 / (3+4)	
		O-alkylate	Ortho-alkylate	Para-alkylate			*O*-	*C*-
1: 0.5	11.3	4.9	3.9	2.6	0.72	1.5	5.4	23.6
1: 1	37.3	14.5	13.5	9.3	0.64	1.5	4.8	13.7
1: 2	42.0	9.0	22.0	11.0	0.2	2.0	2.1	8.2

3-A.3.7 Influence of catalyst poisoning:

The effect of acidity on the two major reactions was investigated by systematic poisoning of BEA (15) with small amounts of sodium and potassium. The acidity of the poisoned catalysts calculated from TPD of NH_3 is presented in Chapter 2, Table 2.5, Fig. 2.3 a and b. As already pointed out (Chapter 2), the strong acid sites are suppressed to a greater degree by the K-ions than the weak acid sites. The performances of the poisoned catalysts are compared in Fig.3-A.7. As expected, conversion decreases with increase in alkali metal loading. It decreases from 37.4 % to 9.22 % with the addition of 0.4 mmol of K per g. The *O*-/*C*-alkylate ratio is not significantly affected by K-loading. This is surprising in view of the observations of the earlier workers that *O*-alkylation can take place on weaker acid sites while much stronger acidity is needed to catalyze *C*-alkylation. The o-/ p- ratio increases on K- poisoning. It is generally believed that both the o- and p-alkylates are the primary products, though some o- to p- transformation could occurs on strong acid sites [6,8,12]. The steady increase in the o-/ p- ratio with K-poisoning may be due to the suppression of the isomerization of the o- to the p- isomer.

The results of Na poisoning (Fig. 3-A.7B) are similar to those noticed for K-poisoning. Conversion and *O*- and *C*- alkylate production decrease with increasing Na-content. Though the o-/ p- ratio decreases as noticed in the case of K, the *C*-/ *O*- alkylate

ratio decreases at only large Na-loading. The reason for this is not clear. Differences in poisoning between Na and K could arise from the difference in basicity of the two ions and their locations inside the zeolite pores and on the external surface.

A kinetic analysis of the above studies was carried out and the rate constants calculated for total conversion, *O*- and *C*-alkylate production are presented in Fig. 3-A8 A (a) and (b), respectively for K and Na- poisoning. All the three k values show a decrease as the potassium or sodium loading increases. A noticeable decrease in k-value for *O* -alkylation is observed even at the lowest concentration of K (0.1 mmol/g), while the *C* - alkylation reaction is less affected (Fig. 3-A.8 A (a)). A plot of the k-values as a function of the number of strong acid centers in the samples is presented in Fig. 3-A.8 B. It is seen that both the *O*- and *C*-alkylation activities are directly related to the strong acidity.

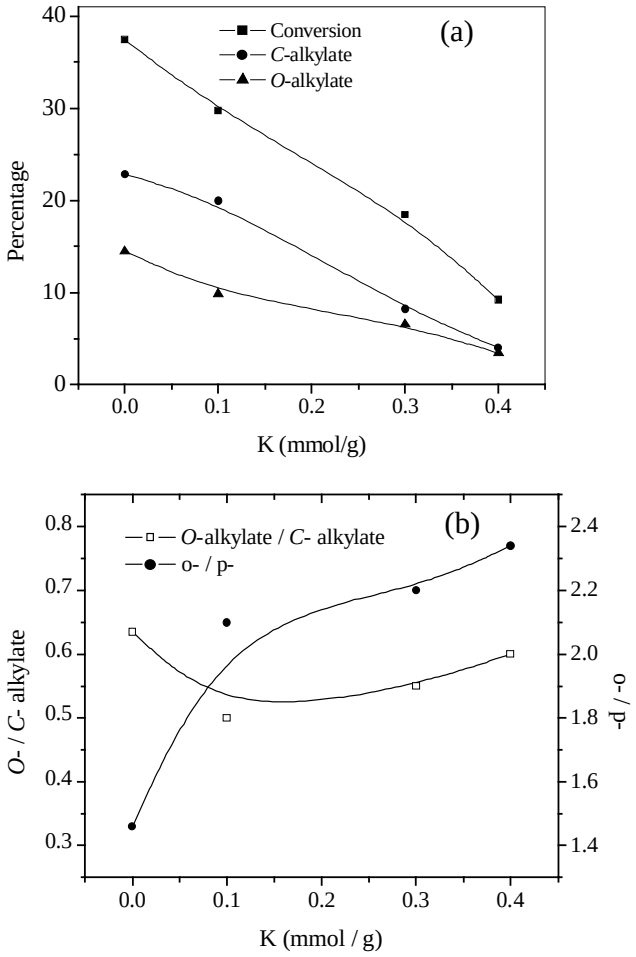

Fig. 3-A.7A. Influence of K-loading on a) conversion and yields of *O*- and *C*- alkylate and b) *O*-/*C*- alkylate and o/p ratios (catalyst = BEA, 0.2g; temperature: 373 K; phenol:1-octene (mole) = 1; duration of run = 6h)

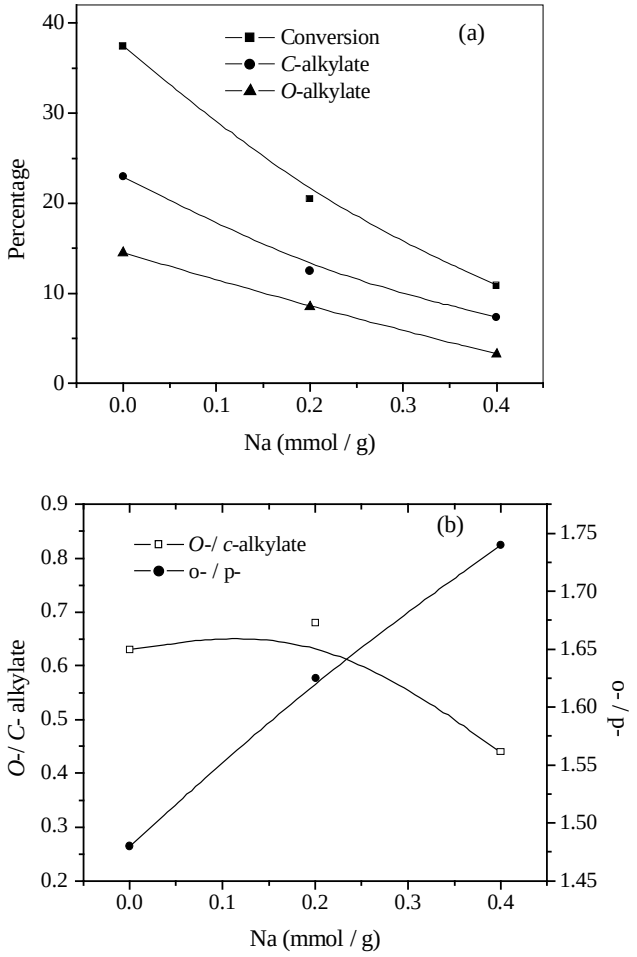

Fig. 3-A 7B. Influence of Na-loading on a) conversion and yields of *O*- and *C*- alkylate and *O*-/*C*-alkylate and o-/p-ratios (catalyst = BEA, 0.2g; temperature: 373 K; phenol:1-octene (mole) = 1, duration of run = 6h)

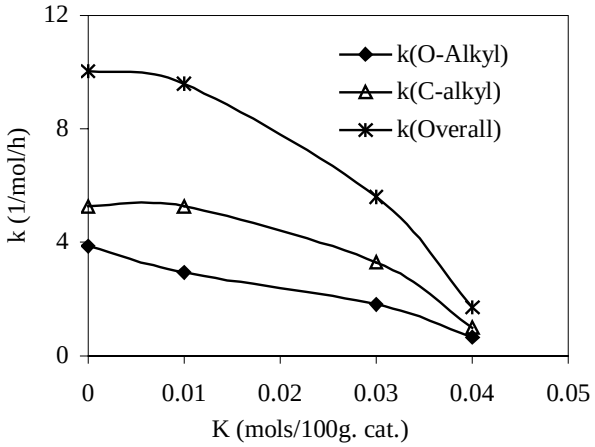

Fig. 3-A.8A (a) Effect of poisoning of BEA-15 (with potassium) on the rate constants of different reactions in alkylation of phenol with 1-octene (temperature: 373 K; catalyst weight: 0.2 g; phenol: 0.01 mol; phenol : 1-octene (mole) =1)

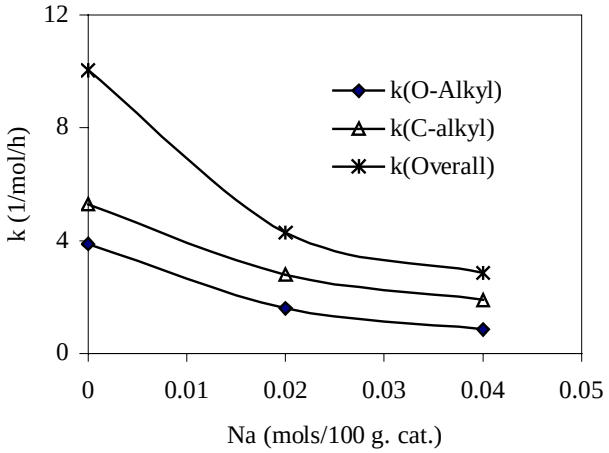

Fig. 3-A.8A (b) Effect of poisoning of BEA-15 (with sodium) on the rate constants of different reactions in alkylation of phenol with 1-octene (temperature: 373 K; catalyst weight: 0.2 g; phenol: 0.01 mol; phenol: 1-octene =1)

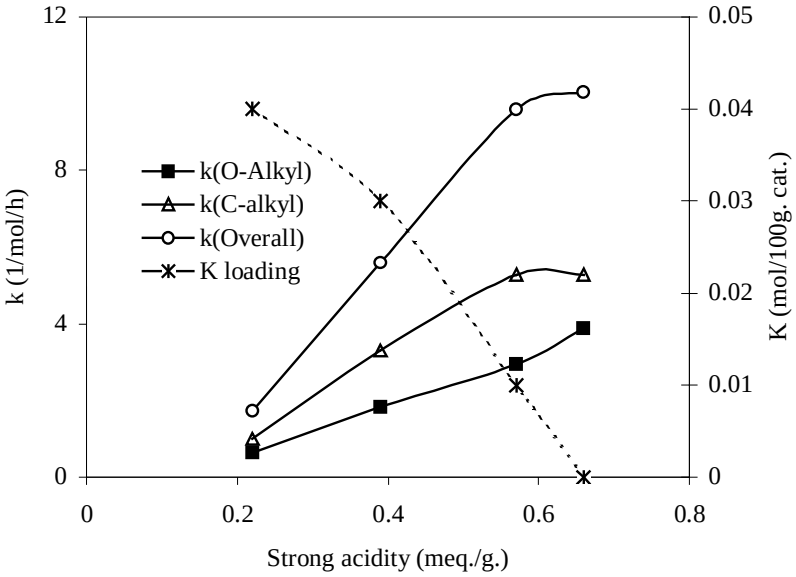

Fig. 3-A.8B Influence of acidity and K-content on the reaction rate constants in the alkylation of phenol BEA(15) poisoned with potassium

3-A.4.8 Influence of zeolite type:

A comparative study of the activities of the three large pore zeolites, viz. BEA(15), MOR(11) and FAU(15) (H-USY) in the alkylation of phenol with 1-octene was carried out. The results of the reaction carried out at 373 K are presented in Table 3-A.3. The ratio of skeletal isomers is also presented in the table.

Table 3-A.3: Effect of zeolite type on conversion and product yield in the alkylation of phenol with 1-octene (temperature: 373 K; catalyst quantity: 0.2 g.; reaction time: 6h; atmosphere: N_2)

Zeolite	Conversion of phenol (%)	Product yield (%)			*O*- / *C*-alkylate	o-/ p-	2 / (3+4)	
		O-alkylate	Ortho-alkylate	Para-alkylate			*O*-	*C*-
BEA(15)	37.3	14.5	13.5	9.3	0.64	1.45	4.8	13.6
FAU(15)	30.5	18.2	8.0	4.2	1.49	1.90	5.8	6.4
MOR(11)	10.3	2.4	4.4	3.6	0.30	1.22	6.7	17.6

The data collected at different run duration for MOR and FAU (H-USY) are presented in Figs. 3-A.9 and 3-A.10. The data of BEA was presented in Fig. 3-A.2. The relative activity of the zeolites for the reaction, in terms of phenol conversion (at 6h; Table 3-A.3) is in the order: BEA > FAU > MOR. The lower activity of MOR is probably due to its 2-dimensional pore structure and the absence of large pore intersections that can accommodate the reaction transition state. Conversion increases rather rapidly on both BEA and MOR with run duration (Figs. 3-A.2 and 9), but in the case of FAU, the increase with time is only marginal (Fig. 3A.10). It is likely that polymeric products (large molecules) are rapidly formed inside the large α-cages and mesopores in the FAU (H-USY) and poison the strong acid sites. BEA and MOR favour *C*-alkylate formation, and FAU favours *O*-alkylate formation; the *O*-/*C*- ratios obtained (at 6h) over BEA, MOR and FAU are, respectively, 0.6, 0.3 and 1.5. Examining the trend in the *O*-/*C*- ratio, it is found that it increases with time over MOR and FAU, but decreases in the case of BEA.

All the three catalysts favour the *o*-isomer formation; the o-/p- ratios (at 6h) over BEA, MOR and FAU are, respectively, 1.5, 1.2 and 1.9. The lowest o-/p- ratio observed for MOR suggests that product or transition state shape selectivity may be operating in the catalyst. In all the three zeolites, the o-isomer is formed preferentially due to kinetic effects. The 2/ (3+4) ratios for C-alkylate are larger (in case of all the three zeolites) than for the O-alkylate (Table 3-A.3). This suggests that the internal olefins react relatively more rapidly (than the terminal olefin) at the *O*-position than at the *C*-positions.

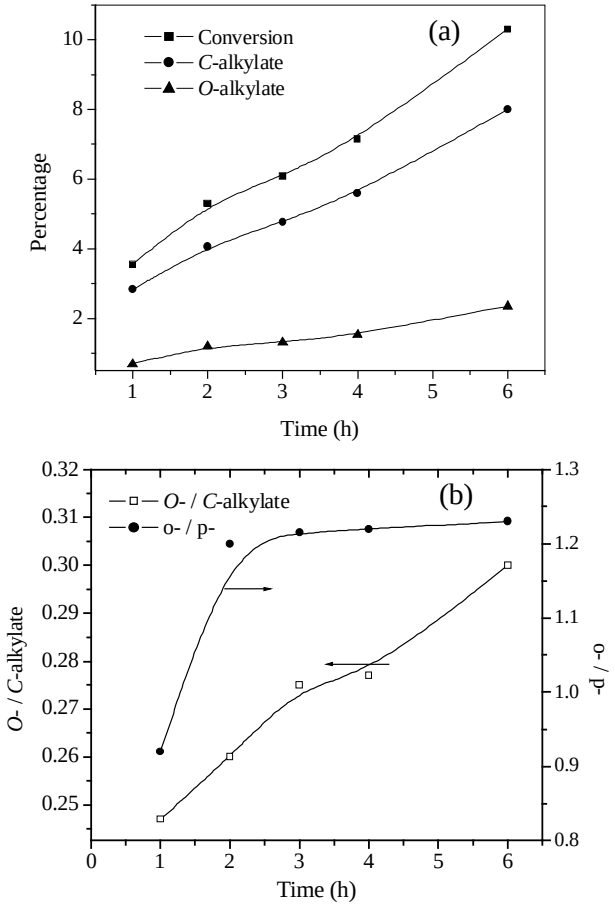

Fig. 3-A.9. Influence of duration of run on a) conversion and yields of *O*- and *C*- alkylate and b) *O*-/*C*- alkylate and o-/p-ratios (catalyst = MOR(11), 0.2g; temperature: 373 K; phenol:1-octene (mole) = 1)

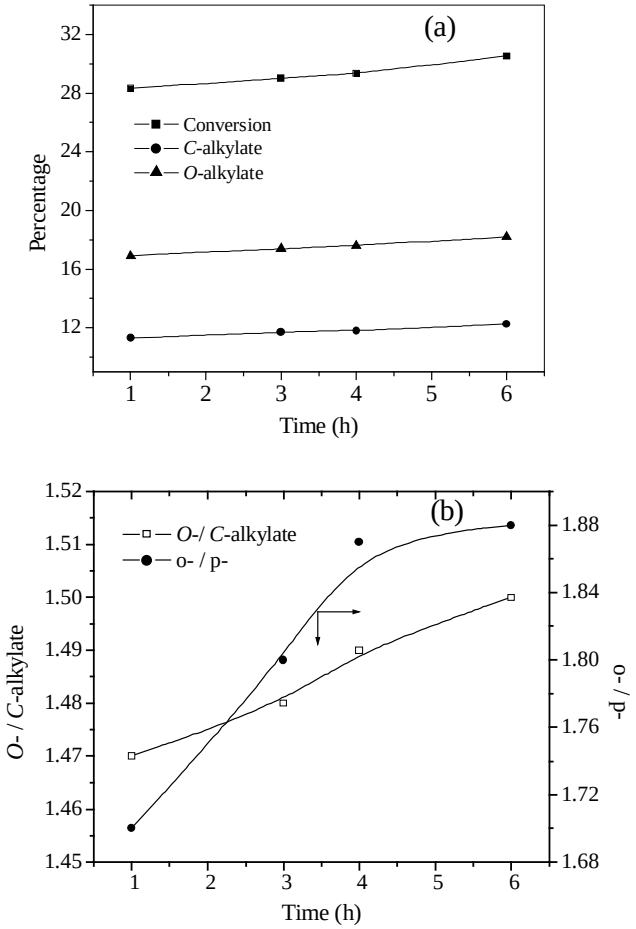

Fig. 3-A.10. Influence of duration of run on a) conversion and yields of *O*- and *C*-alkylate, and b) *O*-/*C*- alkylate and o-/p-ratios (catalyst = FAU(15) (H-USY), 0.2g; temperature: 373 K; phenol:1-octene (mole) = 1)

3-A.4 Conclusions:

Alkylation of phenol with 1-octene has been investigated over zeolite beta (BEA). The influence of different process parameters on the reaction was studied. The products of the reaction are phenyl octyl ether (from alkylation at the *O*-atom) and o- and p-octyl phenols (from alkylation at the *C*-atoms). The *C*- and *O*- alkylation reactions occur in parallel. During the reaction, simultaneous isomerization of 1-octene to the internal olefins occurs. As a result, isomeric products based on the attachment of the phenoxy or phenyl group at different positions (2-, 3- and 4-) in the C_8-chain are formed. The major isomeric product is the 2- isomer. The studies carried out in the temperature range of 343 to 393 K reveal that thermodynamic equilibrium conversion is reached only at about 393K at the end of 6 h of reaction. A comparison of the activity of BEA has also been made with those of two other large pore zeolites, mordenite (MOR) and H-USY (FAU) with nearly similar Si/Al ratios. The activity of the three zeolites is in the order BEA> FAU > MOR. BEA and MOR favour *C*-alkylation while, FAU favours *O*-alkylation. A kinetic analysis of the two parallel alkylation reactions, assuming second order kinetics, has been presented.

3-A.5 References:

1. (a) J. Xu, A. Yan, Q. Xu, React. Kinet. Catal. Lett., 62 (1997)71.

   (b) S. Balsaam, P. Beltrame, P.L. Beltrame, P. Carniti, L. Forni and G. Zuretti, Appl. Catal., 13 (1984) 161. (c) R. Pierantozzi, A. F. Nordquist, Appl. Catal. , 21 (1986) 263.

2. K. Zhang, C. Huang, H. Zhang, S. Xiang, S. Lui, D. Xu, H. Li, Appl. Catal. A., 207 (2001) 183.

3. (a)K. Zhang, C. Huang, H. Zhang, S. Xiang, S. Lui, D. Xu, H. Li, Appl. Catal. A., 166 (1998) 89. (b) A.V. Krishnan, K. Ojha, N.C. pradhan, Org. Proc. Res and Dev. 6 (2002)132.

4. S. Subramaniam, A. Mitra, C.V.V. Satyanarayana, D.K. Chakrabarty, Appl. Catal. A., 159 (1997) 229.

5. A. Sakthivel, S.K. Badamali, P. Selvam, Micropor. Mesopor. Mater. , 39 (2000) 457.

6. S.K. Badamali, A. Sakthivel, P. Selvam, Catal. Lett., 65 (2000) 153.

7. L.B. Young, Eur. Pat. Appl.0,029,333 (1980) Mobil Oil Co.

8. R.F. Parton, J.M. Jacobs, D.R, Huybrechts and P. A. Jacobs, Stud. Surf Sci. Catal., 46 (1988) 163.

9. H.R. Sonawane, V.G. Naik, B.C. Subba Rao, Indian J. Chem.,3 (1965) 26

10. H.R. Sonawane, M.S. Wadia, B.C. Subba Rao, Indian J. Chem., 6 (1968) 72.

11. H.R. Sonawane, M.S. Wadia, B.C. Subba Rao, Indian J. Chem., 6 (1968) 297.

12. S. Namba, T. Yashima, Y. Itaba, N. Hara, Stud. Surf. Sci. Catal., 5 (1980) 105.

13. R.C. Reid, J.M. Praunitz and T.K. Sherwood, “Properties of Gases and Liquids”, 3rd eds. Mc Graw Hill Book Co. (1988) Chapter 6 pg 150.

14. E.V. Sobrinho, D. Cardoso, E.F. Souza-Aguair, J. Braz. Chem. Soc., 9 (3) (1998) 225.

Chapter 3-B

Alkylation of Naphthalene with 2-Propanol

3-B.1 Introduction:

In naphthalene alkylation, electrophilic substitution in the α- position is kinetically preferred though the β-isomer is more stable. There is a strong hindrance for bulkier molecules at the α-position due to interaction with hydrogen in the 8-position [1]. This may not affect the rate of alkylation, but certainly affects the thermodynamic stability of the compound. MOPAC (Molecular Orbital Package Software) calculations [2] provides useful insights into shape selective alkylation. Due to higher frontier electron densities in the α-position (carbon 1, 4, 5 and 8) compared to β-position (carbon 2, 3, 6, and 7) in naphthalene, α-substitution of naphthalene is favored electronically. As β,β'-dialkylates are the desired products, this calls for the use of a shape selective catalyst to impose steric restriction to enhance β-substitution and limit α-substitution.

Several research groups [3,4] have found that 2,6-DIPN (2,6-di-isopropyl naphthalene) can be obtained with high selectivities over H-mordenite (H-MOR) by the alkylation of naphthalene with propene and iso-propanol. Horseley et al. [5] have shown by computer simulation that the diffusion of 2,6-DIPN inside the mordenite pore channel is easier than that of 2,7-DIPN. They concluded that such a difference in energy barrier may partially account for the observed higher selectivity of 2,6-DIPN in mordenites despite the critical diameters of both being very similar. Also, dealumination of mordenite [6] showed improvement in selectivity towards the product. This may be attributed to reduced contribution of external acid sites and reduction of unit cell dimensions [6d]. Poisoning of the external acid sites by silylation [7], by adsorption of water [8] and by deposition of cerium oxide [9] was found to enhance the selectivity of H-MOR for the formation of 2,6-DIPN. In the case of H-Y (FAU), the supercages provide enough space for multiple

reactions that lead to the preferential formation of the thermodynamically stable β-isopropyl naphthalene and the 2,6 and 2,7-isomers. Hence, no characteristic selective production of the 2,6-isomer with respect to the 2,7-isomer could be observed on Y zeolites [10].

Though considerable literature is available on the isopropylation of naphthalene over zeolites, studies using isopropyl alcohol or bromide as alkylating agents have been carried out in the presence of organic solvents [11]. The present work has been undertaken to study the isopropylation of naphthalene in the absence of organic solvents [12]. The influence of reaction parameters has been studied and the activity of different zeolites has been compared.

3-B.2 Experimental:

3-B.2.1 Materials:

BEA, MOR and FAU zeolites with different Si/Al ratios were used in this study. Details of the source and the methods used in the preparation of the samples have been reported in Chapter 2, section 2.1. The preparation of REY used in the studies is described in the same section. The reaction procedure, characterization and discussion are presented in Chapter 2, sections 2.3, 2.4 and 2.5 respectively. H-ZSM-5 and H-MCM-22 used in these studies were obtained from pilot plant unit of Catalysis Division at NCL, Pune, India.

3-B.3 Characterization of Zeolites:

The zeolites were characterized for their structure and chemical composition by XRD and chemical analysis, respectively. The XRD patterns of the zeolites showed good crystalinity and are comparable to the standard XRD patterns available in literature.

Si/Al ratios of the zeolites were determined by chemical analysis. The unit cell composition of the zeolites was calculated based on the Si/Al ratios. The Si/Al ratio and surface areas are presented in Table 3B.1. The Si/Al ratio varies from 2.3 to 20.4.

Table 3-B.1: Composition and surface areas of the zeolites

Zeolite	Si/Al	S_{BET} (m^2/g)
H-beta (BEA(15))	15.0	650
H-mordenite (MOR(11))	11.0	560
H-Y (FAU(2.6))	2.4	880
RE-Y (RE-FAU)	2.4	720
H-ZSM-5 (MFI)	20.4	413
H-MCM-22 (MWW)	2.7	505

3-B.4 Results and Discussion:

The isopropylation of naphthalene was carried out over six zeolites H-beta, H-Y, RE-Y, H-mordenite, H-MCM-22 and H-ZSM-5. The studies were carried out at different process conditions [temperatures of 448, 473 K and 498 K, pressures (with N_2) of 15 to 90 bars, IPA/naphthalene mole ratios of 1 to 3 and different periods of time (1.5 – 9h)] in the case of H-beta.

Isopropylation of naphthalene produces first the monoalkyl naphthalenes (α- and β-isopropyl naphthalenes; 1- and 2-IPN). The two isomers undergo further alkylation to produce the dialkylnaphthalenes. The isopropanol rapidly dehydrates into propene, which is the major alkylating agent. The various isopropyl naphthalenes that are formed in the reaction are shown in Scheme 3-B.1. Inter-conversions between the various isomers through isomerization have not been shown in the scheme.

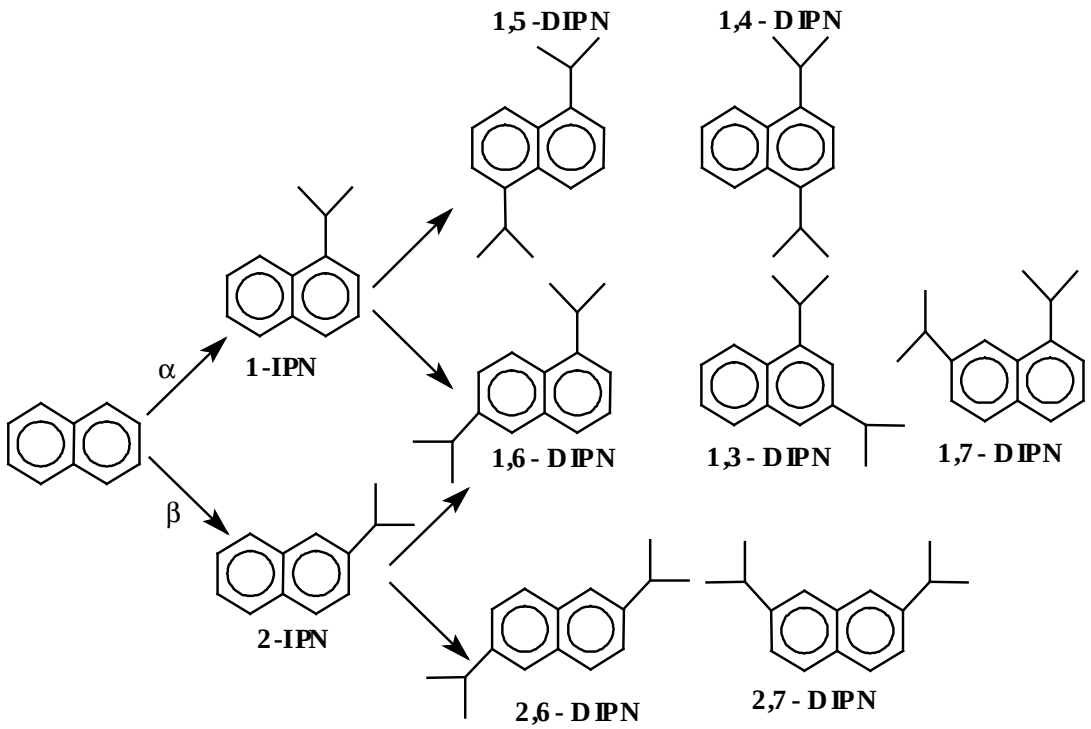

Scheme 3-B.1: The mono and isomeric diisopropyl naphthalenes formed during the isopropylation of naphthalene

3-B.4.1 Comparison of activities of zeolites:

The results of the isopropylation of naphthalene with isopropyl alcohol carried out over the zeolites are presented in Table 3-B.2. The zeolites may be arranged in the following order based on their performance w.r.t. naphthalene conversion, diisopropylnaphthalene (DIPN) selectivity and 2,6-/2,7-DIPN ratio.

H-beta > RE-Y > H-mordenite > H-Y > H-MCM-22 > H-ZSM-5 (conversion and DIPN selectivity)

H-mordenite > H-beta > H-Y > RE-Y (2,6-/2,7-DIPN ratio)

Naphthalene conversion is the highest for H-beta and RE-Y followed by H-mordenite. The lower conversion over H-Y is probably due to its possessing weaker acidity as a result of its high Al content. Due to the presence of RE-ions, RE-Y possesses stronger acidity than H-Y. The high conversion observed over H-beta can be attributed to a combination of two factors; the 3-D channel system made up of twelve-membered rings enabling rapid diffusion of the reactant and product molecules and the strong acidity arising from its large Si/Al ratio. Even though, H-mordenite (MOR(11)) possesses strong acid sites as in H-beta (BEA(15)) (Chapter 2, Table 2.4), its activity is lower due to its unidimensional pores (pore dimensions: BEA, 0.75 x 0.55nm; MOR, 0.67 x 7.1nm) and consequent diffusion limitations. H-ZSM-5 and H-MCM-22 exhibit lower activity due to their narrower pores and pore windows, which are made up of 10-membered rings. The small conversion noticed over these zeolites (Table 3-B.2) is probably due to the reaction at the external surface. Under the conditions of the reaction (473 K, IPA / naphthalene ratio = 2), the calculated equilibrium conversion of naphthalene is greater than 99%. The fact that the values are far below equilibrium value for all the zeolites investigated is probably due to poisoning/ deactivation of the catalyst by water and coke. Analysis of the gaseous fraction at the end of the run revealed it to be mainly propylene, suggesting that the observed lower conversions (than equilibrium value) is not due to depletion of olefin through oligomerization reactions.

DIPN selectivity follows the same trend as conversion. One would expect DIPN selectivity to be a function of catalyst activity, the concentration of MIPN in the reaction mixture and the zeolite pore dimensions. It appears that all the above effects are responsible for the observed trend in DIPN selectivity. As expected, among the large pore zeolites (mordenite, beta and Y), the 2,6-/2,7- ratio is highest for H-mordenite due to its unidimensional pore system. The ratios for H-ZSM-5 and H-MCM-22 are rather low due to

the absence of any shape selectivity as the reaction occurs mostly at the external surface. Besides, DIPN yield over these zeolites is very low and the reported ratios may not be accurate due to analytical errors.

Table 3-B.2: Comparison of activity of zeolites in isopropylation of naphthalene

Zeolite	Conv. (%)	Product yields (%)				DIPN selectivity (%)	Selectivity ratios	
		MIPN[1] (α)	MIPN[1] (β)	DIPN[2]	Others[3]		β / α	2,6-/2,7-
H-beta	63.4	21.9	15.3	18.3	8.0	28.8	0.7	0.9
H-mordenite	43.6	23.7	9.1	8.2	2.5	18.8	2.6	3.3
H-Y	22.1	6.4	12.7	2.0	1.1	9.0	0.5	0.6
RE-Y	62.4	13.9	27.7	15.4	5.4	24.7	0.5	0.5
H-ZSM-5	3.8	0.8	1.6	0.3	1.0	8.6	0.5	2.2
H-MCM-22	5.3	1.5	2.0	1.3	0.5	24.7	0.8	1.5

Reaction conditions: temperature: 473 K; pressure: 90 bars (with N_2); naphthalene: 0.02mol; IPA: 0.04mol; catalyst weight:1g.

[1]: MIPN = monoisopropylnaphthalene; [2]: DIPN = diisopropylnaphthalene;

[3]: mostly poly alkylated products and oligomers of propylene

3-B-4.2 Influence of process parameters:

The influence of temperature, naphthalene / IPA mole ratio, N_2 partial pressure are presented in Table 3-B.3 and the influence of duration of run (contact time) is presented in

Fig. 3-B.1. The experiments (except the last three in Table 3-B.3) were carried out over H-beta.

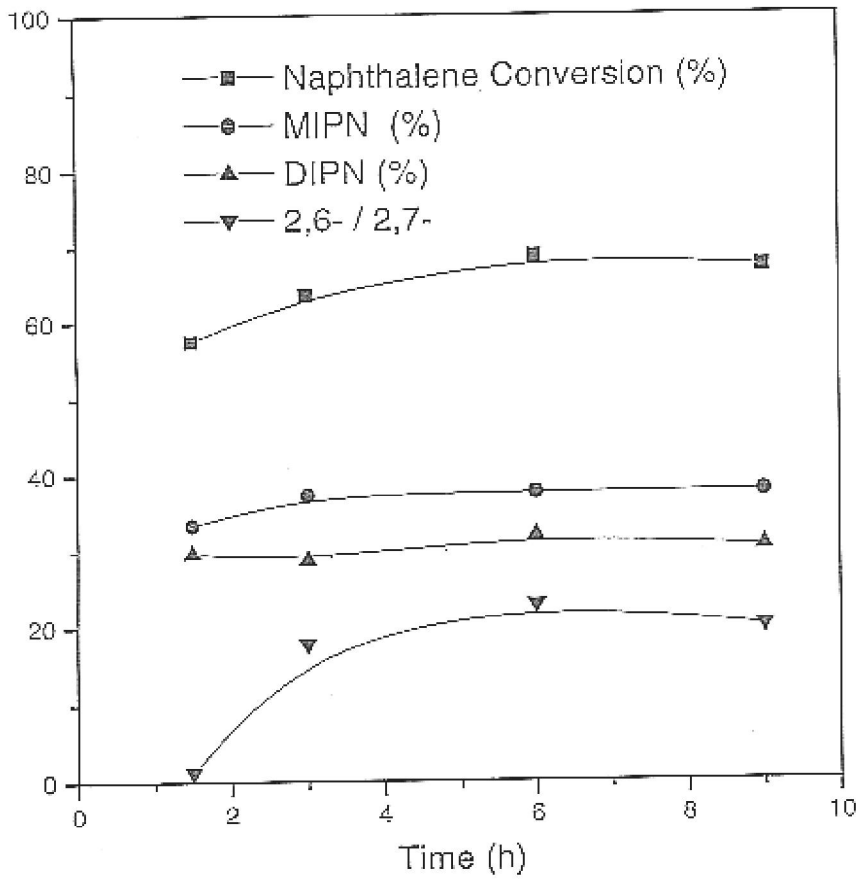

Fig. 3-B.1. Influence of duration of run on conversion and product distribution. (Reaction conditions: temperature: 473 K; pressure: 90 bars (with N_2); naphthalene: 0.02mol; IPA: 0.04mol; catalyst weight: 1g)

On increasing the reaction duration from 1.5 to 6h, conversion increased from 57.4 to 68.5% (Fig. 3-B.1). There was not much change on increasing the reaction time further to 9 hours. Similar trends are also observed for DIPN yield. The 2,6/ 2,7 –DIPN selectivity ratio increases to a maximum of 22.8 at the end of 6h after which it decreases slightly on further increase in reaction time. This shows that at the beginning of the reaction, the 2,6-isomer is formed in larger amounts by alkylation of MIPN inside the pore system and

isomerisation of 2,7-DIPN. Carrying out the reaction for prolonged periods leads to inter-conversion among the dialkyl isomers on the external surface leading to a small decrease in ratio.

When the temperature is increased from 448 to 473 K, naphthalene conversion increases from 34.0 to 63.4 %. On further increasing the temperature to 498 K, conversion decreases to 56.5%. This is probably due to rapid initial coking of the catalyst at higher temperatures and not due to any equilibrium limitation. The β/α ratio increases with increase in temperature again due to thermodynamic reasons; the β isomer is thermodynamically more stable than the α isomer at higher temperatures. Selectivity for DIPN also increases (14.2 to 30.9) with temperature (from 448 to 498 K).

The influence of the relative concentrations of IPA and naphthalene on the reaction was studied by varying the IPA to naphthalene mole ratio from 1 to 3. As the mole ratio is increased from 1 to 2, there is an increase in conversion from 52 to 63%. There is also a corresponding increase in the formation of dialkylates. However, on increasing the mole ratio from 2 to 3, there is a deterioration in the performance of the catalyst, as seen from the decrease in the conversion and selectivity values. This may be because, at higher concentrations of IPA, the effect of propene oligomerisation and cracking leading to coke deposition on the catalyst becomes significant. This results in a decrease in the activity of the catalyst and hence lower conversion and selectivity values. Besides, the larger amount of water formed from IPA (at higher IPA content) might also be poisoning the catalyst more.

The influence of pressure on the reaction was studied by varying the pressure from 15 to 90 bars at a reaction temperature of 473 K. Table 3-B.3 shows that there is less effect of pressure (as expected) as compared to that of temperature. There is a small decrease in conversion, followed by a small increase when the pressure is raised from 15 to 46 and

Table 3-B.3- Influence of reaction parameters on isopropylation of naphthalene over H-beta[1]

Parameter			Conv.	Product yields (%)				Selectivity	Selectivity ratios	
Temp (K)	Press. (bar)	IPA/Naph. (mole ratio)	(%)	MIPN (α)	MIPN (β)	DIPN	Others	for DIPN	β/ α	2,6/2,7
448	90	2	34.0	25.7	10.1	3.2	1.0	14.3	0.65	1.1
473	90	2	63.4	21.4	15.8	18.3	8.0	28.8	0.74	0.9
498	90	2	56.5	11.6	18.2	17.4	9.2	30.9	1.57	1.0
473	90	1	51.9	11.8	22.0	13.7	4.4	26.5	1.86	1.0
473	90	3	51.6	19.9	13.9	12.1	5.8	23.4	0.70	1.5
473	15	2	58.7	16.6	15.6	18.3	6.2	31.1	0.94	0.9
473	46	2	55.8	19.8	14.3	15.3	6.4	27.4	0.72	1.0
473	90	2	43.6	9.1	23.7	8.2	2.5	18.8	2.60	3.3
473[2]	-	2	35.4	7.6	19.2	5.9	2.7	16.7	2.53	3.1
473[3]	-	2	11.5	3.0	5.7	0.8	2.0	7.2	1.91	3.1

[1]: Catalyst wt.: 1g.; N_2 used for pressurization; last 3 experiments carried out over HM; [2]: no solvent or N_2 used; [3]: cyclohexane (50ml) used as solvent; MIPN = monoisopropylnaphthalene; DIPN = diisopropylnaphthalene; others = mostly poly alkylated products and oligomers of propylene

further to 90 bars. There is a gradual decrease in concentration of MIPN, the DIPN concentration decreases a little and comes back to the initial value of 18.2 % and the 2,6/ 2,7-DIPN selectivity ratio remains between16.2 and 18.7 on increase in reaction pressure.

Much of the reported work on alkylation of naphthalene using IPA have been carried out in an organic solvent. The use of large organic molecules as solvents in reactions involving zeolites is likely to create difficulties due to competitive adsorption of the solvent and counter diffusion problems. In this study, we have carried out the reactions in the absence of an organic solvent, but in nitrogen medium. To examine the influence of using a solvent, a reaction was carried out in using cyclohexane as solvent and another in the absence of any added material. The results of these experiments and that done in N_2 are presented in Table 3-B.3. The conversion and selectivity values are low when the reaction is carried out neat (only with IPA and naphthalene) or when cyclohexane is used as the reaction medium. Moreau et al. had earlier reported a lower conversion (~20%) under similar conditions using cyclohexane as solvent.

3-B.5 Conclusions:

The alkylation of naphthalene with isopropanol was carried out over various zeolites (H-beta, H-Y, RE-Y, H-mordenite, H-MCM-22 and H-ZSM-5) in the absence of organic solvent, using nitrogen as the reaction medium. A comparison of the activity of H-Y, RE-Y, H-beta and H-mordenite in the isopropylation of naphthalene with isopropanol shows that H-beta is the most active. RE-Y is more active compared to its H-form. H-MCM-22 and H-ZSM-5 were poor catalysts for the reaction, mainly because the active sites are inaccessible to the reactant naphthalene. Though conversion over H-mordenite is lower than over H-beta and RE-Y, 2,6-DIPN selectivity is highest over this zeolite due to its shape selective nature.

The reaction is rapid over H-beta and maximum product yields are reached in three hours at 473 K. However, further increase in temperature to 498 K, leads to a decrease in

the catalyst activity, due to deactivation of catalyst by coking. Highest conversion of naphthalene is observed when stoichiometric amount of IPA (IPA/naphthalene mole ratio = 2) is used. On increasing the mole ratio from 2 to 3, there is a deterioration in the performance of the catalyst. This is probably due to the oligomerization of propylene leading to coke deposition on the catalyst. A comparison of the reaction in cyclohexane, N_2 and without any medium shows that the reaction proceeds better in N_2 with higher activity and selectivity.

3-B.6 References:

1. J.S. Beck and W.O. Haag, "Alkylation of aromatics, Handbook of Heterogeneous Catalysis", edited by G. Ertl, H. Knozinger, J. Weitkamp, vol. 5, (1997).
2. C. Song, X. Ma, A.D. Schmitz, H. Harold; Appl. Catal. A., 182 (1999) 175.
3. (a) A.D. Schmitz, C. Song, Prepr. Pap.- Am. Chem. Soc. Div. Of Fuel Chem., 39 (1994) 986. (b) J.H. Kim, T. Matsuzaki, K. Takeuchi, T. Hanoka, Y. Kubota, X. Tu, M. Matsumoto, Microporous Mater., 5 (1995) 113. (c) J.H. Kim, T. Matsuzaki, K. Takeuchi, T. Hanoka, Y. Kubota, Y. Sugi, X. Tu, M. Matsumoto, Trans. Mater. Res. Soc. Jpn., 15 A (1994) 153. (d) A.D. Schmitz, C. Song, Catal. Today, 31 (1996) 19.
4. (a) C. Song, S.Kirby, Prepr. Am. Chem. Soc; Div. Petro. Chem. 38 (1993) 784 (b) S.J. Chu, Yu Wen-Chen, Ind. Engg. Echem. Res. 33 (1994) 3112.
5. J. A. Horsley, J. D. Fellmann, E. G. Derouane, M. C. Freeman, J. Catal., 147(1994) 231.
6. (a) K.M. Reddy, C. Song, Catal.Today, 31 (1996) 137. (b) D. Mravec, J. Chylik, M. Michvocik, M. Hronec, A. Smieskova, P. Hudec, Chem. Papers., 52 (1998) 218. (c) C. Song, A. D. Schmidtz, Sekiyu Gakkaishi, 42 (1999) 287. C. A. 131: 300754. (d) C. Song, A.D. Schmidtz, M. Reddy, Proc. 12th Int. Zeolite Conf., Vol.2, edited by Treacy M M J, Materials Research Soc., Warrendale, Pa, (1999) 1133. (e) Y.Sugi, T. Matsuzaki, T. Hanaoka, Y. Kubota, J.H. Kim, T. Tu, M. Matsumoto, Stud. Surf. Sci. Catal., 90 (1994) 397. (f) J.H. Kim, T. Matsuzaki, K. Takeuchi,T. Hanaoka, Y. Kubota, Y. Sugi, T. Tu, M. Matsumoto, Trans. Mater. Chem. Soc. Jpn., 15A (1994) 153. (g) A.D. Schmidtz, C. Song, Catal. Today, 31 (1996) 19 (h) A.D. Schmidtz, C. Song, Catal. Lett., 40 (1996) 59.
7 P. Moreau, A. Finiels, P. Geneste, J. Catal., 136 (1992) 487.
8 A.D. Schmidtz, C. Song, Catal. Lett., 40 (1996) 59.

9 (a) J.H. Kim, Y.Sugi, T. Matsuzaki,T. Hanaoka, Y. Kubota, T. Tu, M. Matsumoto, S. Nakata, A. Kato, Appl. Catal. A., 131(1995) 15. (b) D. Mravec, J. Chylik, M. Michvocik, M. Hronec, A. Smieskova, P. Hudec, Che. Pap., 52 (1998) 218.(c) Y.Sugi, J.H. Kim, T. Matsuzaki, T. Hanaoka, Y. Kubota, T. Tu, M. Matsumoto, Stud. Surf. Sci. Catal., 84 (1994) 1837. (d) Y. Sugi, T. Hanaoka, Sekiyu Gakkaishi, 41 (1998) 193. C.A. 129: 27605. (e) D. Mravec, M. Michvocik, M. Hronec, Pet. Coal, 39 (1997) 27. C.A. 128: 275633. (f) I. Tseng, J. Wu, Y. Chen, J. Chin. Inst. Chem. Eng., 30 (1999) 93. C. A. 131: 103742. (g) Y.Sugi, K. Nakajima, S. Tawada, J.H. Kim, T. Hanaoka, T. Matsuzaki, Y. Kubota, K. Kunimori, Stud. Surf. Sci. Catal., 125 (1999) 359.

10 J. Wang, J. Park, Y. Lee, W. Chul, J. Catal., 220 (2003) 265.

11 C. Song, S. Kirby, Microporous Mater., 2 (1994) 467.

12 (a) I. Matthew, S. Mayadevi, S. Sabne, S.A. Pardhy, S. Sivasanker, React. Kinet. Catal. Lett., 74 (2001) 119. (b) I. Matthew, S. Sabne, S. Mayadevi, S.A. Pardhy, S. Sivasanker, Indian J. Chem. Tech. 8 (2001) 469.

Chapter 4

Acylation of Aromatics

4.1 Introduction:

Friedel-Crafts acylation of aromatics using mineral acids has proved to be of great importance in organic chemical synthesis. Considerable efforts are being made to find suitable recyclable and environment-friendly solid acid catalysts, which can successfully carry out acylation reactions with anhydrides and acids as acylating reagents. In this respect, zeolites and in general solid acid catalysts containing Brönsted acid sites have been reported to be suitable catalysts for carrying out the acylation of activated aromatic rings such as anisole with carboxylic acids [1,2]. Synthetic zeolites are solid acids that can be tailored to suit the desired reaction and are therefore promising heterogenous catalysts for acylation reactions. Zeolites with different acid strength distributions, framework Si/Al ratios and structures can be used to tune the reaction to achieve the desired conversion and product selectivity, especially when other competing side reactions are present. It can be expected that the combination of strong acidity with built-in shape selectivity of zeolites will favour the regioselective formation of the required para-product.

Good yields and selectivities have been reported over large pore zeolites with pores and cavities sufficiently large to fit the Weyland's Friedel-Crafts intermediates. In the case of anisole, the aromatic ring is highly activated and, therefore, the acidity of the zeolites is sufficient to carry out such reactions [3,4]. The activity of various cation-exchanged Y-type zeolites in the acylation of toluene has been studied using octanoic acid as acylating agent [5]. The most efficient catalysts were the rare earth exchanged zeolites (70% exchange). These gave 75% yield of the acylated product with 94% selectivity for the para-isomer. The earliest results were published by Chiche et al.[6] who studied the acylation of toluene and p-xylene with straight chain carboxylic acids catalyzed by CeNa-Y in the liquid phase. They observed a para-isomer yield of at least 94% with all acids studied. The high positional selectivity was attributed by the authors to the shape selectivity of the zeolites. In the

acylation of p-xylene, the maximum yield of the acylated product was found to be proportional to the chain length for acids of carbon numbers C_{12} to C_{20}. For longer chains, the yield decreased suggesting that large substrates could not penetrate the cavities and interact with the active sites. It was therefore reasonably supposed that the reaction occurred in the intracrystalline space (inside the porous network) instead of only on the surface.

Ma et al.[7] studied in detail the Friedel-Crafts acylation of anisole with alkanoic acids, anhydrides and substituted benzoic acids over zeolites. When carboxylic acids were used as acylating agents, the activity of the Y zeolite increased with its Lewis acidity, showing that the Lewis acid sites were more active than the Brönsted acid sites. The mechanism suggested was an attack by the electrophilic intermediate, formed from the acylating agent over the zeolite acid sites, at the aromatic ring of anisole. The structure of the electrophilic intermediate would depend on the acylating reagent and the nature of zeolite acid sites. The carboxylic acid would lead to the protonated and coordinated carboxylic acid as the electrophile, respectively, over the Brönsted and Lewis acid sites. The protonated carboxylic acid would preferentially attack at the oxygen atom of anisole and yield the phenyl carboxlic ester, while the coordinated carboxylic acid and acylium ion would predominantly react with the aromatic ring leading to the Friedel-Crafts acylated product, 4-acyl anisole. Freese et al.[8] have reported the Friedel-Crafts acylation of anisole by acetic anhydride and the Fries rearrangement of the ester in the liquid phase over the H-form of various zeolites. Zeolite beta was found to be most active catalyst for acylation compared to H-Y and H-ZSM-5. The selectivity for the para-isomer was higher than 99% with the formation of only trace amounts of ortho-isomers. By-products from the scission of the C-O bond of anisole, methanol and phenol, were not observed. It was also observed that the activity of the zeolite was strongly dependent on run time. Comparing the activities of

NH_4-Y and H-Y, it appeared that the presence of Brönsted acid sites was a necessary prerequisite for catalytic activity. On the other hand, dealumination of H-beta (Si/Al = 90), i.e. a reduction of the number of Brönsted acid sites, increased the catalytic activity in the initial stages though the final conversion was similar to that of the parent BEA (Si/Al = 12). This behavior was attributed to different factors. Besides change in acidity, dealumination is accompanied by changes in pore distribution. The improved diffusion in the initial stages was suggested to lead to an initial higher activity until coking reactions became predominant. Consequently, the decrease in activity at longer run duration was attributed either to coke deposition or mass transfer limitations. Smith et al. have reported that H-beta can be recovered, regenerated and reused to give almost the same yield as that given by the fresh zeolite [9]. When Friedel-Crafts acylation of aromatics was performed with carboxylic acids over cation exchanged montmorillonite, the ketone yields were found to be dependent upon the nature of the interlayer cation and on the acid chain length [10]. The use of α,β-unsaturated organic acids such as acrylic, crotonic and methyl crotonic acids as acylating agents for the acylation of anisole over heteropoly acids (HPA) has been reported by Castro et al. [11]. As these acids can both acylate and alkylate, a study of the competing reactions was of interest. It was observed that the catalyst was more active for acylation than alkylation also its activity was reported to be greater than that of zeolites H-Y and H-beta. The use of Fe or Zn salts impreganated on K-10 montmorillonite clays as acylation catalysts was also studied by Yadav et al. [12]. It was observed that the catalyst could be reused with no significant effect on the conversion if it was again impregnated with ferric chloride or zinc chloride. Studies on the benzoylation of toluene [13] over super acids reveal that the yields of products are higher when benzoyl chloride is used rather than the anhydride. Benzoylation of veratrole over large pore zeolites has been reported [14]. The effect of various reaction parameters on the initial rate of the reaction of veratrole with benzoic

anhydride over H-Y zeolite was studied. Benzouhanova [15] studied the acylation of several substrates (such as benzene, naphthalene or aromatic heterocycles) over different zeolite catalysts using acid chlorides, anhydrides and carboxylic acids. The mechanism of acylation in the presence of zeolites was supposed to include acylium cation as the electrophilic species. The acylation of benzofuran and 2-methyl benzofuran in a fixed bed reactor over Y zeolite showed that 2-methyl benzofuran was twice as active as benzofuran. About 100 % conversion with 95 % selectivity were obtained in the acylation of 2-methyl benzofuran [16]. An interesting study on catalyst deactivation in the acylation of anisole with acetic anhydride over zeolite beta catalyst was made by Rohan et al. [17]. p-Methoxyacetophenone was selectively and rapidly formed on the fresh catalyst. However, a rapid deactivation occured which could be attributed to a large extent to the retention of di- and triacylated anisole in significant amounts in the large mesopore volume of the zeolite, thereby leading to blocked pores and deactivation. A review of the acylation of several aromatic compounds has been presented by Jasra [18]. Acylation of aromatics such as anisole, toluene, veratrole, 2-methoxy naphthalene and isobutylbenzene over solid acid catalysts and the application of the acylated products have been discuss ed.

4.2 Experimental:

4.2.1 Materials:

BEA, MOR and FAU zeolites with different Si/Al ratios were used in this study. Details of the source and the methods used in the preparation of the samples have been reported in Chapter 2, section 2.1. Hexanoic, octanoic and decanoic acids used in the experiments were obtained from s.d Fine Chemicals, India, Merck, India and Aldrich, USA respectively.

Details of the characterization of the samples and the experimental methods adopted in carrying out the acylation reaction and product analysis are also presented in Chapter 2, section 2.5, and 2.3 respectively.

4.3 Results and Discussion:

The catalysts used in these studies were BEA, MOR and FAU with different Si/Al ratios. The samples were characterized by adsorption, XRD and TPD (of NH_3) studies. The results of these studies have been presented in Chapter 2 section 2.5 (Fig. 2.1 and Fig. 2.2 and Tables 2.4) and discussed. The general observation is that the acidity of the zeolites decreases, as expected, with Si/Al ratio.

The acylation of anisole with long chain acids produces mainly the ketone (4-methoxy phenyl alkyl ketone) and small amounts of the ester (phenyl alkanoate) as shown in Chapter 1, section 1.5.4, Scheme 1.4 and Fig. 4.1 (a). The acylation of anisole was found to occur predominantly at the p-position (4-position). The formation of the m-isomer was not noticed at the experimental conditions used though a small amount of the o-isomer was found, especially at higher temperatures. As the yield of the o-isomer was small in most of the experiments, it is not being reported separately. Some workers have reported the formation of small amounts (a few percent) of the o- and m-isomers [7,8] while others [5,9] have not reported their formation. It appears that the production of the o- and m-isomers is more noticeable when anhydrides are used as the acylating agents [8]. The ester product was formed in very small amounts (a few percent) in all the experiments. The formation of the ester is a result of the demethylation of anisole and esterification of the phenol formed. However, methanol was not detected in the product due (presumably) to the temperatures used (403 – 428K) in the experiments being much above the boiling point of methanol (338K). It is pointed out that the anisole used did not contain any detectable amount of

phenol and the ester cannot be attributed to any phenol impurity. Diacylation products were also not detected.

The acylation of anisole was carried out with three different long chain acids, hexanoic, octanoic and decanoic acids, in the temperature range of 403 – 428K and different mole ratios of anisole to acid (2 – 8). The reactions were generally conducted over a period of 6h. The catalysts used were BEA, MOR and FAU with different Si/Al ratios. As excess anisole was used in the experiments, the conversions reported are based on the acid.

4.3.1 Hexanoic acid:

The influence of run duration on the acylation of anisole (at 413K and 428 K) with hexanoic acid over BEA(15) is presented in Fig. 4.1. The reaction proceeds rapidly in the beginning and slows down after about 4 h especially at 428 K. The major product is 4-methoxyphenyl hexyl ketone along with small amounts of the ester (phenyl hexanoate). As the ester formation is noticed from the beginning (even at 1h), it is also, apparently, a primary product formed from anisole.

The influence of catalyst (BEA(15)) amount on the reaction is presented in Fig.4. 2. A three-fold increase in catalyst amount from 0.05 g to 1.5 g increases conversion by only about 1.3 times. Such a limited increase is often noticed when catalyst loadings is increased, and could arise form thermodynamic or mass-transfer limitations [8].

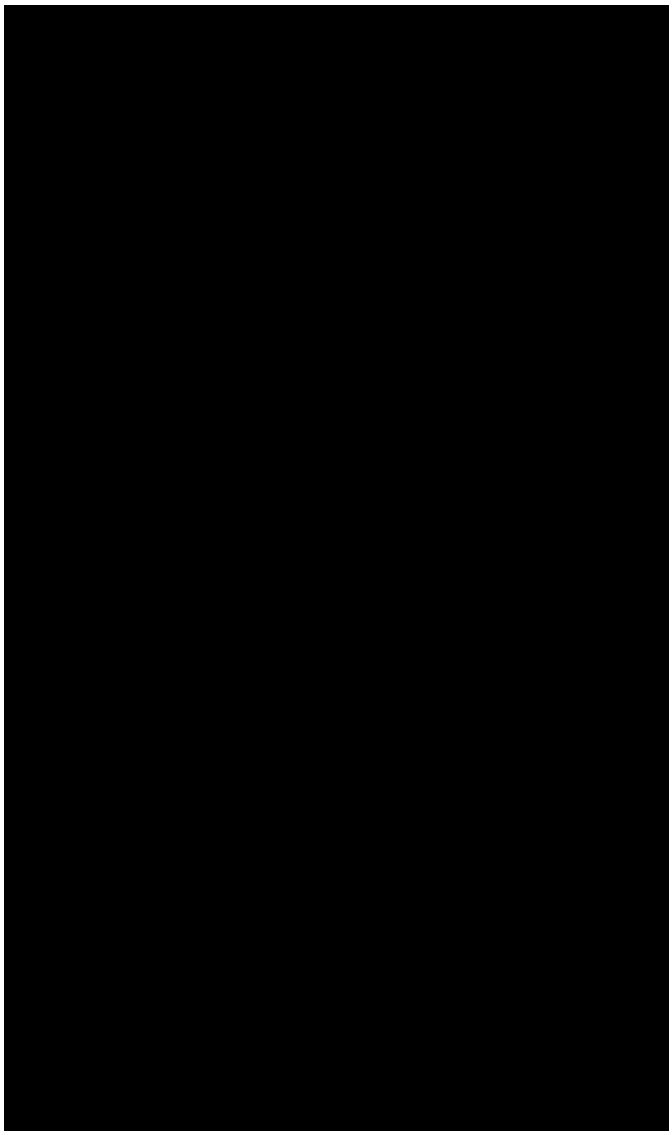

Fig. 4.1. Influence of run duration on conversion, formation of ketone and ester in the acylation of anisole with hexanoic acid: (a) temperature: 413K and (b) temperature: 428K (catalyst = BEA(15), 0.15g; anisole: hexanoic acid (mole) = 4:1)

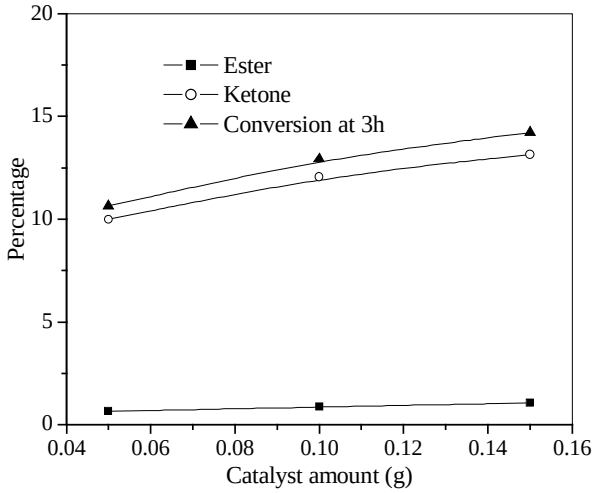

Fig. 4.2. Influence of catalyst amount on conversion, formation of ketone and ester in the acylation of anisole with hexanoic acid (catalyst = BEA(15), temperature: 413K, anisole : hexanoic acid (mole) = 4:1)

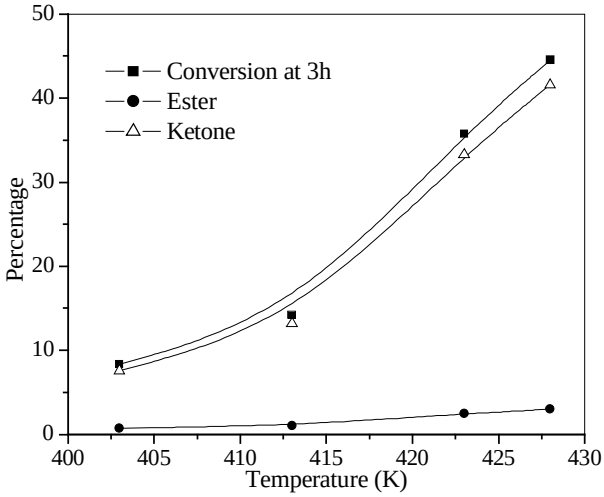

Fig. 4.3. Influence of temperature on conversion, formation of ketone and ester in the acylation of anisole (catalyst = BEA(15), 0.15 g; anisole: hexanoic acid (mole) = 4:1)

The influence of temperature on the reaction over BEA(15) is presented in Fig. 4.3. A rapid increase in conversion, along with increase in the yields of both the ketone and the ester, is noticed with increase in temperature. A kinetic analysis of the reaction was carried out assuming a pseudo-first order reaction and the activation energy (E_a) for the reaction was calculated from the k values at the different temperatures. The E_a values are 22.4, 22.5 and 15.8 kcal $mole^{-1}$ for the overall reaction, for the formation of the ketone and the ester, respectively. The large Ea value obtained over the catalyst (BEA(15)) suggests the absence of external mass transfer effects. The influence of anisole: hexanoic acid mole ratio on conversion and product yields is presented in Fig. 4.4.

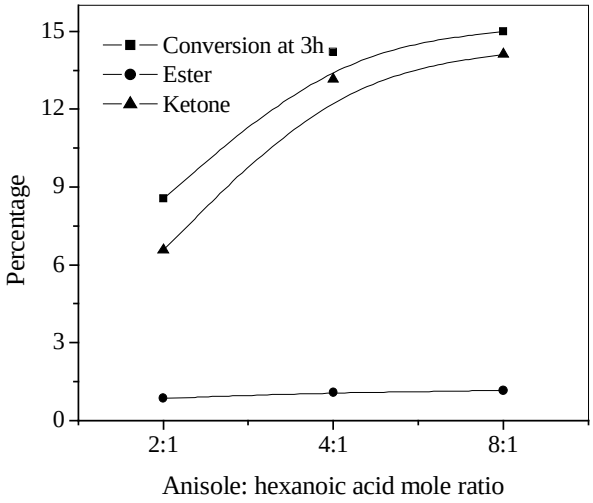

Fig. 4.4. Influence of mole ratio on acylation of anisole with hexanoic acid (catalyst = BEA(15), 0.15 g; temperature: 413K)

A general increase in conversion of the acid and ketone yield is noticed (as expected) with increase in the amount of anisole. However, the ester yield does not increase as rapidly as the ketone.

The reaction was also investigated over MOR, FAU and BEA with different Si/Al ratios. A plot of the activity of the three zeolites (at 413 K) is presented as a function of run duration in Fig. 4.5.

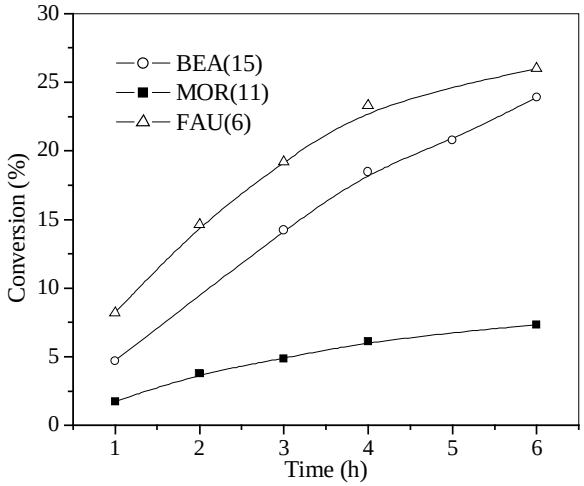

Fig. 4.5. Influence of run duration on conversion of hexanoic acid over BEA(15), MOR(11) and FAU(6). (Catalyst amount = 0.15 g, temperature: 413K; anisole: hexanoic acid (mole) = 4:1)

At this temperature, the order of reactivity of the zeolites is, FAU(6) > BEA(15) > MOR(11). This observed order is due to the effects of both zeolite structure and Al-content. The influence of Al content of the three zeolites on conversion and product yields is presented in Fig. 4.6 a – d. In the case of BEA, a general increase in conversion is noticed with decrease in Al content, i.e. increasing dealumination. A similar, but less pronounced, trend is found in the case of FAU and MOR also. Corresponding plots of k values as a function of Si/Al ratios for the three zeolites are presented in Fig. 4.7 a – c. These plots also show similar trends. Similar results have also been noticed in the Claisen rearrangement of allyl phenyl ether (Chapter 5). Ma et al. have also reported a similar trend during the acylation of anisole with propionic acid in a batch reactor in the absence of a solvent [7] over FAU samples with different Si/Al ratios. They have explained the increase in activity on dealumination to be due to the creation of Lewis acid centers. Freese et al. have reported

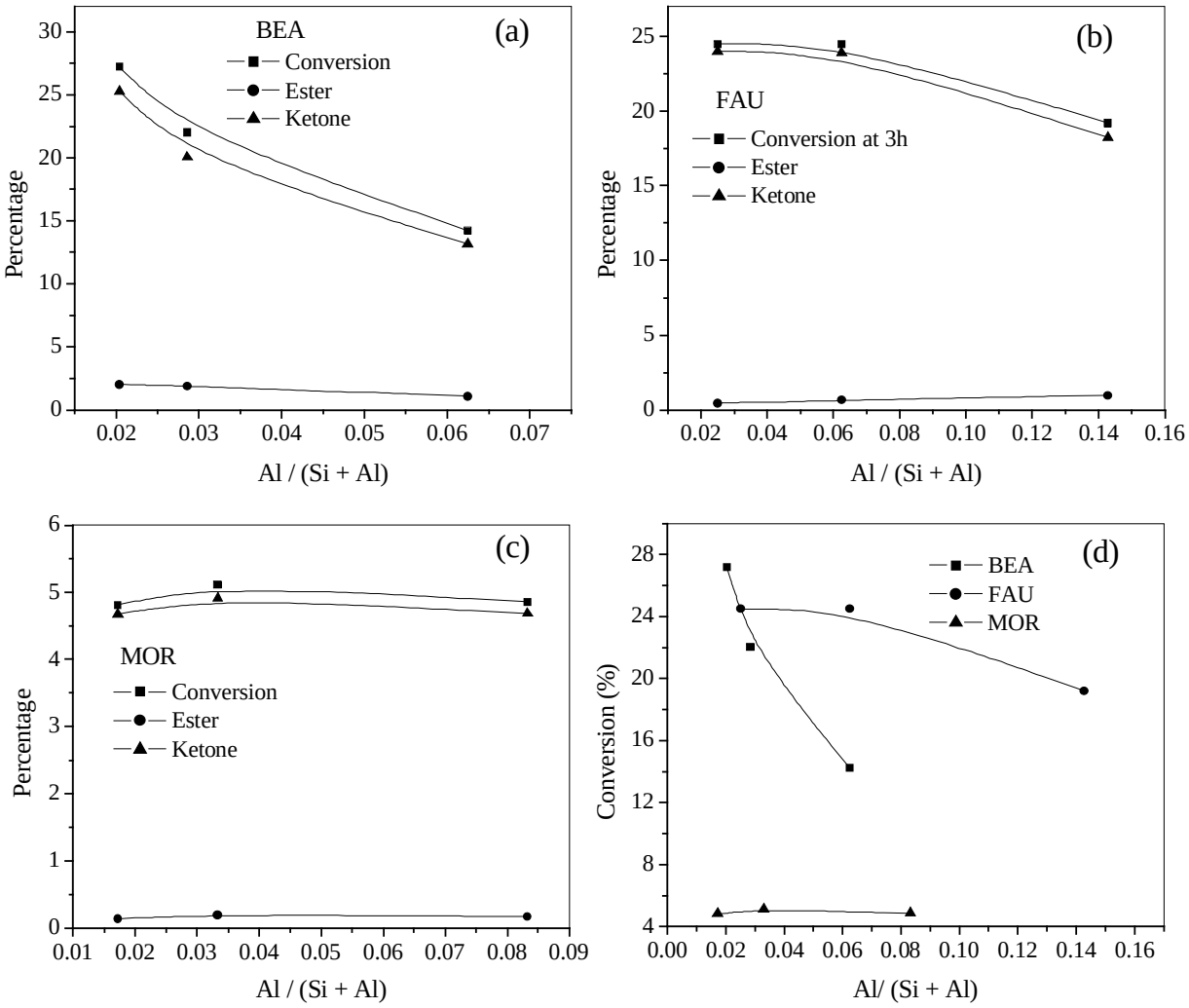

Fig. 4.6. a-c) Influence of Al content of zeolites BEA, FAU and MOR on conversion and product yields and d) comparison of the three zeolites for influence of Al content on conversion in acylation of anisole with hexanoic acid (Catalyst amount = 0.15 g; temperature: 413K; anisole: hexanoic acid (mole) = 4:1)

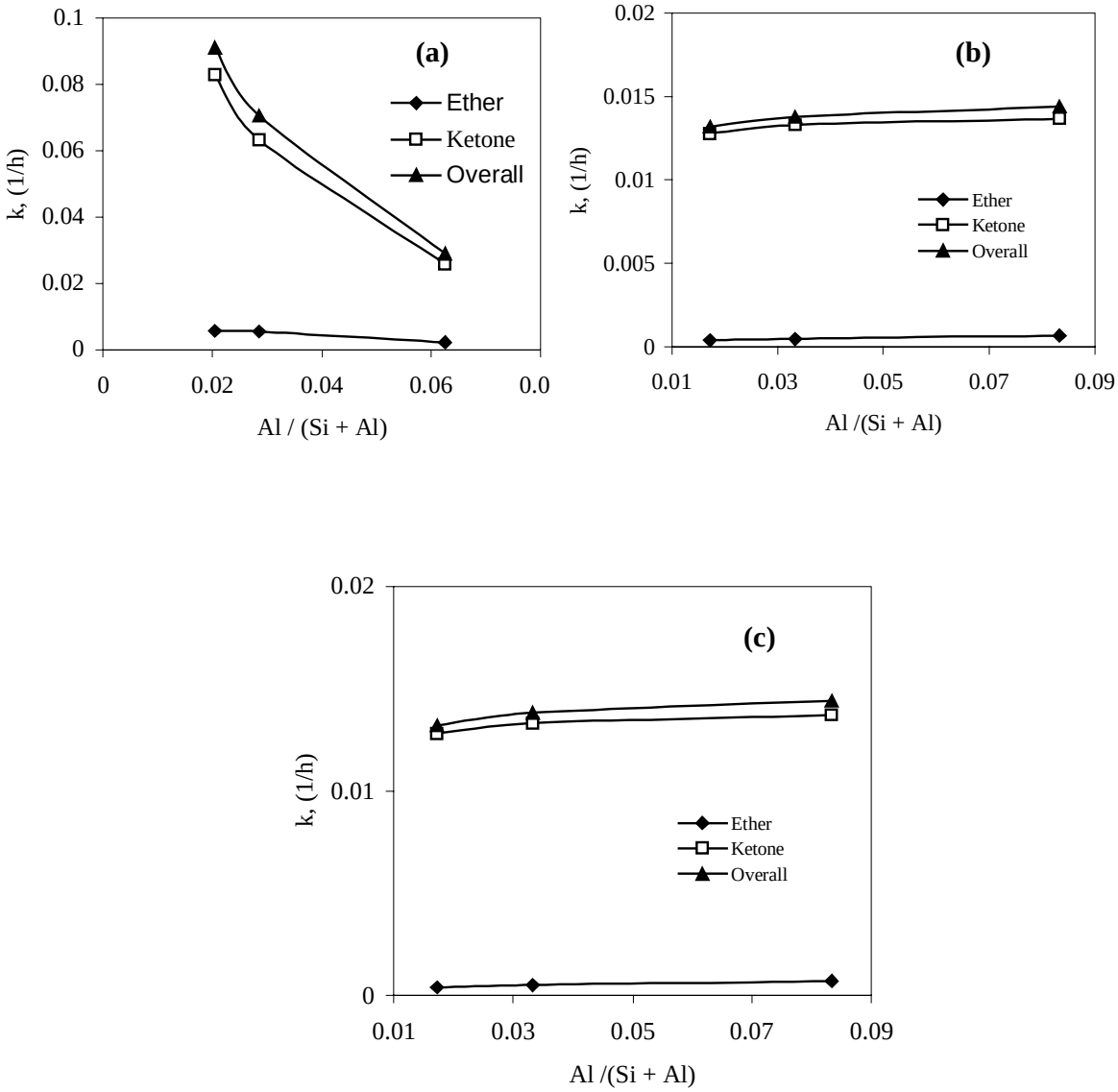

Fig. 4.7. Influence of Al content of zeolites (BEA, FAU and MOR (a, b and c respectively)) on rate constant k in the acylation of anisole with hexanoic acid (catalyst amount = 0.15 g; temperature = 413 K; anisole: hexanoic acid (mole) = 4:1)

an increase in the initial activity of BEA (Si/Al = 12) on dealumination (to Si/Al = 90) and have attributed this to increased mass transfer in the dealuminated sample [8].

It is likely that both effects are involved in the present case. Based on the data obtained at different Si/Al ratios of the zeolites, the activity of the three zeolites at a constant Al content (Al/Si+Al ratio of 0.02; Si/Al = 49) is reported in Table 4.1. The order of activity is now BEA > FAU > MOR. MOR has a rather low activity, presumably due to the presence of diffusion effects in its narrow channels.

Table 4.1: Comaprison of zeolites BEA, FAU and MOR at constant Al content (Al / (Si+Al) ratio of 0.02; Si/Al = 49)

Zeolite	Al / (Si + Al)	Rate constant, k (1/h)		
		Ether	Ketone	Overall
BEA	0.02	0.0057	0.0830	0.0911
FAU	0.02	0.0014	0.0757	0.0777
MOR	0.02	0.0004	0.0128	0.0132

4.3.2 Octanoic acid:

The influence of temperature on conversion and product yields in the acylation of anisole with octanoic acid is presented in Fig. 4.8. A general increase in conversion and product yields with increase in temperature is observed. A comparison of the activity of thethree zeolites (BEA(15), FAU(6) and MOR(11)) is presented in Fig. 4.9. An activity order similar to that noticed in the case of hexanoic acid is noticed: FAU(6) > BEA(15) > MOR(11).

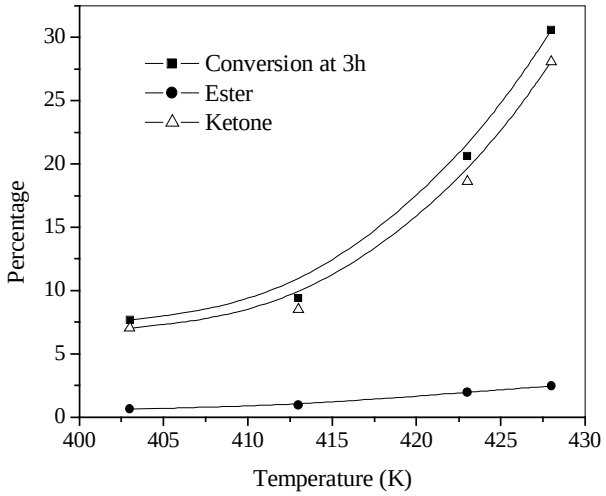

Fig. 4.8 Influence of temperature on conversion and product yields in the acylation of anisole with octanoic acid (Catalyst = BEA (15), 0.15 g; temperature: 413K; anisole: octanoic acid (mole) = 4:1)

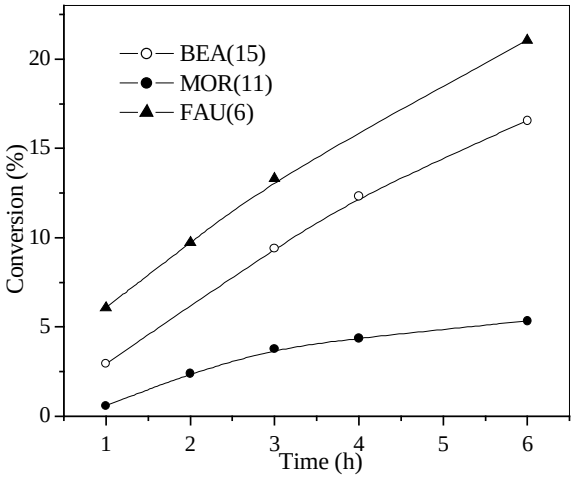

Fig. 4.9. Comparison of the activity of the three zeolites (BEA(15), FAU(6) and MOR(11)) in the acylation of anisole with octanoic acid (Catalyst amount = 0.15 g; temperature: 413K; anisole: octanoic acid (mole) = 4:1)

4.3.3 Decanoic acid:

The influence of temperature on acylation with decanoic acid are presented in Fig. 4.10 and the activity of the three wide pore zeolites are compared in Fig. 4.11. The order activity of the zeolites in this case is slightly different: BEA(15) > FAU(6) > MOR(11). The reason for the difference in the case of decanoic acid is not clear. It could be related to the greater hydrophilic nature of BEA compared to FAU and the stronger adsorption of the more hydrophobic C_{10}-acid.

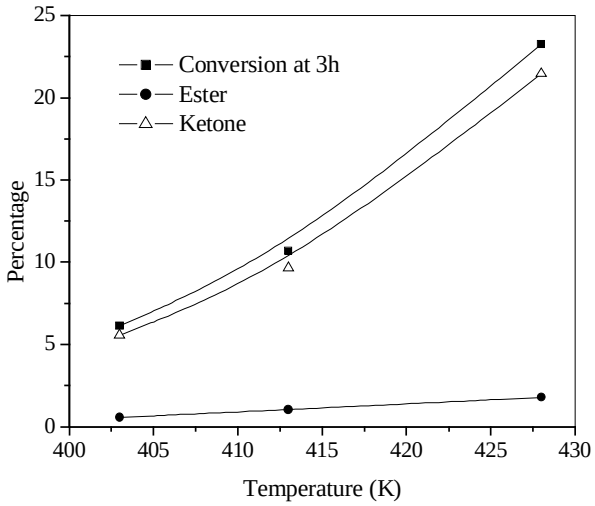

Fig. 4.10. Influence of temperature on conversion and product yield in the acylation of anisole with octanoic acid (Catalyst = BEA (15), 0.15 g; temperature: 413K; anisole: decanoic acid (mole) = 4:1)

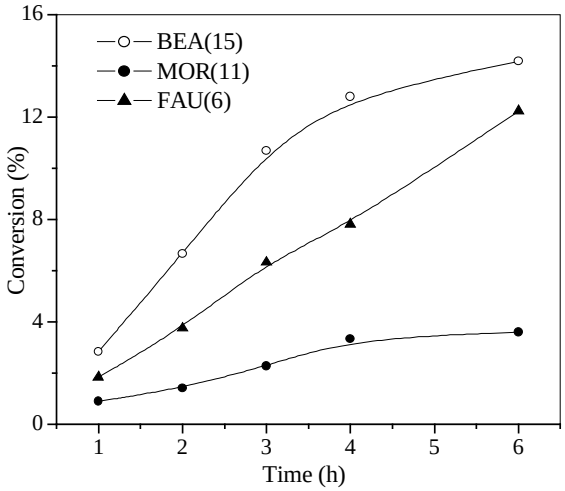

Fig. 4.11. Comparison of the activity of the zeolites (BEA(15), FAU(6) and MOR(11)) in the acylation of anisole with octanoic acid (Catalyst amount = 0.15 g; temperature: 413K; anisole: decanoic acid (mole) = 4:1)

4.3.4. Influence of C-number of acylating agent:

A comparison of the reactivity of the three acids, hexanoic, octanoic and decanoic, at different temperatures is presented in Table 4.2. The p-isomer is the major product in all the cases along with a small amount of the o-isomer (Table 4.2). The reactivity of the acid is found to decrease with its C-number at all the temperatures. The decrease is probably due to decrease in diffusivity with increase in molecular size of the acid.

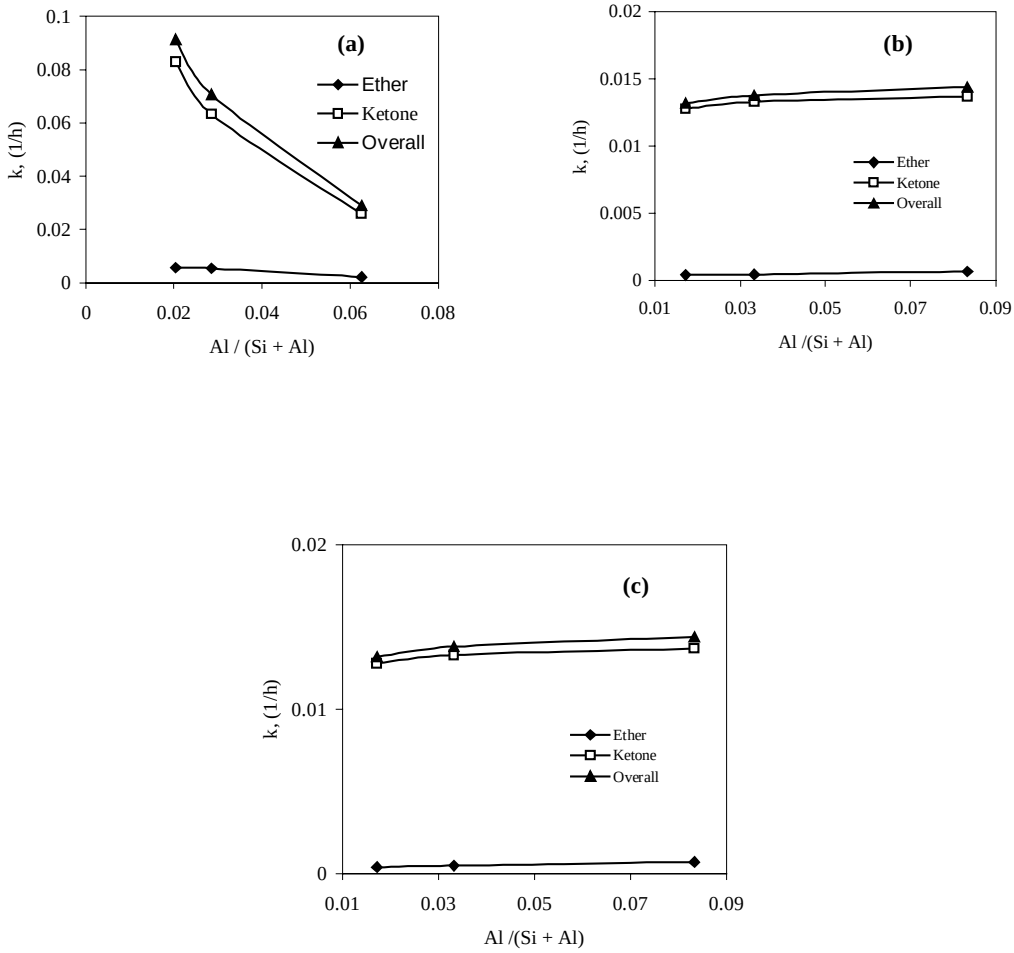

Fig. 4.12. Relationship between the rate constants and carbon number of the carboxylic acid in the acylation of anisole at different temperatures (Catalyst = BEA(15), 0.15 g; temperature: 413 K; anisole : acid (mole) = 4:1)

This suggests the occurrence of the reaction inside the pores of the zeolites. Based on the data obtained at different temperatures and at different run durations, the reaction rate constants (k) were calculated. The data are reported in Fig. 4.12 a, b and c for the overall reaction, ketone and ester formation respectively. The k-values decrease generally with increasing C-number, the decrease being more pronounced at higher temperatures. The activation energy values (E_a) calculated from the k-values are presented in Fig. 4.13 as a function of the C-number of the acid. It is noticed that the Ea values decrease with increasing C-number for ketone formation and for the overall reaction. However, Ea for ester formation is not significantly dependent on the C-number of the acid.

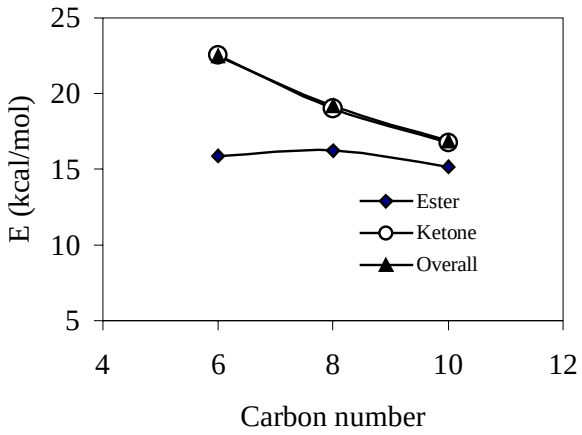

Fig. 4.13 Relationship between the activation energy and the number of carbon atoms in the carboxylic acid in the acylation of anisole (Catalyst = BEA(15), 0.15 g; temperature: 413 K; anisole : acid (mole) = 4:1)

The influence of zeolite structure (type) on the reactivity of the three acids is compared in Table 4.3. The orders of the activity of the three zeolites are similar for hexanoic acid and octanoic acid (FAU(2.6) > BEA(15) > MOR(11)) but different for decanoic acid (BEA(15) > FAU(2.6) > MOR(11)). The k-values for the reactions over the three zeolites using the three acids are presented in Fig. 4.14. A general trend of decreasing k-value with C-number is noticed for all the zeolites for the overall reaction and for ketone

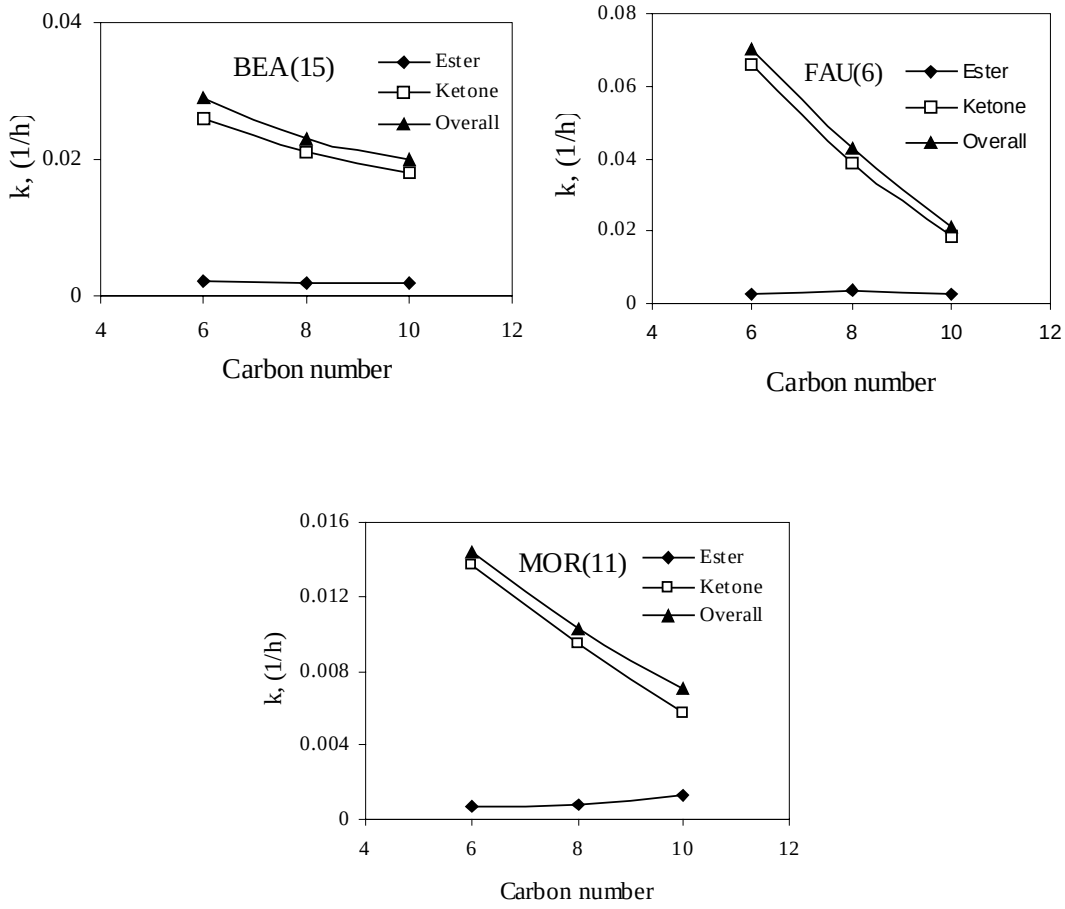

Fig. 4.14. Influence of carbon number of the acid on the k-values of zeolites BEA, FAU and MOR in the acylation of anisole (Catalyst amount = 0.15g, temperature = 413 K, anisole: acid (mole) = 4:1).

Table 4.2: Comparison of the reactivity of hexanoic, octanoic and decanoic acids, at different temperatures in the acylation of anisole (Catalyst = BEA(15), 0.15g; anisole: acid (mole) = 4:1)

Temp. (K)	Hexanoic acid				Octanoic acid				Decanoic acid			
	Conv. (mol%)	Product Distribution (mol %)			Conv. (mol%)	Product Distribution (mol %)			Conv. (mol%)	Product Distribution (mol %)		
		o-	p-	Ester		o-	p-	ester		o-	p-	ester
403	17.0	0.3	15.2	1.5	12.3	0.3	11.0	1.0	10.8	0.3	9.5	1.0
413	23.9	0.5	21.5	1.9	16.5	0.5	14.4	1.6	14.2	0.4	12.4	1.4
423	44.2	0.8	40.6	2.8	35.2	0.8	31.0	3.4	22.5	1.0	20.0	1.5
428	56.3	1.0	51.0	4.3	42.6	1.0	38.0	3.6	31.1	1.2	27.7	2.2

Table 4.3 : Comparison of zeolites BEA (15), MOR (11) and FAU (6) in the acylation of anisole with long chain acids (Catalyst amount = 0.15 g; temperature = 413 K; anisole : acid = 4:1)

Catalyst	Hexanoic acid				Octanoic acid				Decanoic acid			
	Conv. (mol%)	Product Distribution (mol %)			Conv. (mol %)	Product Distribution (mol %)			Conv. (mol%)	Product Distribution (mol %)		
		o-	p-	Ester		o-	p-	ester		o-	p-	ester
BEA(15)	23.9	0.5	21.5	1.9	16.5	0.5	14.4	1.6	14.2	0.4	12.4	1.4
MOR(11)	7.4	0	7.0	0.4	5.3	0	4.9	0.4	3.6	0	2.9	0.7
FAU(6)	26.0	0.6	24.0	1.4	21.1	0.5	18.7	1.9	12.2	0.6	10.1	1.5

formation. The decrease is less pronounced for BEA than for MOR and FAU. Ester formation appears to be much less affected by C-number of the acid.

4.4 Conclusions:

The acylation of anisole with long chain carboxylic acids (hexanoic, octanoic and decanoic) has been investigated over the large pore zeolites BEA, FAU and MOR. The products of the reaction are the ketone (major) and the ester (minor). Acylation occurs predominantly at the 4- (p-) position with small amounts of the o-isomer also being formed. The m-isomer could not be detected. The reactivity of the acid decreases with carbon number due (presumably) to increasing diffusion resistance with C-number. The orders of the activity of the three zeolites arre similar for hexanoic acid and octanoic acid (FAU(6) > BEA(15) > MOR(11)) but different for decanoic acid (BEA(15) > (FAU(6) > MOR(11)). Based on stidies using zeolites with different Si/Al ratios, it is concluded that, at a Si/Al ratio of 49, BEA is about 4 and 14 times more active than FAU and MOR, respectively.

4.5 References:

1. A.Corma, M.J. Climent, H. Garcia, J. Primo, Appl. Catal. A., 49 (1989) 109.
2. C. De Castro, J.Primo, A. Corma, J.Mol. Catal., 134 (1998) 215.
3. G. Harvey, A, Vogt, H.W. Kouwenhoven, R. Prins, Catalysis, (1994) 363.
4. H. van Bekkum, A.J. Hoefnagel, M.A. van Koten, E.A. Gunnewegh, A.H.G. Vogt, H.W. Kouwenhoven, Stud. Surf. Sci. Catal., 83 (1994) 374.
5. C. Gauthier, B. Chiche, A. Finnels, P. Geneste, J. Mol. Catal., 50 (1989) 219.
6. B. Chiche, A. Finnels, C. Gauthier, P. Geneste, J. Org. Chem., 51 (1986) 2128.
7. (a)Y. Ma, Q.L. Wang, W. Jiang, B. Zuo, Appl. Catal. A., 165 (1997) 199. (b) M.Y. Dao, Q.L. Wang, J.X. Dong, Z.C. Ming, Q.Qim, Chem. Lett., 7 (1996) 233. (c) Q.L.Wang, M.Y. Dao, J.X. Dong, Y. Lio, Q.Qim., Chem. Lett., 7 (1996) 99.
8. U. Freese, F. Heinrich, F. Roessner, Catal. Today, 49 (1999) 237.
9. K. Smith, Z. Zhenhua, P.K.G. Hodgson, J. Mol. Catal. A., 134 (1998)121.
10. B. Chiche, A. Finnels, C. Gauthier, P. Geneste, J. Mol. Catal. A., 42, (1987), 229.
11. C.Castro, A. Corma, J. Primo, J. Mol. Catal. A. , 177 (2002) 273.
12. V.G. Yadav, S. B. Chandalia, Indian J. of Chem. Tech., 7 (2000) 112.
13. K. Arata, H. Nakamura, M. Shouji, Appl. Catal. A., 197 (2000) 213.
14. T. Raja, A. P.Singh, A.V. Ramaswamy, A. Finiels, P. Moreau, Appl. Catal. A., 211 (2001) 31.
15. C.P. Benzouhanova, Appl. Catal. A., 229 (2002) 127.
16. F. Richard, H. Carreyre, G. Perot, J. Catal., 159 (1996) 427.
17. D. Rohan, C, Canaff, E. Fromentin and M. Guisnet, J. Catal., 177 (1998) 296.
18. R.V. Jasra, Bull. Catal. Soc. of India, 2 (2003) 157.

Chapter 5

Rearrangement of

Allyl aryl ethers

5.1. Introduction:

Claisen rearrangement, is the concerted pericyclic sigmatropic rearrangement of allyl phenyl ethers to the corresponding o-allylphenols which normally takes place on heating the ethers at elevated temperatures (> 473 K). Migration of the allyl group to the para position is observed only if both the ortho positions are occupied. The ortho-Claisen rearrangement is characterized by the shift of the double bond in the allylic group. This allylic shift is absent in para-Claisen rearrangement. Solid acid catalysts containing Lewis and Brönsted acids, however, catalyze the reaction at lower temperatures [1, 2]. The o-allylphenols undergo cyclization in the presence of acids to produce dihydrobenzofuran derivatives [3].

Reports of the use of zeolitic materials as catalysts in Claisen rearrangement are limited. Pitchumani et al. have observed shape selectivity in ZSM-5 and ZSM-11 during their study of photo-assisted Claisen rearrangement [4]. The diastereoselective asymmetric induction in the thio-Claisen rearrangement over zeolites was reported by Sreekumar et al. [4a]. The synthetic utility of zeolites (Y, beta, ZSM-5 and EMT) as a versatile catalyst for diastereoselective Claisen rearrangement of various S-allyl γ-hydroxy ketene dithiacetals was presented. All S-allyl γ-hydroxy ketene dithiacetals underwent rapid and diastereoselective thio-claisen rearrangement into *anti*-α-allyl β-hydroxy dithioesters in good yields at room temperature in hexane. In the un-catalysed thio-claisen rearrangement, the major product was the *syn* isomer. In zeolite mediated reactions, the *anti* isomer was the only product.

Shelden et al. have investigated the use of H-BEA and H-MOR in the rearrangement of allyl phenyl ether (APE) in benzene medium [5, 6]. The rearrangement led to the formation of 2-allyl phenol and its further cyclization to 2-methyldihydrobenzofuran. The reaction was accompanied by the formation of dimers and oligomers, especially over H-BEA. The formation of these side products could be suppressed by triphenyl phosphine treatment of

the catalyst. This treatment led to better selectivities to the major reaction products in the case of H-beta. However, mordenite showed no improvement. A remarkable result was obtained when the rearrangement was performed over dealuminated mordenite. The outer surface activity of dealuminated mordenite was only 7% in comparison to H-mordenite, but the selectivity for the rearranged product was found to be higher. The activity per aluminium site was higher for dealuminated mordenite than mordenite. A plausible explanation for the increase of activity (per Al^{3+}) is the creation of mesopores during the dealumination process. Mesopores improve the accessibility of the reactants to the zeolites, thereby improving the performance of the catalyst though the number of active sites is decreased. Greyghton et al. have reported the multifunctional probe, allyl 3,5-di-tert-butylphenyl ether, for testing the outer surface acidity of zeolites [6a]. The Brönsted acid catalyzed Claisen rearrangement of the probe molecule, followed by the cyclization of the primary product to 4,6-di-tert-butyl-2-methyldihydrobenzofuran illustrates the use of the probe to provide information regarding the outer surface acidity of H-MOR and H-BEA. This reaction proved to be useful for the investigation of the effects of various modifications of H-MOR on outer surface acidity [6a].

The results of the Claisen rearrangement of APE over zeolites beta, mordenite and Y are presented in this chapter. The effect of different zeolites and their aluminium content, reaction conditions and solvents on conversion and product selectivity is discussed. The reaction has also been investigated using three isomeric allyl cresyl ethers and the diallyl ether of hydroquinone with zeolite beta as the catalyst. A kinetic analysis of the formation of the different products under various reaction conditions is also presented.

5.2 Experimental:

5.2.1 Materials:

BEA, MOR and FAU zeolites with different Si/Al ratios were used in this study. Details of the source and the methods used in the preparation of the samples have been reported in Chapter 2, section 2.1.

Details of the characterization of the samples and the experimental methods adopted in carrying out the reaction and product analysis are also presented in Chapter 2, section 2.5 and 2.3.4. The different allyl aryl ethers used in this work were synthesized by allylation of the corresponding phenols with allyl bromide and purification by standard methods is presented in (Chapter 2 section 2.2). The purity of the prepared materials was > 98%. The methodology adopted in the kinetic analysis is presented in section 2.7 of Chapter 2. The experimental data have been analyzed assuming first order series and parallel reactions. The relevant equations used are presented in Chapter 2, section 2.7.

5.3 Results and Discussion:

5.3.1. Claisen rearrangement of allyl phenyl ether:

The possible reaction scheme reported for the thermal reaction is shown in Fig. 5.1 [7]. It is reported that the ether first undergoes rearrangement to produce allyl hexadienone followed by enolization to give o-AP which cyclizes to give 2,3-dihydro-2-methyl benzofuran (benzofuran) [7]. However, the intermediate allyl hexadienone could not be identified in any of the products in this study. Depending on the solvent used, other side products (Chapter 2, Fig. 2.9) were formed in the reaction.

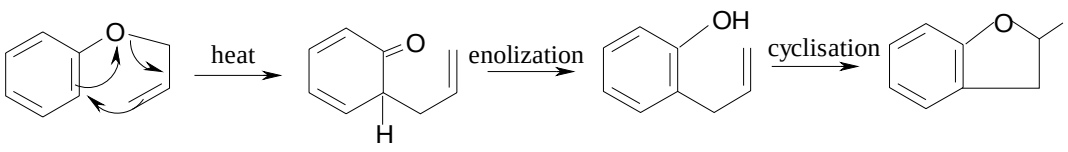

Fig. 5.1. Reaction scheme for the Claisen rearrangement of allyl phenyl ether

5.3.2 Influence of duration of run:

5.3.2.1 Beta:

The effect of run duration (up to 6 hours) on conversion of APE and product yields over H-beta at 353 K are presented for the inert solvent dichloroethane (EDC) in Fig. 5.3 (a) and for toluene in Fig. 5.3 (b). In general, both conversion and benzofuran (furan) formation increase with run duration while o-AP decreases.

(a)

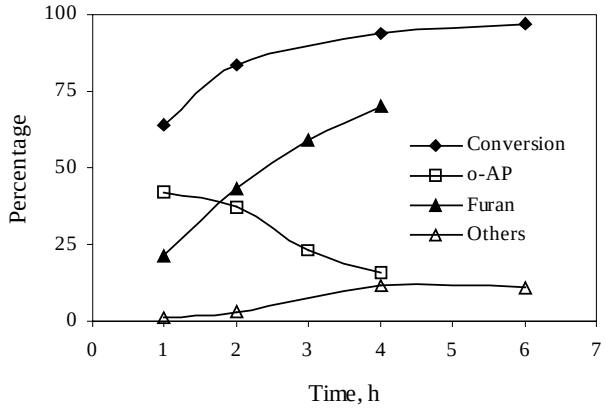

(b)

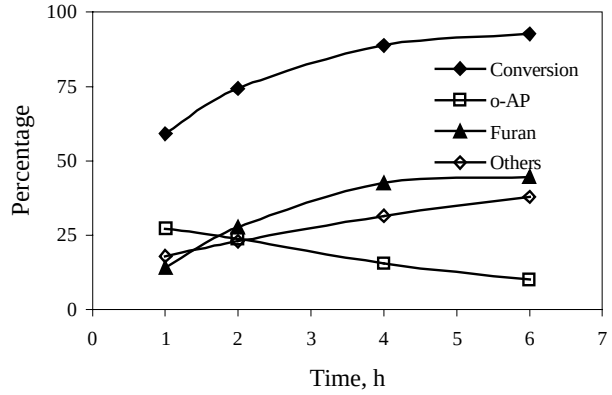

Fig. 5.3. Influence of duration of run on APE conversion and product yields (temperature: 353 K; catalyst: H-beta, 0.1g; APE: 0.00125 mole) solvent: (a)EDC; (b) toluene

Actually, o-AP goes through a maximum (as is expected for a consecutive reaction), although this is not seen in these figures due to the absence of data at short run durations in these experiments. When toluene is used as the solvent, a substantial amount of the byproducts is also produced.

5.3.2.2 Mordenite:

The influence of duration of run on APE conversion and product yields are presented in Fig. 5.4. It is seen that conversion, and concentrations of both o-AP furan increase with reaction time. There is no side product formation for the reaction on mordenite, as EDC was used as the solvent. The reaction is sluggish over mordenite, as compared to beta, indicating that beta is more active than mordenite, even though the number of acid sites (both strong and weak) in mordenite is higher than that in beta (Chapter 2, Table 2.4). This may be due to the one dimensional pores in mordenite offering greater diffusional resistance to the reactant and product molecules.

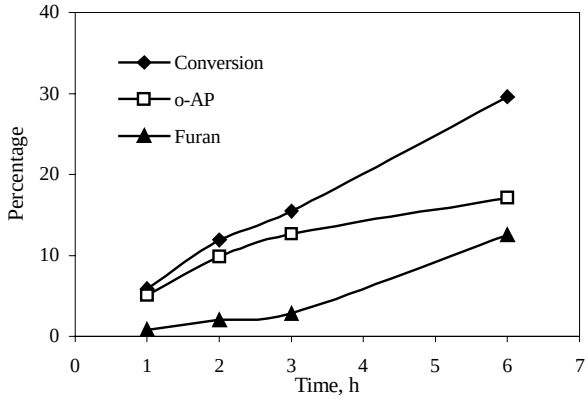

Fig. 5.4. Influence of duration of run on APE conversion and product yields (temperature: 353 K; catalyst: H-mordenite, 0.1 g; APE: 0.00125 mole; solvent: EDC)

5.3.2.3. Faujasite:

The influence of reaction time on conversion and yields of products in the Claisen rearrangement of APE in EDC over faujasite (zeolite Y) is presented in Fig.5.5. There is no

formation of side products in this case too. The conversion and the concentrations of o-AP and furan reach a plateau at the end of 2 hours indicating that the reaction has stopped at approximately 22 % conversion even though FAU is more acidic (both strong and weak) and possess a larger total surface area than beta and mordenite (Chapter 2, Table 2.4). It appears that deactivation / poisoning of the active centers present inside the large α-cages of the zeolite by the reaction products occurs rapidly (causing the reaction to stop at the end of 2h in the case of zeolite Y (FAU(2.6)).

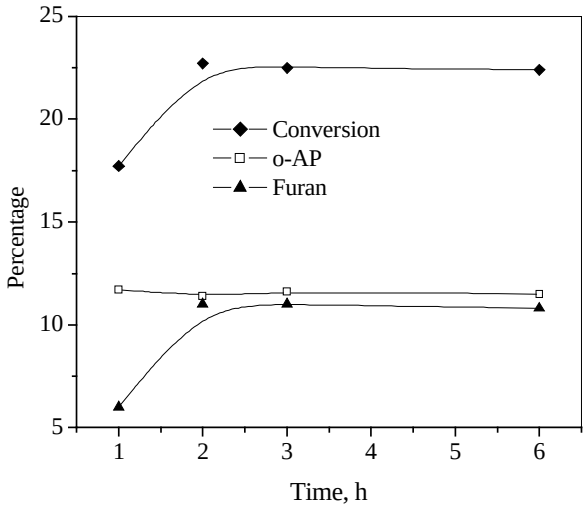

Fig. 5.5. Influence of duration of run on APE conversion and product yields (temperature: 353 K; catalyst: Faujasite (FAU 2.6), 0.1 g; APE: 0.00125 mole; solvent: EDC)

5.3.3 Influence of catalyst weight:

The influence of catalyst weight on conversion of APE and product yield in two different solvents are presented in Fig. 5.6 (a) and (b) (catalyst, H-beta). The nature of the conversion curve is similar to the reaction behavior with duration of run. It increases up to a catalyst weight of 0.08 g beyond which there is no appreciable change due to the attainment of nearly 100 % conversion. The selectivity for o-AP decreases with catalyst weight, which is the typical behavior for the intermediate in a consecutive reaction.

(a)

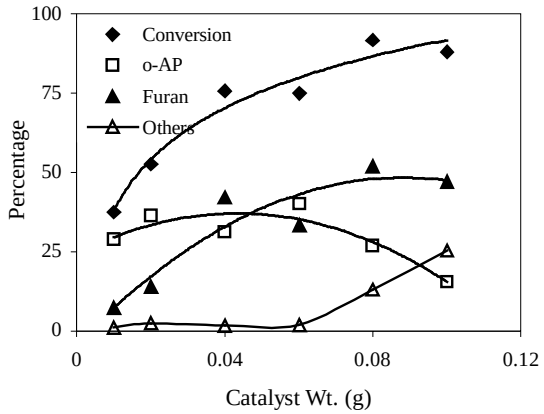

(b)

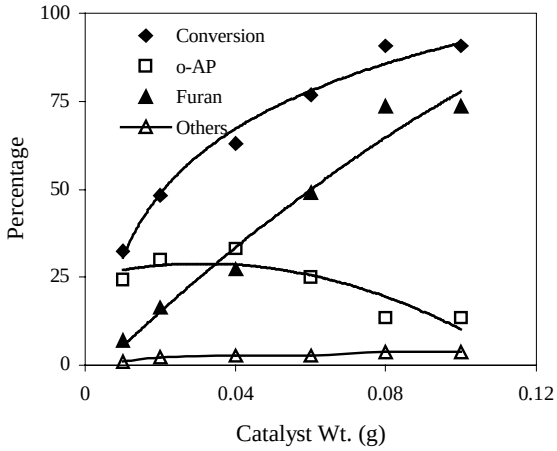

Fig. 5.6. Influence of catalyst weight on APE conversion and product yields (temperature: 353 K; catalyst: H-beta; APE: 0.00125 mole; reaction time: 3h) (a) solvent: EDC; (b) TCE

.

Benzofuran selectivity and the side products formation increase with catalyst weight. An increase in catalyst weight also results in an increase in the side products formation at the expense of benzofuran when toluene is used as the solvent (Fig. 5.6 (a)). A catalyst weight of 0.08 g was used in most of the subsequent experiments

5.3.4. Influence of solvent:

The reaction of APE over H-beta produces both the primary product, 2-allyl phenol (o-AP) and the secondary product, 2-methyl 2,3-dihydrobenzofuran when it is carried out in an inert solvent like EDC or TCE (tetrachloroethane). The nature of the solvent is found to affect the reaction rate. The order of reactivity in the solvents is benzene > EDC > toluene > TCE >> ACN (acetonitrile). In ACN, the reaction does not proceed beyond the first step with 100 % selectivity for o-AP (conversion: 7.5 % at the end of 6 h). The influence of the solvent on zeolite catalyzed reactions can be complex. The solvent may affect the reactivity of the reaction intermediate, it may also adsorb strongly and poison the active sites, cause substrate exclusion from the surface due to strong adsorption effects and increase the resistance to diffusion of the reactants and the substrates inside the channels. In the case of the solvents used, all except ACN and DMF have low polarities (dielectric constants between 2.2 and 2.4 at 293K). The reason for the low to negligible activity observed in DMF and ACN may be primarily due to their strong adsorption owing to their large dielectric constant (37.6 and 37.5, respectively) and exclusion of the substrate molecules from the active centres. An interesting solvent effect has been reported by Pitchumani et al., who observed that shape selectivity effects were noticeable only when water and not n-hexane was used as a solvent in their study of photo Claisen rearrangement of allyl phenyl ether sorbed in the pores of hydrophobic MFI and MEL zeolites [4] suggesting that the reaction could not occur inside the pores when n-hexane was used. n-Hexane was

preferentially adsorbed inside the pores of the hydrophobic zeolites excluding the substrate molecules.

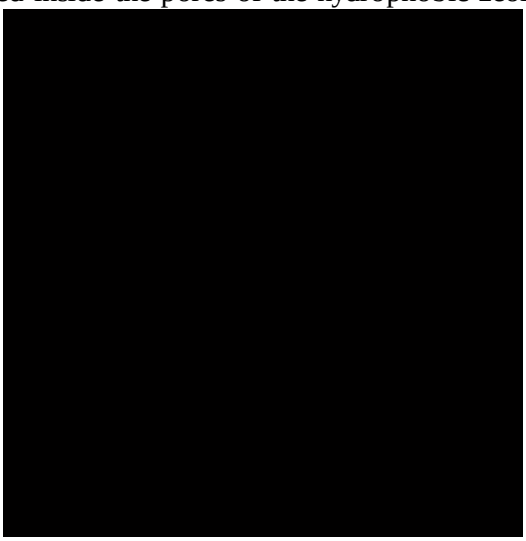

Fig. 5.7 Influence of solvent on conversion of APE (Table 5.1) and product distribution. (reaction time: 1 h; temperature: 353 K; catalyst weight: 0.1 g; APE: 0.00125 mole)

The conversion of APE and the distribution of the different products formed are presented in Fig. 5.7. The side products formed in benzene and toluene have been identified to be mainly the reaction (alkylation) products between the solvent and the intermediate allyl phenol (Chapter 2, Fig. 2.9).

5.3.5 Influence of aluminium content:

Negligible reaction occurrs in the absence of a catalyst and when a purely siliceous, high surface area material (MCM-41) is used as the catalyst, even at 373 K [8]. This suggests that the reaction is catalyzed by the acid centers on zeolites. Very surprisingly, both conversion and selectivity in the Claisen rearrangement are found to be inversely dependent on the Al content of the zeolites, as can be seen from Fig. 5.8-5.10. As the Al content of the zeolites decrease (increase in the Si/Al ratio), the strong and weak acidity decrease. However, the APE conversion is more over the dealuminated catalysts. Dealumination is known to create mesopores in zeolite crystals giving the reactant greater access to the acid centers. In general, dealumination increases the diffusivity of the reactants

and products. It appears therefore that the reaction occurs mainly on the external surface of the zeolite crystallites, presumably at the pore mouths, and dealumination enhances the accessibility of the acid sites to the reactant molecules by creating a mesopore system in the crystallites, thus enhancing the accessibility of the acid centers, thereby increasing the productivity of the Al-ions. In the case of zeolites, molecular diffusion can increase by many orders of magnitude when the pore diameter increases even by a few angstroms. Thus, the positive effect of increased diffusion of the molecules greatly offsets the decrease in the number of acid centers. This is clearly seen in Fig. 5.8(b) – 5.10 (b) wherein the TOF is plotted against Al content. Al-ions in the dealuminated samples are found to be catalytically more effective.

Another explanation for the observation of increasing activity on dealumination may be the creation of new Lewis acid sites during dealumination that are much more active for the reaction than the Brönsted acid sites. Earlier workers have reported the formation of Lewis acid sites during the steam dealumination of FAU and a continuous increase in Lewis/ Brönsted ratio with decreasing Al content [9,10]. They observed a similar increase in conversion with dealumination during their investigation of anisole acylation [9,10].

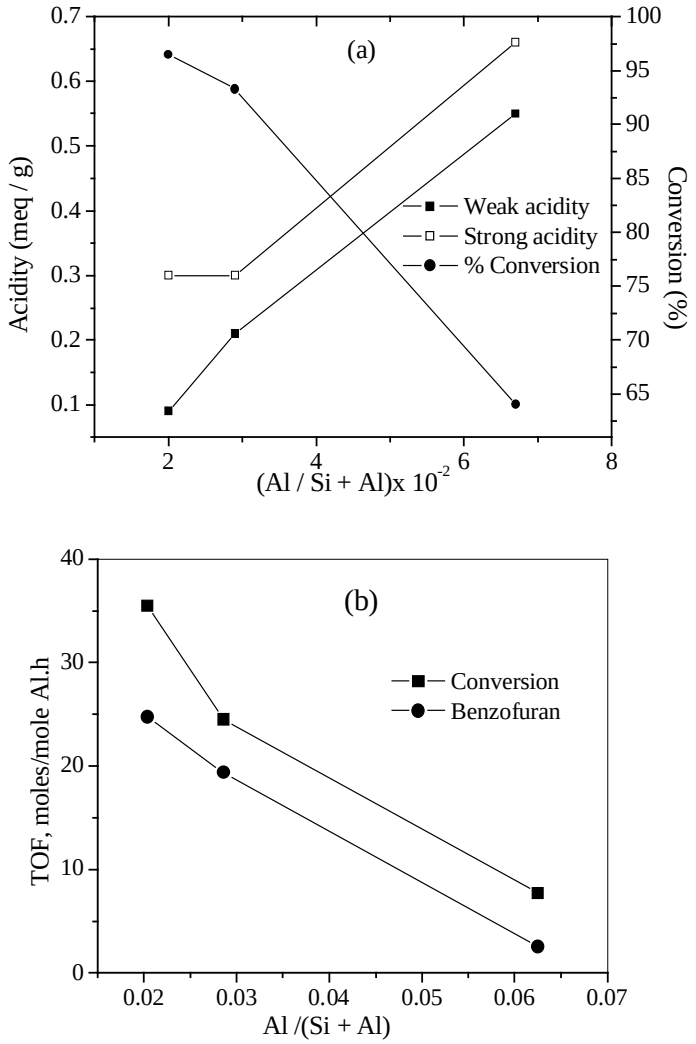

Fig. 5.8. Influence of Al content on (a) acidity and APE conversion and (b) turnover frequencies (TOF) for conversion of APE and benzofuran formation (reaction time: 2 h; temperature: 353 K, catalyst: beta (0.1 g); APE: 0.00125 mole; solvent: EDC)

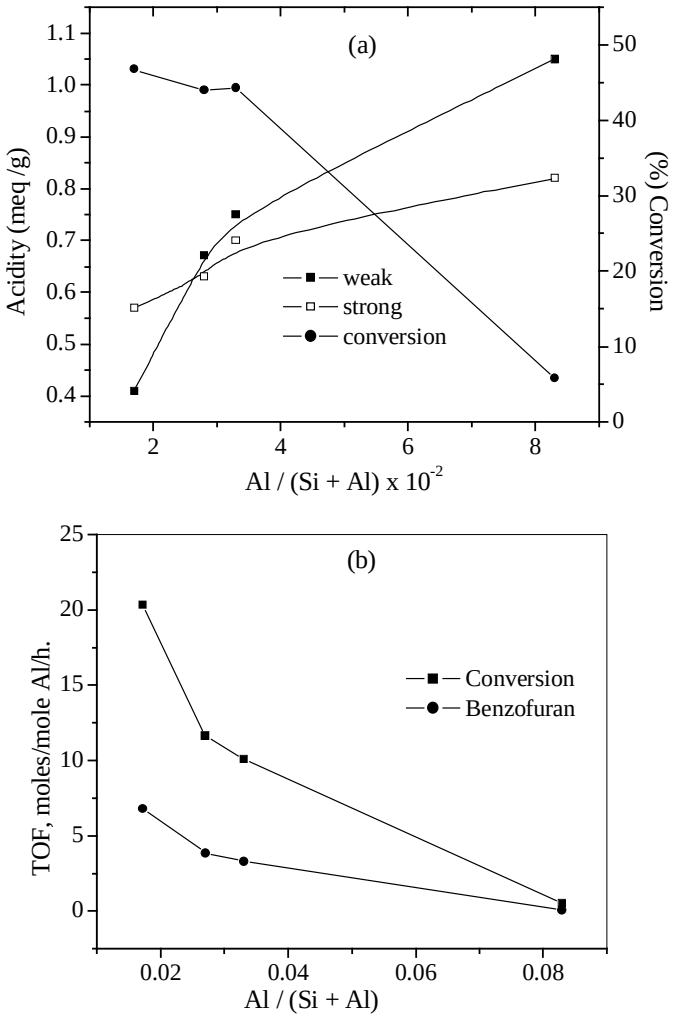

Fig. 5.9 Influence of Al content on (a) acidity and APE conversion and (b) turnover frequencies (TOF) for conversion of APE and benzofuran formation (reaction time: 2 h, temperature: 353 K; catalyst: mordenite (0.1 g); APE: 0.00125 mole; solvent: EDC)

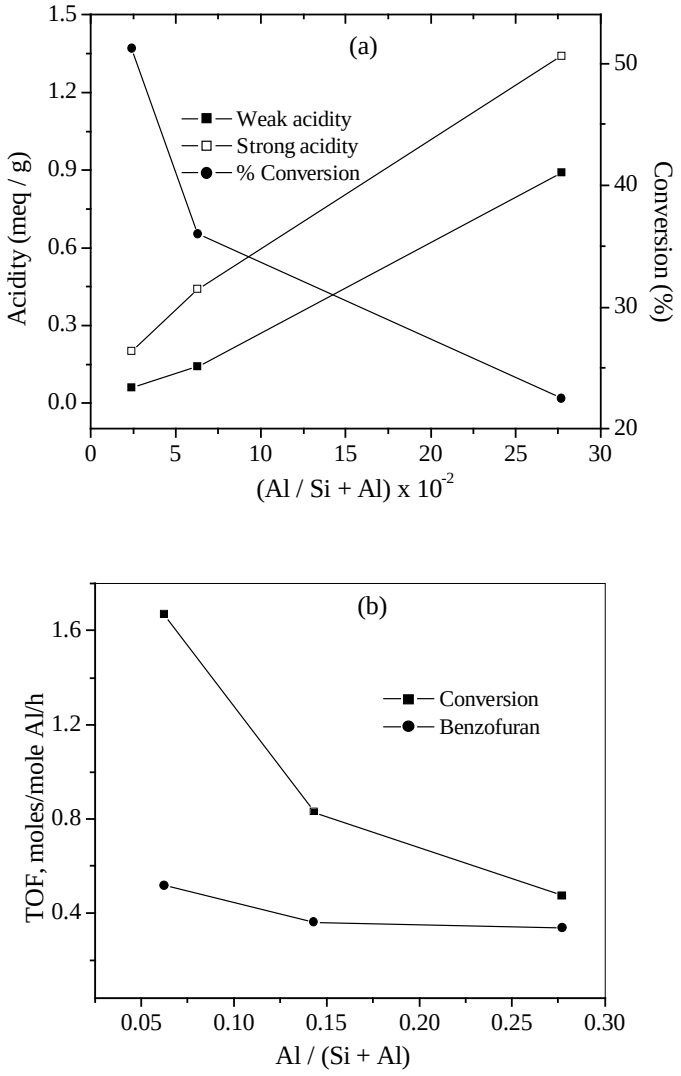

Fig. 5.10. Influence of Al content on (a) acidity and APE conversion and (b) turnover frequencies (TOF) for conversion of APE and benzofuran formation (reaction time: 2 h; temperature: 353 K; catalyst: faujasite (0.1 g); APE: 0.00125 mole; solvent: EDC)

5.3.6. Comparison of substrate reactivity:

A comparison of the reactivity of APE (1) with allyl o-cresyl ether (A(oC)E, 2), allyl (m-cresyl) ether, (A(mC)E, 3) and allyl (p-cresyl) ether, (A(pC)E, 4) was carried out at 353 K with EDC, toluene and benzene as the solvents over zeolite beta (Table 5.1). The products formed from the different substrates are also presented in Fig. 5.11. (a). The general trend observed on the reactivity of the different substrates (based on 1 h reaction time) in the three solvents are: EDC, 4 > 1 > 2 > 3; benzene, 1 > 4 > 2 > 3 and toluene, 1 > 4 > 3 > 2. The order of reactivity of the substrates observed in the inert solvent EDC probably reflects the inherent reactivity of the molecules arising from electronic and steric effects of the substitution of the CH_3 group in the ring. The order of reactivity in benzene and toluene is similar. The exact reasons for this order in the reactive solvents are not clear though one would expect the competitive adsorption of the solvent molecules and the reactivity of the intermediate allyl phenols with the solvents during the reaction to be responsible. Substrate 2 produces, interestingly, the p-allyl derivative (IV) (Fig. 5.11. (a)) in substantial amounts due to blockage of one o-position and lower selectivity for the ring product. Substrate 3 produces two allyl phenols (VI and VII) and two ring products (VIII and IX) (Fig. 5.11. (a)). The conversion and the product yields for APE in the three solvents are presented in Table 5.1. The presence of the methyl group in the benzene ring in APE influences the reactivity of the substrates. The o-cresyl derivative (2) (Fig. 5.11. (a)) is less reactive than APE (1) due to the blockage of an o-position. On the other hand, the p-isomer (4) is most reactive, nearly 85 % conversion taking place in about 0.25 h. The m-isomer is the least reactive, about 45 % conversion taking place in 1 h. However, in the case of compounds 3 and 4, the reaction stopped at about 1 h, presumably due to rapid catalyst poisoning. The reasons for the rapid fouling of the catalyst by these substrates or their reaction products are not clear.

Substrate	Product
1 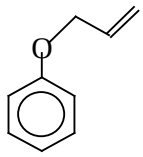	(I) 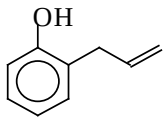 (II) 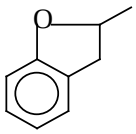
2 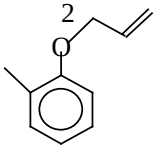	(III) 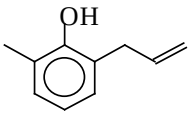 (IV) 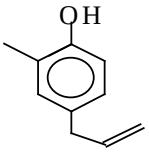 (V) 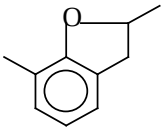
3 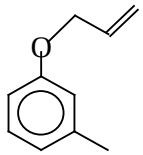	(VI) 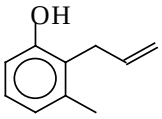 (VII) 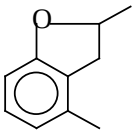 (VIII) 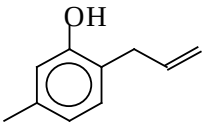 (IX) 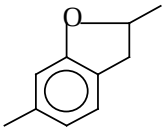
4 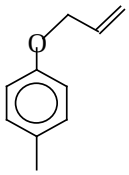	(X) 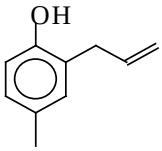 (XI) 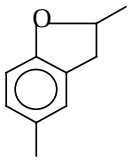

Fig. 5. 11 (a) The products of Claisen rearrangement of different substrates

Another substrate that was investigated (in EDC overBEA(15)) was the diallyl ether of hydroquinone. The direct products of the reaction are presented in Fig.5.11. (b). Two diallyl hydroquinone (A and B), two phenol molecules containing one furan ring and one

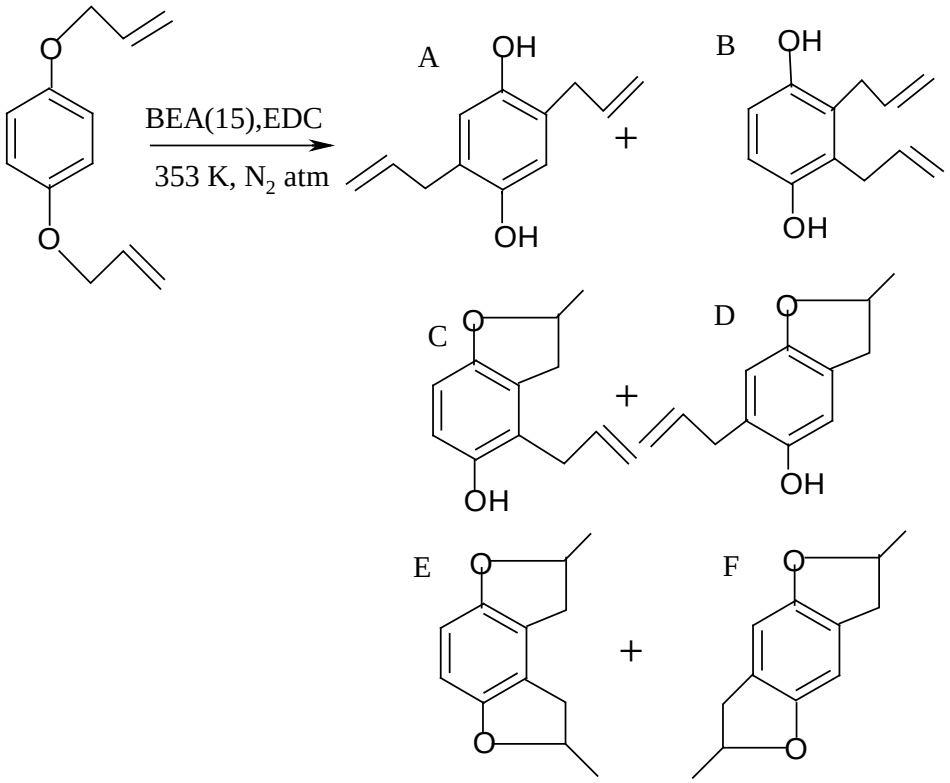

Fig. 5.11. (b) The products of Claisen rearrangement of diallyl ether of hydroquinone.

allyl group (intermediates C and D) and two three ring compounds (E and F) are produced. The influence of run duration at 353 K on conversion and the three types of compounds are presented in Fig. 5.12. It is seen that the conversion of the diether is quite substantial over BEA at 1h (~ 85 %), though it does not increase much with run duration (~ 90 % at 6h), presumably due to strong adsorption of the large product molecules on the catalyst and its deactivation. The yield of the final ring products (E and F) is much more than the others even at a run duration of 1h suggesting the rapid transformation of the diallyl compounds (A and B) into the difuran ring compounds (E and F). In the case of APE, the ring compound

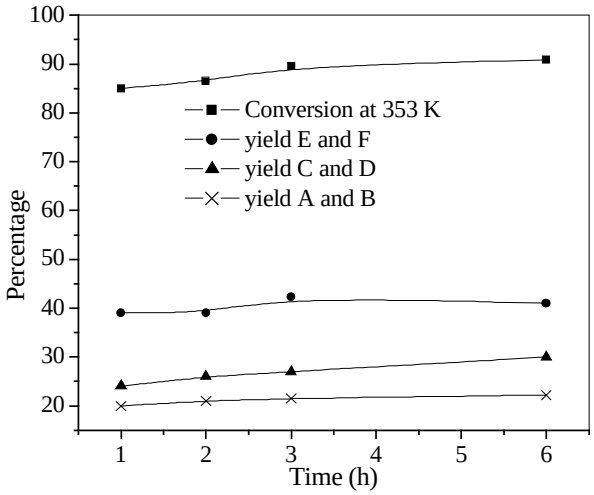

Fig. 5.12. Influence of run duration on conversion and product distribution in the Claisen rearrangement of the diallyl ether of hydroquinone (catalyst: BEA(15), 0.08g; diallyl ether of hydroquinione: 0.001 mole; temperature: 353 K; solvent: EDC)

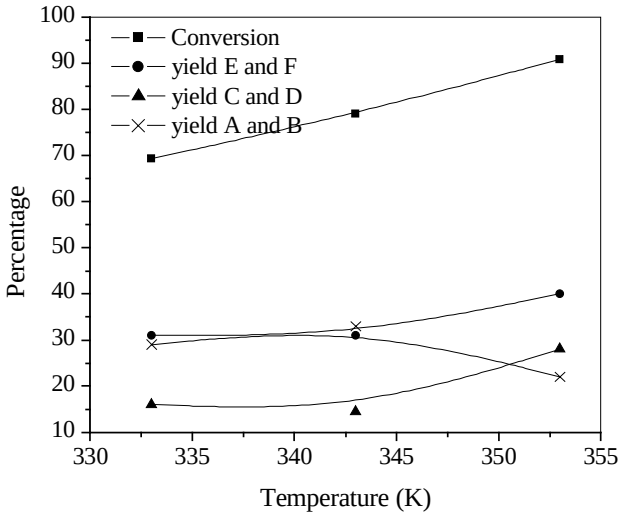

Fig. 5.13. Influence of temperature on conversion and product formation in the Claisen rearrangement of the diallyl ether of hydroquinone (catalyst: BEA(15), 0.08g.; diallyl ether of hydroquinione: 0.001 mole; temperature: 353 K; solvent: EDC)

increases with run duration and is substantially more than the allylic phenol only after 2h (Fig. 5.3 a).

The influence of temperature on conversion and product formation is presented in Fig. 5.13. It is noticed that the double furan ring compounds (E and F) and single furan ring compounds (C and D) increase with temperature at the expense of the diallyl hydroquinones (A and B).

Table 5.1: Comparison of reactivity and product distribution in the Claisen rearrangement of APE and allyl cresyl ethers in different solvents (reaction time: 1h; catalyst H-beta (0.1g); temperature: 353K; APE: 0.00125 mole)

Solvent	APE				o-cresyl ether				m-cresyl ether				p-cresyl ether			
	Conv. (%)	Product distribution (%)			Conv. (%)	Product distribution (%)			Conv. (%)	Product distribution (%)			Conv. (%)	Product distribution (%)		
		AP	Furan	Other		AP	Furan	Other		AP	Furan	Other		AP	Furan	Other
Benzene	89.4	14.9	36.1	38.4	37.4	29.5	4.7	3.2	9.6	6.2	0.3	3.1	57.2	42.7	8.9	5.5
Toluene	59.2	27.1	14.1	18.0	28.0	24.4	2.1	1.5	24.0	18.1	2.7	3.2	43.5	3.9	36.0	3.6
EDC	64.4	21.	42.0	1.0	53.5	49.3	4.2	-	45.3	31.4	11.1	2.8	84.5	57.2	25.0	2.3

5.3.7. Mechanism of the reactions:

Plausible mechanisms for the initial Claisen rearrangement to produce the allyl phenol and the subsequent conversion of the phenol into the ring compound or byproducts are presented in Fig.5.14 (a), (b) and (c). The steps are catalyzed by acid centers. In the first step, namely the formation of the intermediate allylphenol, the acid site protonates the -O- of the ether to form the phenol. This is followed by intramolecular rearrangement of the protonated (adsorbed) species into the o-allyl phenol as shown in Fig. 5.14(a). The allyl phenol is next protonated at the allylic double bond to produce the secondary carbonium ion that reacts again intramolecularly with the phenolic 'O' to produce the benzofuran (Fig. 5.14b)). When the reaction is carried out in the presence of the aromatic solvents benzene or toluene, an electrophilic substitution takes place on the aromatic ring of benzene or toluene to produce the byproducts (Fig. 5.14(c)).

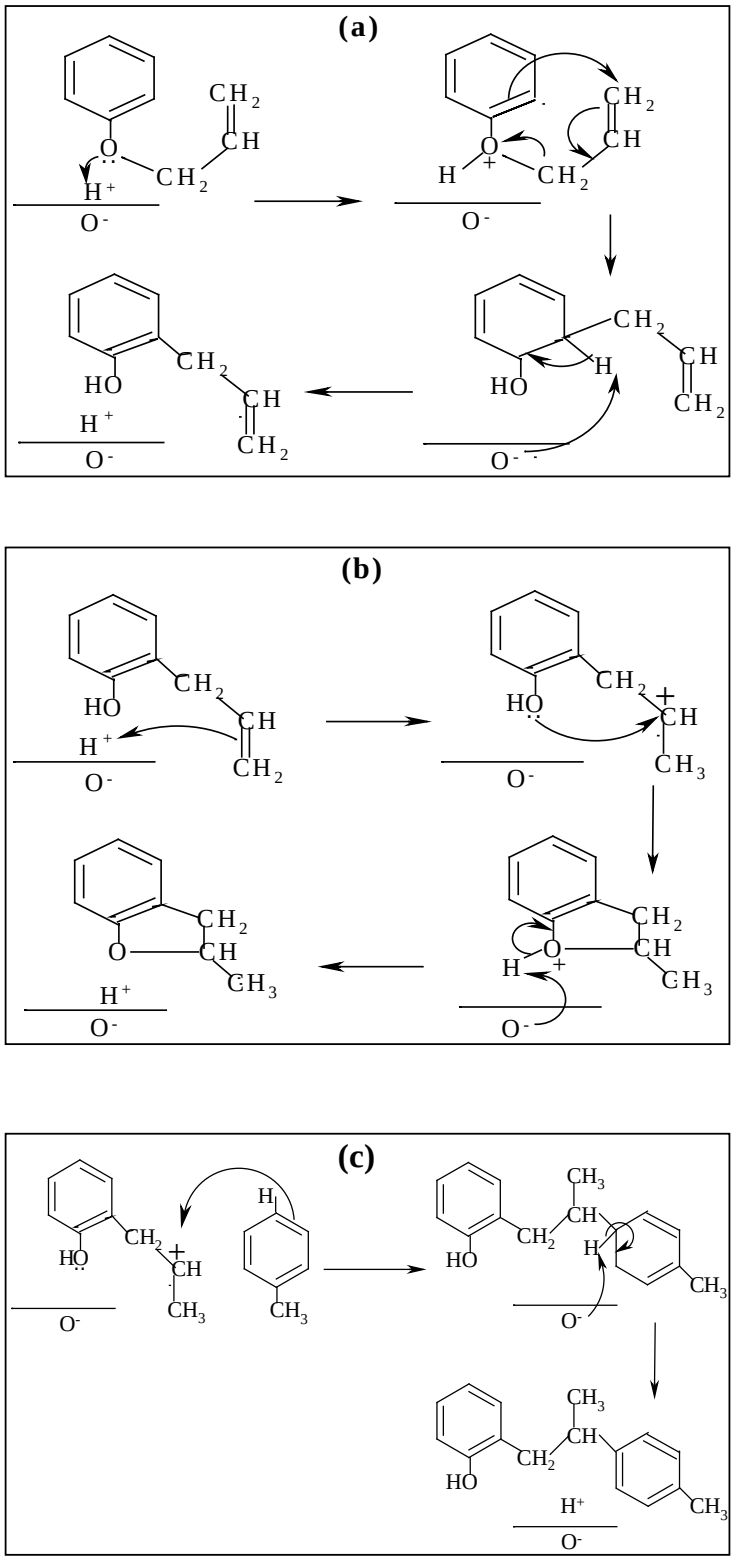

Fig.5.14. Plausible reaction mechanisms for (a) the formation of AP, (b) the formation of ring product and (c) the formation of byproducts over zeolite catalysts

5.4. Kinetic Analysis:

5.4.1 Beta

Two typical parity plots for the rearrangement of APE in toluene and in tetrachloroethane (TCE) are presented in Fig. 5.15 (a) and (b) respectively. In the figure, the lines represent compositions based on the kinetic equation (Chapter 2, section 2.7). The symbols represent the concentration of the individual components relative to the initial concentration of APE. It can be seen that the kinetic predictions are in good agreement with the experimental data confirming first order consecutive and parallel reaction kinetics(Chapter 2, section 2.7).

The rate constants of the various steps over H-beta for different temperatures and solvents (toluene and TCE) are presented in Table 5.2. The rate constants were derived assuming a consecutive first order reaction as described in Chapter 2, section 2.7. The rate constant for the disappearance of the substrate (APE) is k_1, while k_2' and k_2" are the rate constants for the formation of the benzofuran derivative and side-products, respectively. It is noticed from the table that the reaction is much faster (k_1 values are larger) in toluene than in TCE. This is especially so at higher temperatures. On the other hand, k_2' is of similar magnitude in both the solvents (at a given temperature) suggesting a similar activity of the catalyst (BEA(15)) for ring product formation in both the solvents. The formation of side-products (k_2") as already mentioned is substantial in toluene and negligible in TCE. The apparent activation energies (Ea) calculated for the different steps and are also presented in Table 5.2. The rate constants for the conversion of different substrates at 353 K in toluene are presented in Table 5.3. The order of reactivities of the substrates in toluene are APE > A(pC)E > A(mC)E > A(oC)E.

(a)

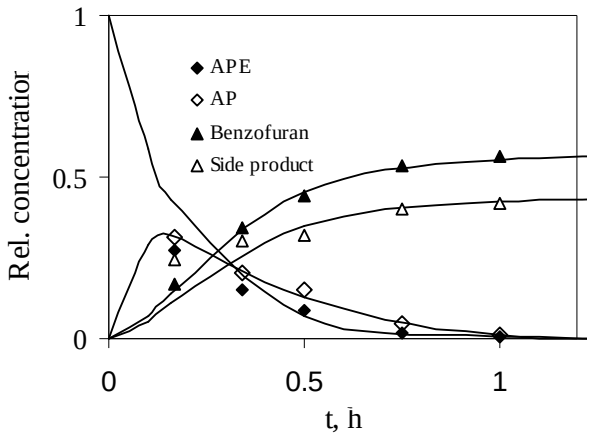

(b)

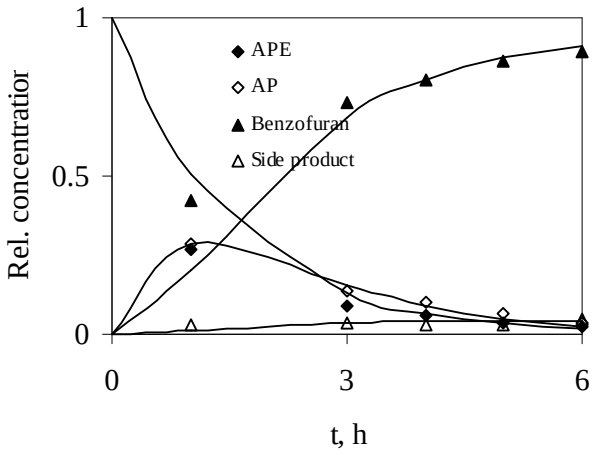

Fig. 5.15 Parity plots for the reaction (catalyst weight: 0.1 g; APE: 0.00125 mole). The symbols represent experimental concentrations relative to the initial concentration of the reactant. (a) solvent: toluene; temperature: 373 K; (b) solvent: TCE; temperature: 353 K

The influence of aluminium content on the reaction kinetics in EDC over the catalysts H-beta, mordenite and faujasite are presented as a plot of rate constant versus Si/Al ratio for the two reaction steps, in Figs. 5.16. The figures show that the conversion of APE

and the formation of benzofuran are both sensitive to the aluminium content, and the sensitivity depends on the zeolite type.

Table 5.2: Effect of different solvents on the rate constant and activation energies (substrate: APE; catalyst: H-beta)

Solvent	Temperature (K)	Rate constant (1/h) for		
		Depletion of APE (k_1)	Formation of furan (k_2')	Formation of side product (k_2")
Toluene	343	0.11	0.08	0.07
	363	5.65	0.37	0.49
	383	11.43	0.94	1.44
	Activation Energy (kcal/mol)	30.0	12.9	20.8
TCE	343	0.19	0.24	0.02
	363	0.74	0.33	--
	383	3.69	0.89	--
	Activation Energy (kcal/mol)	18.2	14.1	--

Table 5.3: Influence of substrate on the reaction rate constants (temperature: 353 K; solvent: toluene; catalyst: H-beta)

Precursor	Rate constant (1/h) for		
	Depletion of substrate (k_1)	Formation of benzofuran (k_2')	Formation of side products (k_2")
APE	0.71	0.10	0.08
A(oC)E	0.25	0.07	0.04
A(mC)E	0.43	0.53	0.23
A(pC)E	0.51	0.16	0.17

In the case of beta, k_1 and k_2 pass through a maximum with increase in the Si/Al ratio. Corresponding to this, t_{max}, the time at which the concentration of the intermediate product is maximum, passes through a minimum. When the rate constants for the consecutive reactions are maximum, the time required for reaching the maximum concentration of the intermediate is the minimum. The sensitivity of the reactions for change in aluminium content is different for beta, mordenite, and faujasite. In the case of beta, the formation of benzofuran is more sensitive to the Si/Al ratio, than the conversion of APE as can be seen from the higher slopes of the k_2 curve with increse in the Si/Al ratio. In the case of mordenite, k_1 is more sensitive to the Si/Al ratio as compared to k_2. In the case of faujasite, k_1 is small and is not sensitive and k_2 increases with increase in the Si/Al ratio. Further, k_2 at all times is higher than k_1. The t_{max} in this case decreases with increase in the Si/Al ratio.

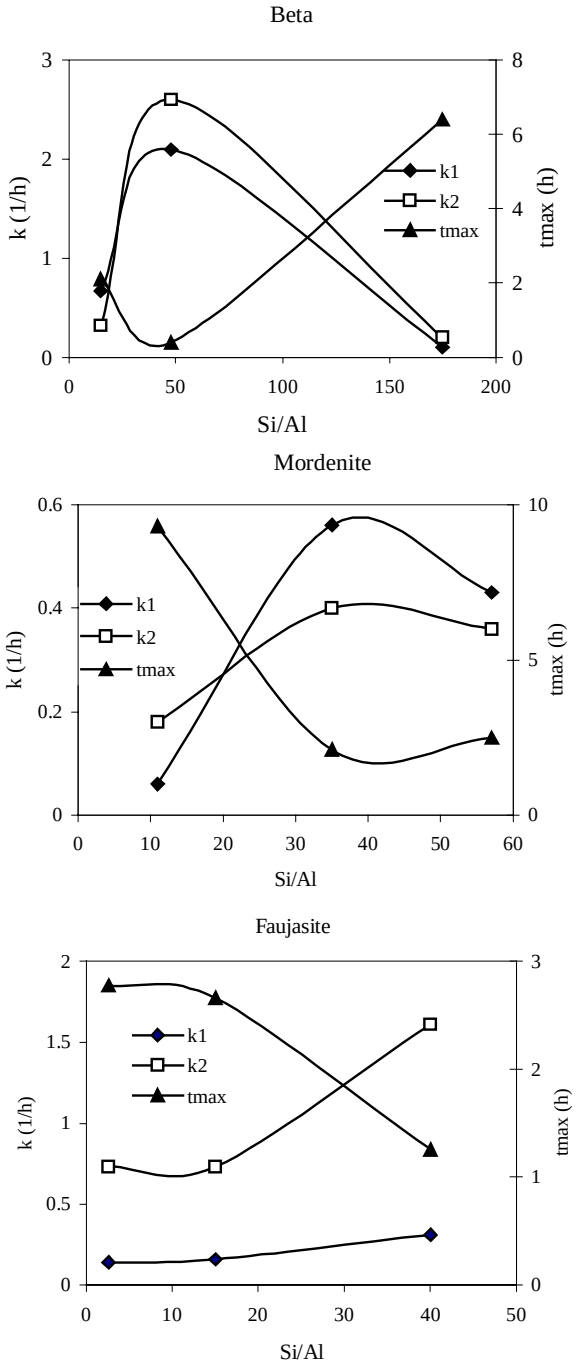

Fig. 5.16. Influence of aluminium content on the rate constants of the two steps and the time maximum concentration of o-AP in the Claisen rearrangement of APE over zeolite beta, mordenite and faujasite (solvent: EDC; temperature: 353K)

5.4.2. Comparison of activity of zeolites:

The zeolites beta and faujasite have similar large surface areas and pore volumes (Chapter 2, Table 2.3). The external surface of beta is roughly three times as large as that of faujasite (zeolite Y). Mordenite has total surface area much smaller than both beta and Y. Its external surface area is similar to that of Y. The acidity (both strong and weak) of beta is much lower than that of both mordenite and Y. Faujasite (zeolite Y) has the maximum acidity.

The reactivity of these zeolites is related to their acidity and surface area. Beta, having the highest external surface area and lower acidity gives the highest conversion and formation of benzofuran (Figs. 5.8 - 5.10). The conversion of APE over mordenite and Y are considerably lower than that over beta. This suggests that the reaction probably takes place predominantly over the external surface of the catalyst. It is also possible that the product molecules are more strongly adsorbed in MOR and FAU than BEA. The combined effect of the low external surface and deactivation due to strong adsorption of the reaction products may be the reasons for the observed poor performace of mordenite and Y, despite having higher acidity compared to beta.

5.5 Conclusions:

The Claisen rearrangement of allyl phenyl ether, allyl cresyl ethers and diallyl ether of hydroquinone occurs rapidly over zeolite beta even at temperatures as low as 353K. The initial products formed (o-allylphenols) cyclize readily into benzofuran derivatives. An increase in the temperature of the reaction or the amount of catalyst increases the formation of the ring product. The reaction proceeds rapidly both in inert solvents such as EDC and TCE, and in reactive solvents such as benzene and toluene. In the latter solvents, the intermediate allyl phenols react with the solvent to produce byproducts. The acidity of the zeolites, measured by the TPD of ammonia, decreases progressively on increasing levels of

dealumination with nitric acid. However, the activity of the catalysts increase with increasing dealumination and decreasing number of acid sites. This is attributed to the reaction occurring mainly at the pore-mouths and at the external surface of the zeolite crystallites and dealumination increasing the accessibility of the acid centers to the reactant molecules through creation of mesopores. The conversion is poor in mordenite and zeolite Y despite their possessing higher acidity compared to beta. This may be due to (i) their low external surface areas and (ii) their easy deactivation due to strong adsorption and slow desorption of the poduct specie from the zeolite surface. A kinetic analysis reveals that the reaction follows a typical first order consecutive and parallel reaction kinetics. The rate constants for the different substrates and catalysts derived from the kinetic analysis enable a better understanding of the reactivity of the different substrates. Plausible mechanisms for the different reaction steps based on acid catalysis have been proposed.

5.6 References:

1. J. March, "Advanced Organic Chemistry", 4th Eds., Wiley, New York, (1992).
2. (a) R.P. Lutz, Chemical Rev., 84 (1984) 205. (b) D.S. Tarbell, Org. React. 2 (1944) 1.
3. K. Pitchumani, M. Warrier, V. Ramamurthy, Res. Chem. Intermediates, 25 (1999) 623.
4. K. Pitchumani, M. Warrier, V. Ramamurthy, J. Amer. Chem. Soc., 118 (1996) 9428. (a) R. Sreekumar, R. Padmakumar, Tet. Lett. 38 (1997) 2413.
5. J.A. Elings, R.S. Downing, R.A. Sheldon, Stud. Surf. Sci. Catal., 94 (1995) 87.
6. R.A. Sheldon, J.A. Elings, S.K. Lee, H.E.B. Lempers, R.S. Downing, J. Mol. Catal. A: Chemical, 134 (1998) 129. (a) E.J. Creyghton, J.A. Elings, R.S. Downing, R.A. Sheldon, H.van Bekkum, Microp. Mater., 5 (1996) 299.
7. V.G.S. Box, P.C. Meleties, Heterocycles, 48 (1998) 2173
8. N.T. Mathew, S. Khaire, S. Mayadevi, R. Jha, S. Sivasanker, J. Catal., 229 (2005) 105.
9. (a) Y. Ma, Q.L. Wang,. W. Jiang, B. Zuo, Appl. Catal., A: General, 165, (1997), 199. (b) M.Y. Dao, Q.L. Wang, J.X. Dong, Z.C. Ming, Q. Qim, Chem. Lett., 7 (1996) 233. (c) Q.L. Wang, M.Y. Dao, J.X. Dong, Y.Lio, Q. Qim, Chem. Lett., 7 (1996) 99.
10. U. Freese, F. Heinrich, F. Roessner, Catal. Today, 49 (1999) 237.

Chapter 6

Heck Reaction of Aryl Halides with Olefinic Compounds

6.1 Introduction:

The Heck reaction consists of the coupling of aryl halides onto C=C double bonds that typically bear electron withdrawing groups. The common reaction conditions use a Pd complex as the catalyst, a tertiary amine as the base and an aprotic polar liquid such as dimethyl formamide or dimethyl acetamide as the solvent. The importance of Heck and related reactions stems from the creation of a new C-C bond under conditions that are compatible with the presence of a wide variety of other functional groups and the easy availability of the starting reagents.

The use of homogeneous Pd catalysts to promote this reaction is well established [1-2]. However, these catalysts are expensive (Pd with phosphane or special ligand systems) and also difficult to separate from the reaction mixture for reuse. Therefore, for economic reasons, industrial applications of homogeneous Heck reactions are limited [3]. In addition to the separation problems, deactivation of the homogeneous catalysts by formation of less active or inactive colloidal Pd species is often encountered at the comparatively high reaction temperature. In order to over come the problems arising from the separation, recovery and reuse of the Pd complexes, a variety of heterogeneous catalysts have been investigated for the Heck reaction [4-6]. Since Pd switches between the zerovalent and divalent state in the catalytic Heck cycle, the choice of the support is crucial for retaining both states. The various supports explored for this reaction include Pd supported on carbon, different metal oxides [7,8], clays, mesoporous silica and zeolites [9,10]. Studies have also been reported on Pd nanoparticles [11]. The use of Cu, Ni, Co, and Mn heterogeneous catalysts for the Heck reaction is also known [12]. Polymer supported Pd-complexes have been used for activation of aryl iodides (and bromides) by several groups [14]. The use of microwave irradiation in this reaction has also been reported by Wali et al.[13].

Palladium complexes entrapped in zeolite cages exhibit high activity toward the Heck reaction of aryl bromide with olefins even at a low palladium concentration (0.1%). The activity is determined by the nature of the support and the Pd dispersion. These supported catalysts are easily separated from the reaction mixture and reused without loss in activity after washing. However, Djakovitch and Koehler [9c] observed leaching of active Pd species depending on the zeolite structure. The electronic nature of the aryl bromide has a dominating effect on the reaction yield. The Heck reaction requires the presence of a base as co-catalyst. It is well known that alkali exchanged faujasites are basic solids, whose basic strength increases in the series $Na^+ < K^+ < Rb^+ < Cs^+$and with the framework Si/Al ratio of the zeolite [10b]. However, only a few reports are available on the use of metal supported basic catalysts for the Heck reaction [10,13]. Pd grafted MCM-41 was found to be more active compared to conventional supported Pd catalysts [9a] and was able to activate even the nonreactive substrate, chlorobenzene. However, the activity of the catalyst decreased on reuse.

ETS-10 (Engelhard's titanosilicate-10) is a large pore titanosilicate molecular sieve, first synthesized at Engelhard Corp., USA [15-17]. The framework structure of ETS-10 consists of corner shared oxygen ions of $[TiO_6]^{8-}$ octahedra and $[SiO_4]^{4-}$ tetrahedra. ETS-10 possesses a three dimensional pore system made up of 12-membered ring (12-MR) channels with a pore diameter of 7.6 Å. The Ti/Si ratio of ETS-10 is typically 5. Due to the O_h arrangement of Ti-ions in a tetrahedral framework, each Ti-ion is charge balanced by two alkali metal ions (Na^+ and K^+) making ETS-10 highly basic.

The present study reports the carbon-carbon coupling of different aryl halides with ethyl acrylate over Pd loaded ETS-10 molecular sieve. The influences of Pd content, the nature of the added base and the reactivity of the different substrates and reactants on the coupling reaction (Heck) are now presented in this chapter.

6.2 Experimental

The preparation of ETS-10, Pd-ETS-10 and the reaction procedure are described in Chapter 2 section 2.1 and 2.3.5. respectively.

6. 3 Results and discussion

6.3.1 Influence of Pd content:

Pd loaded ETS-10 samples with different Pd contents (0.2 to 6 wt %) were used in the studies. The reaction of iodobenzene with ethyl acrylate was chosen as the model reaction to test the catalytic activity of the samples. The catalytic activities of the different Pd- ETS-10 samples are plotted as a function of duration of run in Fig. 6.1. The general observation is that the catalytic activity increases with increasing Pd loading. The selectivity for Heck products was > 98 % over all the catalysts.

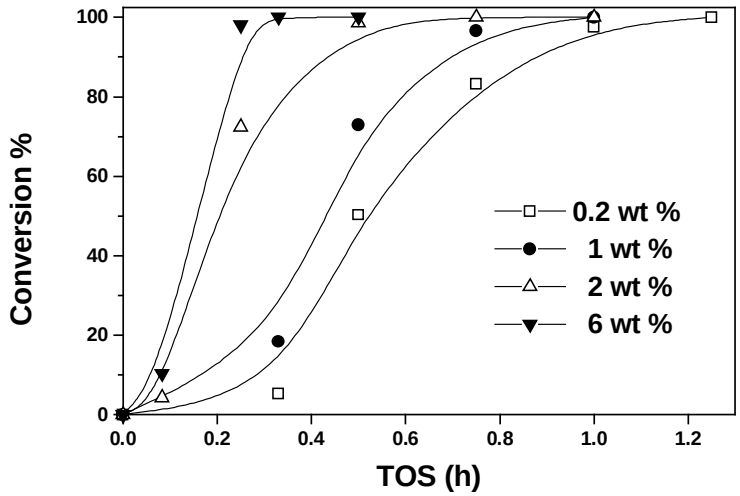

Fig. 6.1. Conversion of the substrate (iodobenzene) over Pd-ETS-10 with different Pd contents (Conditions: catalyst = 0.025 g; temperature: 403 K; substrate: 1 mmol. iodobenzene; and reactant: 5 mmol ethyl acrylate; base = 2 mmol tributylamine (TBA) and solvent:5 g dimethyl formamide (DMF)

The results of studies on the coupling of ethyl acrylate and iodobenzene carried out over 1 wt % Pd-ETS-10 are presented in Table 6.1. A conversion of about 97 % is obtained at about 0.75 h of run duration. The catalyst is found to be recyclable without any loss of activity, the TOF values being 549 for the fresh catalyst and 572 after one recycle (Table 6.1; entries 1 and 2).

Experiments carried out on the 0.2 wt % Pd catalyst are also reported in Table 6.1 (entry 4). The catalyst is quite active in spite of the low (0.2 wt %) Pd loading; a TOF of about 10, 000 is achieved when 5 mmols of iodobenzene are used (Table 6.1; entry 5). The 0.2 wt % catalyst is also recyclable (Table 6.1; entry 6).

Leaching studies were carried out to verify the heterogeneous nature of the reaction. The tests were done on both 0.2 and 1 wt % Pd catalysts (Table 6.1; entries 7 and 3). As the catalysts were reduced in H_2 at 623 K (Chapter 2, section 2.1), the Pd is expected to be present mainly as Pd^0 specie that are not soluble in organic solvents. However, Pd^0 may slowly react with the substrate (iodobenzene) and form complexes that could be leached into the solution.

In a typical leaching experiment, the catalyst was refluxed with iodobenzene at 403 K, for 15 min and separated from the organic layer by centrifuging. Ethyl acrylate was then added to the organic layer. The composition of the clear filtrate was determined by GC. This homogeneous reaction mixture was heated at 403 K and the progress of the reaction was monitored by GC by following iodobenzene conversion. Conversions of 8.1 % and 14.6 % were observed in the case of 0.2 % and 1 wt % Pd catalysts, after 2 h (Table 6.1; entries 7 and 3). A similar experiment was conducted with 1-bromo-4-nitrobenzene and no conversion was observed, in the homogeneous reaction mixture (Table 6.1; entry 9). The conclusion of these leaching experiments is that some leaching of Pd occurs in iodobenzene

Table 6.1: Studies on Heck reaction of different substrates using Pd-ETS-10 and Pd salts

No.	Substrate	Catalyst[a]	TOS (h)	Selectivity (%)	Conversion(%)	TOF[b]	Pd[c] (mg)
1.	Iodobenzene	Pd-ETS-10(1.0)	0.75	98.2	96.7	549	0.25
2.	Iodobenzene[d]	Pd-ETS-10(1.0)	0.75	99.1	95.9	572	0.24
3.	Iodobenzene[e]	Pd-ETS-10(1.0)	2.00	99.2	14.6	170	0.01
4.	Iodobenzene	Pd-ETS-10(0.2)	1.00	98.0	95.7	2,037	0.05
5.	Iodobenzene[f]	Pd-ETS-10(0.2)	1.00	99.1	95.7	10,023	0.05
6.	Iodobenzene[d,f]	Pd-ETS-10(0.2)	1.00	98.3	92.1	9,799	0.05
7.	Iodobenzene[e]	Pd-ETS-10(0.2)	2.00	98.2	8.1	287	0.05
8.	Bromo-4-nitrobenzene	Pd-ETS-10(1.0)	9.00	100	84.3	40	0.003
9.	Bromo-4-nitrobenzene[e]	Pd-ETS-10(1.0)	6.00	-	-	-	0.25
10.	Iodobenzene	$[(NH_3)_4Pd]Cl_2$(1.0)	6.00	72.7	16.1	11	0.25
11.	Iodobenzene	$Pd(OAc)_2$(1.0)	6.00	69.0	6.9	5	0.25

Reaction conditions: catalyst = 0.025 g; temperature: 403 K; substrate: 1 mmol. iodobenzene; reactant: 5 mmol. ethyl acrylate; base: 2 mmol tributylamine (TBA) and solvent: 5 g dimethyl formamide (DMF); [a] = wt% of Pd in the catalyst is given in brackets; [b] = TOF [mole of iodobenzene converted/mole of Pd/h]; [c] = Pd present in the reaction mixture, in catalyst/ in solution; [d] = first recycle; [e] = leaching test and [f] = 5 mmol.iodobenzene,25mmolTBA,20gDMF

and not in 1-bromo-4-nitrobenzene and the leached Pd is less active than the heterogeneous Pd (supported on ETS-10). The Heck reaction was also carried out using the Pd salts, $[(NH_3)_4Pd]Cl_2.H_2O$ and $Pd(OAc)_2$. In these experiments, the amount of the Pd used was equivalent to the Pd present when 1 wt % Pd-ETS-10 was used as the catalyst. These complexes were less active as compared to the (1 wt %) Pd loaded ETS-10 (Table 6.1).

6.3.2 Influence of different bases:

The influence of different bases on conversion and selectivity was investigated (Table 6.2). The reaction was faster when tributyl amine and triethyl amine were used in the case of

both iodobenzene and 1-bromo-4-nitrobenzene (Table 6.2).

Table 6.2: Influence of different bases on the catalytic activity of Pd-ETS-10

Base	TOS (h)	Selectivity (%)	Others (%)	Conversion (%)
Triethylamine	1.00	100	-	95.3
Tributylamine	0.75	98.2	1.8	96.7
K_2CO_3	2.00	100	-	96.7
NaOAc	12.00	97.3	2.7	77.2
K_2CO_3[a)]	12.00	100	-	24.5
Triethylamine[a)]	9.00	98.1	1.9	84.3

Reaction conditions: catalyst: 0.025 g; temperature: 403 K; substrate: 1 mmol iodobenzene; and reactant: 5 mmol. ethyl acrylate; base: 2 mmol. and solvent: 5 g dimethyl formamide (DMF); [a)]: 1-bromo-4-nitrobenzene used as substrate.

6.3.3 Reactivities of different olefins:

The reactivities of different olefins (different acrylates and styrene) are compared in Table 6.3. Ethyl acrylate is found to be the most reactive and selective among the acrylates (96.5 % in 0.75 h). The reactivities of the acrylates are in the order: ethyl acrylate > t-butyl acrylate > methyl acrylate > butyl methacrylate > methyl methacrylate. Styrene is also quite reactive (conv. = 96.7 % and sel. = 80.2 %).

Table 6.3: Reactivities of different olefins in the Heck reaction catalyzed by Pd-ETS-10

Olefin	TOS (h)	Selectivity (%)	Others (%)	Conversion (%)
Methyl acrylate	1.5	100	-	99.7
Ethyl acrylate	0.75	98.2	1.8	96.7
Methyl methacrylate	2.00	100	-	95.2
Butyl methacrylate	2.00	76.5	23.5	77.5
t-Butyl acrylate	1.00	100	-	100
Styrene[a)]	3.00	80.2	19.8	96.7

Reaction conditions: catalyst: 0.025 g; temperature: 403 K; substrate: 1 mmol. iodobenzene; reactant: 5 mmol. ethyl acrylate; base: 2 mmol. tributylamine (TBA) and solvent: 5 g. dimethyl formamide (DMF) a) 2mmol iodobenzene used

6.3.4 Reactivities of different halobenzenes:

A comparison of the reactivities of different halobenzenes is presented in Table 6.4. The reactivities of the different halobenzenes are in the order: iodobenzene > bromobenzene > chlorobenzene (Table 6.4). In the case of 1-halo-4-nitrobenzenes, conversion and

selectivity decrease in the order: 1-iodo-4-nitrobenzene > 1-bromo-4-nitrobenzene > 1-chloro-4-nitrobenzene. In general, it is noticed that electron withdrawing substituents increase conversion.

Table 6.4: Reactivities of different substrates in the Heck reaction catalyzed by Pd-ETS-10

Substrate	TOS (h)	Selectivity (%)	Conversion (%)
Iodobenzene	0.75	98.2	96.7
Bromobenzene	24	77.6	50.1
Chlorobenzene	24	43.8	35.7
1-Iodo-4-nitrobenzene	0.5	100	100
1-Bromo-4-nitrobenzene	9	99.1	84.3
1-Chloro-4-nitrobenzene	12	44.5	40.2
4-Iodophenyl methyl ketone	2	100	87.1
4-Bromophenyl methyl ketone	6	98.2	45.9
1-Chloro-4-iodobenzene	9	98.2	98.5
4-Iodoanisole	3	99.3	64.1

Reaction conditions: catalyst: 0.025 g; temperature: 403 K; substrate: 1 mmol. iodobenzene; reactant: 5 mmol ethyl acrylate; base: 2 mmol. tributylamine (TBA) and solvent: 5 g dimethyl formamide (DMF)

6. 4 Conclusions:

Pd-ETS-10 (reduced in H_2) exhibits a high activity towards the Heck coupling of aryl iodides and bromides with acrylates, under typical reaction conditions. A TON value of

~ 10,000 is achieved for a 0.2 wt % Pd-ETS-10 catalyst. Though some Pd leaches out into solution when iodobenzene is used as the substrate, the reaction is found to proceed mainly by the heterogeneous route. When 1-bromo-4-nitrobenzene is used as the substrate, the reaction is totally heterogeneous. Organic bases lead to higher catalytic activity than inorganic bases and electron withdrawing substituents enhance the reactivity of the aryl halides.

6.5 References:

1. (a) R.F. Heck, "Palladium Reagents in Organic Synthesis", Academic Press, New York, (1985).
2. (a) B.M. Trost, I. Flemming (Eds.), "Comprehensive Organic Synthesis", Vol. 4, p. 585 and 833 and references cited therein. (b) A. de Meijiere, F.E. Meyer, Angew. Chem. 106 (1994) 2473, and references cited therein. (c) W.A. Herrmann, C. Brossmer, C-P Reisinger, T.H. Riermeier, K. Ofele, M. Beller, Chem. Eur. J. (1997) 1357. (d) T. Jeffery, Tetrahedron 32 (1996) 10113. (e) W.A. Herrmann, C. Brossmer, K. Ofele, M. Beller and H. Fischer, J. Mol. Catal. A. Chem. 103 (1995) 133. (f) M. Beller, H. Fischer, K. Kuhlein, C.P. Reisinger and W.A. Herrmann, J. Organomet. Chem. 520 (1996) 257. (g) C. Gurtler and S.L. Buchwald, Chem. Eur. J., 5 (1999) 3107. (h) A.F. Littke, and G. C. Fu, J. Am. Chem. Soc., 123 (2001) 6989. (i) D. Nair, J. T. Scarpello, I. F. J. Vankelecom, L.M. F. D. Santos, L.S. White, R.J. Kloetzing, T. Welton and A.G. Livingston, Green Chem. 4 (2002) 319.
3. I.P. Beletskaya, A. V. Cheprakov, Chem. Rev., 100 (2000) 3009.
4. (a) F.R. Hartley, "Supported Metal Complexes: A New Generation of Catalysts", Riedel, Dordrecht, (1985). (b) Y.I. Ermakov and L.N. Aezamaskova, Stud. Surf. Sci. Catal. 27 (1986) 459.
5. A. Eisenstadt, in "Catalysis of Organic Reactions", ed. by F. E. Hecks, Marcel Dekker, Basel (1988) p. 415.
6. (a) R.S. Varma, K.P. Naicker and P.J. Liesen, Tetrahedron Lett. 40 (1999) 439. (b) B.M. Bhanage, M. Shirai and M. Arai, J. Mol. Catal. A; Chem. 145 (1999) 69. (c) J. Schwarz, V.P.W. Bohm, M.G. Gardiner, M. Grosche, W.A. Herrmann, W. Hieringer and G. Raudaschl-Sicber, Chem. Eur. J. 6 (2000) 1773. (d) B.M. Bhanage, M. Arai, Catal. Rev., 43 (2001) 315.

7. (a) D. Savoia, C. Trombini, A. Umani-Ronchi and G. Verardo, J. Chem. Soc. Chem. Commun. (1981) 541. (b) M. Beller and K. Kuhlein, Synlett. (1995) 441. (c) C.A. Merlic and M.F. Semmelhack, J. Organomet. Chem. 391 (1990) C23. (d) H. Hagiwara, Y. Shimizu, T. Hoshi, T. Suzuki, M. Ando, K. Ohkubo and C. Yokoyama, Tetrahedron Lett. 42 (2001) 4349.

8. (a) R.L. Augustine and S.T. O'Leary, J. Mol. Catal. 72 (1992) 229. (b) M. Hiroshige, J.R. Hauske and P. Zhou Tetrahedron Lett. 36 (1995) 4567. c) F. Zhao, B.M. Bhanage, M. Shirai and M. Arai Chem. Eur. J. 6 (2000) 843.

9. (a) C.P. Mehnert and J.Y. Ying, Chem. Commun. (1997) 2215. (b) C.P. Mehnert, D.W. Weaver and J.Y. Ying, J. Am. Chem. Soc. 120 (1998) 12289. (c) L. Djakovitch and K. Koehler J. Mol. Catal. A., 142 (1999) 275. (d) L. Djakovitch, H. Heise and K. Kohler, J. Organomet. Chem., 584 (1999) 16. (e) L. Djakovitch and K. Koehler, J. Am. Chem. Soc., 122 (2001) 5990. (f) J. Zhao, R. Zhao, L.Mo, S. Zhao, X. Zheng, J. Mol. Catal. A., 178 (2002) 289. (g) M. Dams, L. Drijkoningen, D. De Vos and P. Jacobs, Chem. Commun., (2002) 1062.

10. (a) K. Kohler, M. Wagner and L. Djakovitch, Catal. Today 66 (2001) 105. (b) A. Corma, H.Garcia, A. Levya, A. Primo, Appl. Catal. A., 247 (2003) 41.

11. M.T. Reetz and E. Westermann, Angew. Chem. Int. Ed. 39 (2000) 165.

12. (a) R.J. Peterson, Hydrogenation Catalysis, Noyes Data, Park Ridge, NJ, USA, 1977. (b) A. Farkas, in 5^{th} edn. Ullmann Encyclopaedia vol. A5 (1986) 313. (c) M.V. Rajasekharam and R.V. Chaudhari, Catal. Lett. 41 (1996) 171. (d) S. Iyer, V.V. Thakur, J. Mol. Catal. A., 157 (2000) 275.

13. A. Wali, S.M. Pillai and S. Satish, React. Kinet. Catal. Lett. 60 (1997) 189.

14. (a) D. Villemin, P. A. Jaffers, B. Nacheb, F. Courivaud, Tetrahedron Lett., 38 (1997) 6581. (b) B.M. Bhanage, M. Shirai and M. Arai, J. Mol. Catal A., 145

(1999) 69. (i) R.S. Varma, K.P. Naicker, P. J. Leisen, Tetrahedron Lett., 40 (1999) 439. (j) J. Schwartz, V.P.W. Böhm, M.G. Gardiner, M. Grosche, W.A, Hermann, W. Heiringer, G. Raudashl-Sieber, Chem. Eur. J. 6 (2000) 1773.

15. S.M. Kuznicki, U.S. Patent 5011591 (1991).
16. T.K. Das, A.J. Chandwadkar and S. Sivasanker, Chem. Commum., (1996) 1105.
17. S.B. Waghmode, S.G. Wagholikar and S. Sivasanker, Bull. Chem. Soc. Jpn., 76 (2003) 1989.

Chapter 7

Summary and Conclusions

The use of microporous materials for different types of carbon-carbon bond formation reactions has been explored in the present work. Emphasis has been given to the use of zeolites for a variety of important reactions / rearrangements that involve carbon-carbon bond formation. A wide range of reactions can be categorized as carbon-carbon bond formation reactions. Some of them are presented in Chapter 1, Table 1.3. The most commonly cited are alkylation and acylation of aromatic compounds. Both these reactions are electrophilic aromatic substitution reactions. The present work includes studies on the alkylation of phenol with a long chain olefin (1-octene) over different zeolites, the alkylation of naphthalene with 2-propanol in nitrogen as the reaction medium and acylation of anisole with long chain carboxylic acids.

Certain organic rearrangements are also examples of carbon-carbon bond formation. The most cited are Claisen, Cope, Diels-Alder, Benzidine, Fries and Wolff rearrangements. Organic reactions involving ring formation, expansion or contraction also involve carbon-carbon bond formation. The present work also includes a study of the Claisen rearrangement of allyl phenyl and methyl substituted allyl phenyl ethers and diallyl ether of hydroquinone. In order to understand the reactions better and to obtain effective comparisons of the activity of the different zeolites, kinetic analysis of the data has been carried out. A second order parallel reaction kinetics was assumed for the phenol alkylation, a pseudo first order kinetics was assumed for the acylation of anisole and first order series and parallel reactions were assumed for Claisen rearrangement. As thermodynamic and thermochemical data were not available for the alkylation of phenol with 1-octene, these data were obtained by calculations using Benson's method (Chapter 2).

The coupling of aromatic halides with acrylates and other olefins (Heck reaction) or boronic acids (Suzuki reaction) are also examples of carbon–carbon bond formation reactions. The present work explores the Heck reaction over Pd loaded ETS-10 molecular sieve. The catalyst was specifically chosen because of the basic nature of ETS-10 and the possible synergistic effects of a basic support in the reaction promoted by a base.

Wide pore zeolites beta, mordenite and Y (with different Si/Al ratios) were characterized by XRD, N_2-adsorption and TPD of NH_3. The TPD studies revealed the acidity characteristics of the parent zeolites and their modified (aluminaterd and alkali poisoned) forms. The acidity of the parent zeolites was in the order: FAU(2.6)> MOR(11) > BEA(15), which is also the order of the Al content of the zeolites. Dealumination decreased the acidity of all the three zeolites. K-poisoned the acidity of BEA more than Na. A preferential poisoning of the strong acidity by K was noticed.

Alkylation of phenol with 1-octene was investigated over the zeolites beta (BEA), mordenite (MOR) and Y (FAU) possessing different Si/Al ratios. The influence of different process parameters on the reaction was studied in detail over BEA. The products of the reaction are phenyl octyl ether (from alkylation at the *O*-atom) and o- and p-octyl phenols (from alkylation at the *C*-atoms). The *C*- and *O*- alkylation reactions occur in parallel. During the reaction, simultaneous isomerization of 1-octene to the internal olefins occurs. As a result, isomeric products based on the attachment of the phenoxy or phenyl group at different positions (2-, 3- and 4-) in the C_8-chain are formed. The major isomeric product is the 2- isomer. The studies carried out in the temperature range of 343 to 393 K reveal that thermodynamic equilibrium conversion is reached only at about 393K at the end of 6 h of reaction. A comparison of the activity of BEA has also been made with those of two other large pore zeolites, mordenite (MOR) and H-USY (FAU) with nearly similar Si/Al ratios. The activity of the three zeolites is in the order BEA> FAU > MOR. BEA and MOR favour

C-alkylation while, FAU favours *O*-alkylation. A kinetic analysis of the two parallel alkylation reactions, assuming second order kinetics, has been presented. The rate constants for *C*-alkylation are larger than those for *O*-alkylation in the temperature range of 328 to 393 K. The activation energy (Ea) values calculated from the rate constants are 14.6 kcal $mole^{-1}$ for *O*-alkylation and 12.6 kcal $mole^{-1}$ for *C*-alkylation.

The alkylation of naphthalene with isopropanol (IPA) was carried out over various zeolites (H-beta, H-Y, RE-Y, H-mordenite, H-MCM-22 and H-ZSM-5) in the absence of an organic solvent, using nitrogen as the reaction medium. A comparison of the activity of different zeolites reveals that H-beta is the most active. RE-Y is more active compared to its H-form. H-MCM-22 and H-ZSM-5 are poor catalysts for the reaction, mainly because of the lack of access of the active sites to the reactant naphthalene. Though conversion over H-mordenite is lower than over H-beta and RE-Y, 2,6-DIPN selectivity is highest over H-MOR due to its shape selective nature. The reaction is rapid over H-beta and a conversion of about 63 % is reached in three hours at 473 K. However, at a temperature of 498 K, the catalyst activity is lower presumably, due to initial rapid deactivation of the catalyst by coking. The highest conversion of naphthalene is observed when a stoichiometric amount of IPA (IPA/naphthalene mole ratio = 2) is used. On increasing the mole ratio from 2 to 3, there is a deterioration in the performance of the catalyst. This is probably due to the oligomerization of propylene leading to coke deposition on the catalyst and poisoning by water produced by the dehydration of the alcohol. A comparison of the reaction in cyclohexane, N_2 and in the absence of any medium shows that the reaction proceeds better in N_2 with higher activity and selectivity.

The acylation of anisole with long chain carboxylic acids (hexanoic, octanoic and decanoic) has been investigated over the large pore zeolites BEA, FAU and MOR. The products of the reaction are the ketone (major) and the ester (minor). Acylation occurs

predominantly at the 4- (p-) position of anisole with small amounts of the o-isomer also being formed. The m-isomer could not be detected. The reactivity of the acid decreases with carbon number due (presumably) to increasing diffusion resistance with C-number. The orders of the activity of the three zeolites arre similar for hexanoic acid and octanoic acid (FAU(6) > BEA(15) > MOR(11)), but different for decanoic acid (BEA(15) > (FAU(6) > MOR(11)). Based on studies using zeolites with different Si/Al ratios, it is concluded that, at a Si/Al ratio of 49, BEA is about 4 and 14 times more active than FAU and MOR, respectively.

The Claisen rearrangement of allyl aryl phenol and allyl aryl cresols occurs rapidly over zeolite beta even at temperatures as low as 353K. The initial products formed (o-allylphenols) cyclize readily into benzofuran derivatives. An increase in the temperature of the reaction or the amount of catalyst increases the formation of the ring product. The reaction proceeds rapidly both in inert solvents such as EDC and TCE, and in reactive solvents such as benzene and toluene. In the latter solvents, the intermediate allylphenols react with the solvent to produce byproducts. The acidity of the zeolites, measured by the TPD of ammonia, decreases progressively on increasing levels of dealumination with nitric acid. However, the activity of the catalyst increases with increasing dealumination and decreasing number of acid sites. This is attributed to the reaction occurring mainly at the pore-mouths and at the external surface of the zeolite crystallites and dealumination increasing the accessibility of the acid centers to the reactant molecules through creation of mesopores. The conversion is poor in mordenite and zeolite Y despite their possessing higher acidity compared to beta. This may be due to (i) their low external surface areas and (ii) their easy deactivation due to strong adsorption and slow desorption of the product molecules from their surfaces. A kinetic analysis reveals that the reaction follows typical first order consecutive and parallel reaction kinetics. The rate constants for the different

steps derived from the kinetic analysis enable a better understanding of the reactivity of the different substrates.

Pd-ETS-10 (reduced in H_2) exhibits a high activity towards the Heck coupling of aryl iodides and bromides with acrylates, under typical reaction conditions. A TON value of ~ 10,000 is achieved for a 0.2 wt % Pd-ETS-10 catalyst. Though some Pd leaches out into solution when iodobenzene is used as the substrate, the reaction is found to proceed mainly by the heterogeneous route. When 1-bromo-4-nitrobenzenes used as the substrate, the reaction is totally heterogeneous. Organic bases lead to higher catalytic activity than inorganic bases and electron withdrawing substituents enhance the reactivity of the aryl halides.

The present work is a study of a number of carbon-carbon bond formation reactions over large pore zeolites. As the reactions have been carried out at different experimental conditions, it is not possible to conclude on the relative ease of the reactions over the different zeolites. However, based on the temperatures used and conversions achieved in the reactions in this study it appears that the ease of these reactions over the zeolites investigated is the order: Claisen rearrangement of APE > alkylation of 1-octene > acylation by long chain acids > isopropylation of naphthalene with isopropyl alcohol. However, it is pointed out that this order may change when different substrates are used.

List of Publications:

1. Heck Reaction over Pd-loaded ETS-10 molecular sieve

   S.B.Waghmode, S. G. Wagholikar and S. Sivasanker;

   Bulletin of chemical Society of Japan, 76 (2003) 1989-1992.

2. Benzylic oxidation with H_2O_2 catalyzed by Mn complexes of N,N',N''-trimethyl-1,4,7-triazacyclononane:spectroscopic investigations of the active Mn species.

   T.H. Bennur, S.M. Sabne, S. S. Deshpande, D. Srinivas and S. Sivasanker, Journal of Molecular. Catalysis; A: Chemical, 185 (2002) 71-80.

3. Liquid phase oxidation of amines to azoxy compounds over ETS 10 molecular sieves.

   S.B.Waghmode, S. M. Sabne and S. Sivasanker; Green Chemistry, 3 (2001) 289.

4. Alkylation of naphthalene with t-butanol: use of carbon dioxide as solvent.

   R.P. Marathe, S. Mayadevi, S.M. Sabne and S. Sivasanker; Journal of Molecular. Catalysis; A: Chemical, 181 (2002) 201-206.

5. Studies on isoproplylation of naphthalene over zeolites.

   Ishwarya Mathew, S. Mayadevi, Smita Sabne, S.A. Pardhy and S. Sivasanker; Reaction Kinetics and Catalysis letters, 74(1) (2001) 119-125.

6. Isopropylation of naphthalene over large pore zeolites.

   Ishwarya Mathew, Smita Sabne, S. Mayadevi, S.A. Pardhy and S. Sivasanker; Indian Journal of Chemical Technology, 3 (2001) 469-472.

7. Claisen rearrangement over zeolite beta.

   S. G. Wagholikar, S. Mayadevi, S. Sivasanker, Presented at the 14th International Zeolite Conference, Cape Town, April 2004.

8. Alkylation of anisole over zeolite catalyst: influence of alkylating agents and operating parameters.

   P.V. Surse, S.G. Wagholikar, S.Mayadevi and S. Sivasanker,

   Presented in The Indian Chemical Engineering Congress, 2003, and 56th annual session of the I. I. Ch. E., Orissa state Coordination and R.R.L Bhuwaneshwar, India, Dec. 19-22, 2003.

9. Claisen rearrangement of allyl phenyl ether over zeolites beta, mordenite and Y.

   S. Wagholikar, S. Mayadevi, N.E. Jacob, S. Sivasanker, manuscript under preparation

10. Alkylation of phenol with 1-octene

    S. Wagholikar, S. Mayadevi and S. Sivasanker, manuscript under preparation

11. Alkylation of anisole with long chain acids over zeolite catalyst

    S. Wagholikar, S. Mayadevi and S. Sivasanker, manuscript under preparation